A study of Pyrrolidinium *Bis*(fluorosulfonyl)imide based ionic liquids for lithium metal batteries

Hyun-gook (Martin) Yoon

July 2013

A thesis submitted to the Faculty of Science, Monash University, for the degree of Doctor of Philosophy.

Table of Contents

Abstract

The use of ionic liquids (ILs) as electrolytes for lithium metal secondary batteries was investigated in this thesis. An electrolyte based on *bis*(fluorosulfonyl)imide, or FSI, which has relatively lower viscosity and higher conductivity than the well-known *bis*(trifluoromethylsulfonyl)imide ionic liquids (NTf_2 or TFSI), was investigated for its application in a lithium metal battery. An electrolyte based on dicyanamide, or DCA, which does not have any fluorinated functional group, was also investigated.

The FSI based electrolyte was characterised using various electrochemical, physical and spectroscopic techniques as well as for its performance in Li metal batteries containing a lithium cobalt oxide ($LiCoO_2$) cathode. Unlike the commercial organic liquid based electrolyte, FSI showed good lithium cycle-ability when the lithium salt concentration was exceptionally high, up to 3.2 $mol.kg^{-1}$ or 1 : 1 Li to cation ratio - in spite of its high viscosity. High rate charge and discharge (up to 5C) was achieved with this high salt concentration (and highly viscous) electrolyte in Li | $LiCoO_2$ cells; which is superior to the performance with the standard organic electrolyte. The nature of this unusual behaviour was rationalised with respect to its transference number and the conformational structure of the FSI anion. It was suggested that the change from trans-conformer of FSI to cis-conformer in the presence of Li^+ alters the lithium ion transportation mechanism.

A non-fluorinated dicyanamide (DCA) based ionic liquid was investigated as an alternative electrolyte for its exceptionally low viscosity, high conductivity and lower cost compared to fluorinated electrolytes. It was shown that this electrolyte exhibited good capacity retention for Li | $LiFePO_4$ batteries, achieving 130 $mAh.g^{-1}$ at 50 ^oC. The moisture content of the IL was shown to be extremely important in determining performance and approximately 200 ppm of moisture produced the optimum cycling ability. The physical properties of this DCA ionic liquid containing several different fluorinated lithium salts (lithium *bis*(fluorosulfonyl)imide(LiFSI), lithium *bis*(trifluoromethanesulfonyl)imide ($LiNTf_2$ or LiTFSI)and lithium tetrafluoroborate ($LiBF_4$)) was compared with when LiDCA was added. The solution had the lowest viscosity, highest ionic mobility and highest degree of ionization when Li DCA was added. $LiBF_4$ addition produced the highest viscosity and lowest ionic mobility with the lowest degree of ionization. Unlike the other added salt anion species, BF_4^- was shown to form larger clusters rather than simple ion pairs. The difference of qualitative description of the 'Walden plot' result and 'ionicity' result was compared and this suggested that 'ionicity' (the ratio of the molar ionic conductivity versus the conductivity calculated from Nernst-Einstein equation using NMR self-diffusion coefficients) better represents the behaviour of a salt mixed system than the Walden plot.

Acknowledgements

I would like to express my sincere thanks to my main supervisor, Professor Douglas R. MacFarlane. He gave me this opportunity when I was seeking an opportunity in Australia, guided me when I was lost in research, encouraged me when I was depressed when my research was not progressing as I intended. I thank him for holding trust in me even when I was lost in research and struggling to find a proper direction.

I also would like to thank my supervisor at Deakin University, Dr. Patrick C. Howlett, whose expertise in battery science and ionic liquids, kindness, encouragement and enthusiasm was a great gift to me. His guidance based on his knowledge and experience on data analysis became one of the most important parts of my thesis.

I cannot exaggerate what and how much Dr. Adam S. Best at CSIRO has given to me. He was my teacher when I need a scientific knowledge, my boss when I did my research at CSIRO, and my sincere friend when I need helps outside of research. Not only as a Ph.D. student, but also as a newcomer in Australia, I would not have finished my Ph.D. research without his help.

I also would like to thank Professor Maria Forsyth at Deakin University. She has given me invaluable advices with keen insight and a lot of opportunities. I also thank her for her endurance and actually consoling me when I broke an NMR probe at the beginning of my research resulting delay in research of many other colleagues.

I also thank to Dr. Katya Izgorodina Pas and Dr. Toby Bell, who have given me kind advices during my research period as my panelists.

Special thanks to Dr. Youssof Shekibi, Dr. Paul Bayley, Dr. George Lane, who initiated my research, helped me with their knowledge and experience.

I thanks to Dr. Tony Hollenkamp, Dr. Anand Bhatt, Dr. Thomas Ruther, Dr. Graeme Snook, Mr. Pon Kao, Ms. Thuy Huynh at CSIRO, who gave me valuable advices, helps.

Thank you to all of the members of the Ionic Liquids group at Monash University and Deakin University. Especially, Mr. Tristan Simons, Dr. Timothy Khoo, Mr. Liyu (Leo) Jin, Dr. Katherine Nairn, Dr. Judith Janikowski, Dr. Vanessa Armel, Dr. Usman Ali Rana, Ms. Mega Kar, and Dr. Manoj Ainikalkannath Lazar. I couldn't have done my research without your kind help.

Finally and the most importantly thanks to my wife, Kyungim Lee who always has trusted me when I suddenly resigned from my previous company to start a new life in Australia.

Chemical Abbreviations

AgTf	silver trifluoromethanesulfonate
BOB	*bis*(oxalato)borate
C_2mim, EMI	*N*-ethyl-*N'*-methylimidazolium
C_4mim, BMI	*N*-butyl-*N'*-methylimidazolium
C_3mpip	*N*-propyl-*N*-methylpiperidinium
C_1mpyr	*N,N*-dimethylpyrrolidinium
C_2mpyr	*N*-ethyl-*N*-methylpyrrolidinium
C_3mpyr	*N*-propyl-*N*-methylpyrrolidinium
C_4mpyr	*N*-butyl-*N*-methylpyrrolidinium
DCA	dicyanamide
DMC	dimethyl carbonate
DEC	diethyl carbonate
EC	ethylene carbonate, *1,3*-dioxolan-*2*-one
EMC	ethyl methyl carbonate
FSI	*bis*(fluorosulfonyl)imide
NMP	*N*-methyl-*2*-pyrrolidone
TCB	tetracyanoborate
TCM	tricyanomethanide
TFSI or NTf$_2$	*bis*(trifluoromethanesulfonyl)imide
VC	vinylene carbonate, *1,3*-dioxo-*2*-one

PART A: General Declaration

Monash University

Declaration for thesis based or partially based on conjointly published or unpublished work

General Declaration

In accordance with Monash University Doctorate Regulation 17 Doctor of Philosophy and Research Master's regulations the following declarations are made:

I hereby declare that this thesis contains no material which has been accepted for the award of any other degree or diploma at any university or equivalent institution and that, to the best of my knowledge and belief, this thesis contains no material previously published or written by another person, except where due reference is made in the text of the thesis.

This thesis includes 1 original papers published in peer reviewed journals and 3 unpublished publications. The core theme of the thesis is lithium metal batteries with ionic liquid electrolytes. The ideas, development and writing up of all the papers in the thesis were the principal responsibility of myself, the candidate, working within the School of Chemistry and CSIRO Energy Technology and Deakin University under the supervision of Prof. Douglas MacFarlane (School of Chemistry), Dr. Adam Best (CSIRO Energy Technology) and Dr. Patrick Howlett (Deakin University).

The inclusion of co-authors reflects the fact that the work came from active collaboration between researchers and acknowledges input into team-based research.

In the case of chapter 3 and 4 my contribution to the work involved the following:

[If this is a laboratory-based discipline, a paragraph outlining the assistance given during the experiments, the nature of the experiments and an attribution to the contributors could follow.]

Thesis chapter	Publication title	Publication status*	Nature and extent of candidate's contribution
3	The effect of lithium concentration on mobility and transference number in N-propyl-N-methylpyrrolidinium bis(fluorosulfonyl)imide	Accepted to J. Electrochem. Soc.	Experimentation, experiment planning, manuscript writing. Extent of experimental contribution: 100%
3	Conformational change affecting Li ion mobility in High Li concentration FSI-based ionic liquid electrolytes	Submitted to J.Phys.Chem.C	Experimentation, experiment planning, manuscript writing. Extent of experimental contribution: 100%
4	Lithium electrochemistry and cycling behavior of ionic liquids using cyano based anions	Published in Energy and Environmental Science	Experimentation, experiment planning, manuscript writing. Extent of experimental

			contribution: 70%
4	Ionicity and lithium interfacial properties of N-butyl-N-methylpyrrolidinium dicyanamide ionic liquid - lithium salt electrolytes	Manuscript	Experimentation, experiment planning, manuscript writing. Extent of experimental contribution: 100%

I have /(have not) (circle that which applies) renumbered sections of submitted or published papers in order to generate a consistent presentation within the thesis.

Signed: **Hyungook (Martin) Yoon...**

Date: *10-07-2013*

Chapter 1. Introduction

1-1. Lithium secondary batteries

Lithium secondary batteries are the most widespread electrochemical storage devices due to their high energy densities, high discharge rate characteristics and long cycle life. For decades, they have been used for cellular phones and laptops, electric vehicle (EV) and hybrid electric vehicle (HEV) applications replacing internal combustion engines, the importance of research in this field has grown.[1] The current technology for conventional lithium ion batteries consists of a graphite anode, an organic liquid electrolyte and a lithium cobalt oxide ($LiCoO_2$) cathode. They offer a coulombic capacity over 400 $Wh.L^{-1}$ in the 4.2V to 3.0V voltage window, over 90% of discharge capacity is available at a 1 hour discharge rate (1C) versus the 5 hour discharge rate (0.2C).[2]
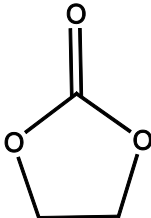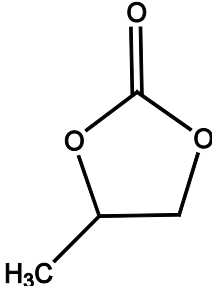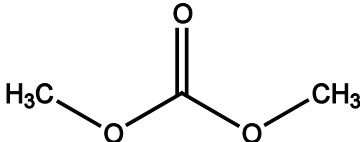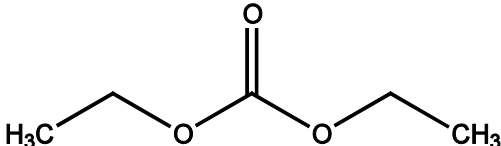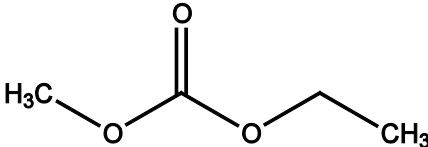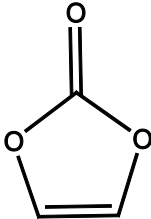
The need for higher capacity with good C-rate and cycle-ability has always been important, but is especially important for application in EVs and HEVs, especially while maintaining good safety characteristics. While a conventional battery for a cellular phone or laptop computer has capacity of 1 - 4 Ah, a single cell for an EV or HEV has a capacity of 7 – 10 Ah.[3] These larger batteries, along with increased energy densities, have generated serious safety concerns because some failure modes, such as internal short circuits, may result in a serious accident due to a large amount of energy being discharged internally in a short time possibly resulting in fire or explosion.

1-2. Electrolytes

Electrolyte research is one of the most important fields with respect to improved safety, as well as other related properties of the device. Even if a researcher finds a novel cathode or anode material which has high capacity or rate performance, without a proper electrolyte having wide electrochemical window, sufficiently high ionic conductivity and good thermal stability, the goal of realising a safe advanced secondary battery cannot be achieved. Almost all potential failure modes of lithium secondary batteries are related to flash ignition of the electrolyte on thermal runaway. The thermal and electrochemical stability of an electrolyte is thus very important. Goodenough, *et al*. summarised the properties of various classes of electrolytes and nominated stability over wide voltage range, low volatility and non-flammability as the most important requirements.[4]

In the case of lithium secondary batteries, whether they are lithium ion batteries or lithium metal batteries, non-aqueous organic liquids (mostly alkyl carbonates) have mainly been used as electrolytes because they have wide electrochemical voltage range and high ionic conductivities. The structures and physical properties of the most commonly used organic liquid electrolyte solvents are shown in Table 1-1.

Table 1-1: Some alkyl carbonates used as electrolytes, melting point, boiling point and

flashing point data were collected from the Merck™ website.[5]

Name	Structure	M.P (^{o}C)	B.P (^{o}C)	F.P (^{o}C)
Ethylene Carbonate (EC)		36	348	150
Propylene Carbonate (PC)		-49	243	123
Dimethyl Carbonate (DMC)		0.5 – 4.7	90	14
Diethyl Carbonate (DEC)		-43	126	31
Ethyl Methyl Carbonate (EMC)		-55	107	25
Vinylene Carbonate (VC)		19 – 22	162	73

The main problem with these organic liquids is that they are volatile and highly flammable.

Their flash points range from room temperature to 150 ^{o}C. There are various failure modes

and testing methods of lithium secondary battery safety. For example, there are tests of

thermal stability of lithium batteries, in which the cell is held at 150 ^{o}C, or tests of external

short endurance, mechanical damage of the cell, or induced voltage over-limit and so on.

However, the many failure modes and testing methods can be divided into three categories

related to the internal failure mechanism. The first failure mode is an internal short

between two electrodes, whether caused by an internal driving force (lithium dendrite

growth may penetrate separator, or unwanted debris) or external driving forces (electrical

short or mechanical damage). The second failure mode is external heating. The final failure

mode is caused by over potential on the cathode (structure collapse when deintercalating Li

I < 0.5 mol fraction, about 4.6V vs. Li |Li^{+}) or electrolyte voltage window. In these failure

modes, the organic liquids are decomposed and result in thermal runaway.[6] Sometimes

ignition is caused by an electrical short because the flash points of organic liquids are low.

Because of these weaknesses of the organic liquid electrolytes, the investigation of

alternative electrolyte systems has become essential for the development of advanced

lithium rechargeable batteries. Thus, the goal of this research includes investigating ionic

liquids as electrolytes for lithium secondary cells, which have wide safety operating regions,

as well as high performance compared to the conventional organic electrolyte.

1-3. Ionic Liquids (ILs)
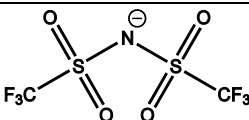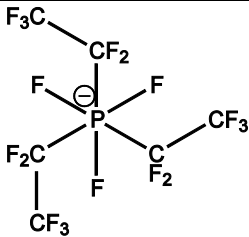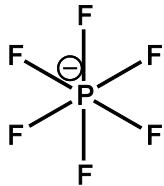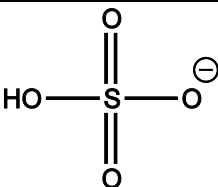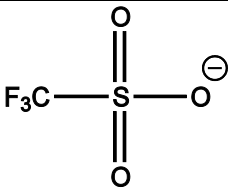
Ionic liquids are salts existing in the liquid phase around room temperature. At room

temperature, normal liquids such as water or alcohol exist in the uncharged state, molecules

in an IL exist as ions. These types of materials are also called "Molten Salts" or "Liquid Salts".

The first room temperature ionic liquid was discovered by P. Walden in 1914 and

chloroaluminate based salts were synthesised by Hurley and Wier, and Wilkes, *et al*. in 1951.

More recently Wilkes and Zaworotko reported hydrolytically stable anions in 1992, which
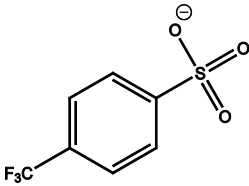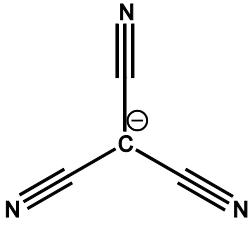
triggered massive research on ionic liquids.[7] The general requirement for classification as an ionic liquid is that the salt needs to have melting point of $100^{\circ}C$ or below.[8] Those having melting points at or below room temperature (RT) are called RTILs.
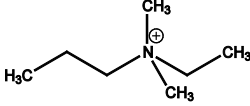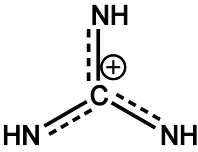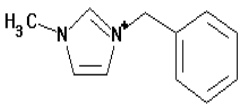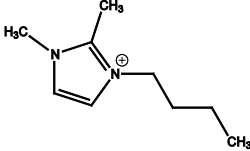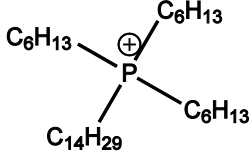
Currently, there are several types of RTIL being researched. These can be classified in several ways, by the different cation and anion species, protic and aprotic characteristics, or for the designated applications. The following Table 1-2 lists classes of anion and cation (data collected from the Merck™ website[5]).
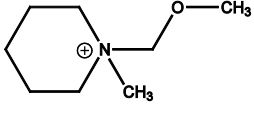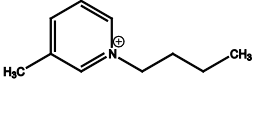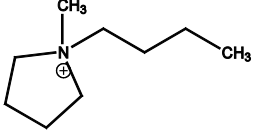
Table 1-2: Ions in RTILs, data collected from the Merck™ website[5]

Anions		Example Structure	Example IL	M.P. ($^{\circ}C$)
Trifluoroacetates			*1*-Butyl-*1*-methylpyrrolidinium trifluoroacetate	31
Borates	Cyanoborates TCB		*1*-Ethyl-*3*-methylimidazolium tetracyanoborate	13
	Fluoroborates		*1*-Ethyl-*3*-methylimidazolium tetrafluoroborate	15
	Oxalatoborates		*1*-Ethyl-*3*-methylimidazolium *bis*[oxalato(2⁻)-O,O⁺]borate	62
Dicyanamides			*1*-Butyl-*3*-methylpyridinium dicyanamide	16

Halides	Chlorides	Cl⁻	*1*-Ethyl-*3*-methylimidazolium chloride	77-79
	Bromides	Br⁻	*1*-Ethyl-*3*-methylimidazolium bromide	65
	Iodides	I⁻	*1*-Ethyl-*3*-methylimidazolium iodide	69
	Fluorides	F⁻	Cetylaminhydrofluoride	122-125
Imides (or Amides)			*1*-Ethyl-*3*-methylimidazolium *bis*(trifluoromethylsulfonyl)imide	-15
Phosphates	Fluoroalkylphosphates, (FAP)		*1*-Ethyl-*3*-methylimidazolium tris(pentafluoroethyl)trifluoro-phosphate	-1
	Fluorophosphates		*1*-Butyl-*3*-methylimidazolium hexafluorophosphate	12
Sulfates			*1*-Butyl-*3*-methylimidazolium hydrogensulfate	38
Sulfonates	Trifluoromethane-sulfonates		*1*-Butyl-*2,3*-dimethylimidazolium trifluoromethanesulfonate	41

Tosylates		1-Ethyl-3-methylimidazolium p-toluenesulfonate (tosylate)	56
Thiocyanate		1-Ethyl-3-methylimidazolium thiocyanate	
Tricyanomethide		1-Butyl-3-methylimidazolium tricyanomethanide	

Cations		Example Structure	Example IL	M.P. (^{o}C)
Ammoniums			Ethyl-dimethyl-propylammonium bis(trifluoromethylsulfonyl)imide	-11
Guanidiniums			Guanidinium tris(pentafluoroethyl)trifluoropho-sphate	155
Imidazoliums	Disubstituted Imidazoles		1-Benzyl-3-methylimidazolium chloride	-23
	Trisubstituted Imidazoles		1-Butyl-2,3-dimethylimidazolium tetrafluoroborate	40
Phosphoniums			Trihexyl(tetradecyl)phosphonium bis(trifluoromethylsulfonyl)imide	

Piperidiniums		*1*-(*2*-Methoxyethyl)-*1*-methyl-piperidinium bis(trifluoromethylsulfonyl)imide	
Pyridiniums		*1*-Butyl-*3*-methylpyridinium dicyanamide	16
Pyrrolidiniums		*1*-Butyl-*1*-methylpyrrolidinium bis(trifluoromethylsulfonyl)imide	-6

One common property of RTILs is that the charge on the anion or cation is spread across the molecule and the charge on the anion can also be shielded by electron withdrawing atoms or functional groups such as fluoride. Another important property of the cation is that it is usually contains large, asymmetric alkyl groups and this results in reduction of the lattice energy of the salt. These two effects of cation and anion result in weak intermolecular forces in the salts, but allow strong long-range intramolecular forces and contribute to the low melting point and to some amount to the non-volatile characteristics. So after the discovery of their quite different characteristics from normal liquids a lot of interest has been focused on ILs.

Due to the attractive characteristics of RTILs, they have been widely investigated for various applications from novel solvents for the chemical industry, to biochemical extractors and corrosion inhibiters for light metals. One of the most attractive possible applications is as electrolytes for solar cells, fuel cells or secondary batteries.[9] While organic liquids show high volatility and flammability (with low flash point), ILs have been regarded as an ideal electrolyte material for lithium batteries due to their non-volatile and non-flammable

characteristics. The attractive properties of ionic liquids for electrolytes are summarised as follows:[10]

1.   Liquid over a wide temperature range, including ambient temperature.

2.   Thermal stability, non-volatility, flame-resistance.

3.   Wide electrochemical window.

4.   Higher conductivity among the novel electrolytes.

5.   Chemical stability.

Since the discovery of new RTILs with high conductivity in the late 1990's, the number of RTIL research papers on lithium batteries has increased drastically. Recently, research on RTILs has mainly been focused on increasing ionic conductivity and adapting cell systems to evaluate charge-discharge characteristics, while early research focused on the IL properties. At the initial stage of applying RTILs as an electrolyte for lithium secondary batteries, $C_2mimNTf_2$ (or EMITFSI) with Li NTf_2 salts were mainly researched because of its hydrophobicity, good air and moisture stability and also high conductivity. In 2004, Garcia, *et al*. reported a cell consisting of $Li_4Ti_5O_{12}$ anode and $LiCoO_2$ cathode and 1M Li NTf_2 in $C_2mimNTf_2$ showing over 90% capacity retention over 200 cycles (1C rate at room temperature).[7] Before that, MacFarlane, *et al*. synthesised and reported the characteristics of pyrrollidinium based ILs, $C_1mpyrNTf_2$ and $C_2mpyrNTf_2$ showing high conductivity (up to 2 x 10^{-4} $S.cm^{-1}$ at 60^oC) in lithium ion doped plastic crystal phases of the ionic liquid.[11]   Later Matsumoto, *et al*. introduced the $(FO_2S)_2N^-$ (or FSI) anion. The FSI based RTILs have lower

viscosity and higher conductivity than NTf$_2$ based RTILs, with slightly narrower electrochemical windows.[12] Guerfi, *et al.* made a cell consisting of natural graphite anode, lithium iron phosphate (LiFePO$_4$)cathode and C$_2$mimFSI or C$_3$mpyrFSI with LiFSI. This cell showed over 360 mAh.g^{-1} of graphite and 160 mAh.g^{-1} of LiFePO$_4$ at the initial discharge and almost no capacity reduction over 40 cycles at 60 ^{o}C at low charge discharge rate (1/24C).[13]

Low viscosity, DCA based RTILs were introduced by MacFarlane, *et al.* in 2001,[14] and recently, Lane, *et al.* reported DCA ILs in cells with a LiFePO$_4$ cathode with 140 mAh.g^{-1}(with LiDCA salts) to 160 mAh.g^{-1} (with LiDCA and LiBOB salts) of their initial capacity remaining after 100 cycles.[15-16]

1-4. Lithium metal batteries

Due to its high theoretical capacity (3860 mAh.g^{-1}), Li metal has been regarded as a promising candidate for the Li battery anode system. While a lithium ion battery, which uses a graphite anode intercalation mechanism:

C$_6$ + e$^-$ + Li$^+$ $\rightarrow$ Li$^+$C$_6^-$ (charging at graphite anode)

Li$^+$C$_6^-$ $\rightarrow$ C$_6$ + e$^-$ + Li$^+$ (discharging at graphite anode)

In a lithium metal battery, lithium ions deposit directly onto the lithium metal anode during charging and are dissolved during discharge as shown below:

Li$^+$ + e$^-$ $\rightarrow$ Li (Charging)
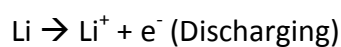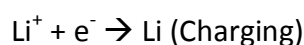
Li $\rightarrow$ Li$^+$ + e$^-$ (Discharging)

Lithium metal has the highest volumetric and gravimetric theoretical capacity amongst all possible anode candidates. However, due to the problem of dendrite formation during charging and discharging, practical use of lithium metal as an anode for secondary battery is limited, so using ionic liquid based electrolytes to establish lithium metal battery safety is one promising alternative approach to make a commercial lithium metal battery possible. Some initial important ionic liquid research related lithium metal batteries are presented in table 1-3.

Table 1-3: Initial RTIL research results for lithium metal batteries

Year	Author	Electrolyte	Result
1992	Wilkes[17]	$C_2mimCH_3CO_2$	Introduction of moisture stable RTIL
1995	Koch[18]	$C_2mimNTf_2$, $C_3dmimNTf_2$	SEI investigation
1996	Bonhote[19]	$C_xmmim[X]$	Physicochemical properties of imidazolium cations with various cation and anion combinations
1997	Fuller[20]	C_2mimBF_4	Physicochemical properties of imidazolium cations.
1999	MacFarlane[21]	$C_xmpyrNTf_2$	High conductivity (up to 2×10^{-4} S.cm^{-1} at 60 ^{o}C) was reported with physical properties investigation in a lithium ion doped plastic crystal phase ionic liquid.
2003	Howlett[22]	$C_2mimNTf_2$ with Li NTf_2 with Li | Li symmetrical cells	Using optical cell, lithium surface was investigated with Raman spectroscopy and growth of lithium dendrite was pictured. In RTIL solution the growth of lithium dendrites are distinctively lower than in conventional organic solution (1M $LiPF_6$ in PC).

In 2003, Howlett, *et al*. discovered that the dendrite formation rate in RTIL as a solvent is reduced compared with conventional organic liquids(Figures 1-1 and 1-2). Research indicating PEO based gel polymer electrolytes also suppress lithium dendrite formation has also been reported. [23]
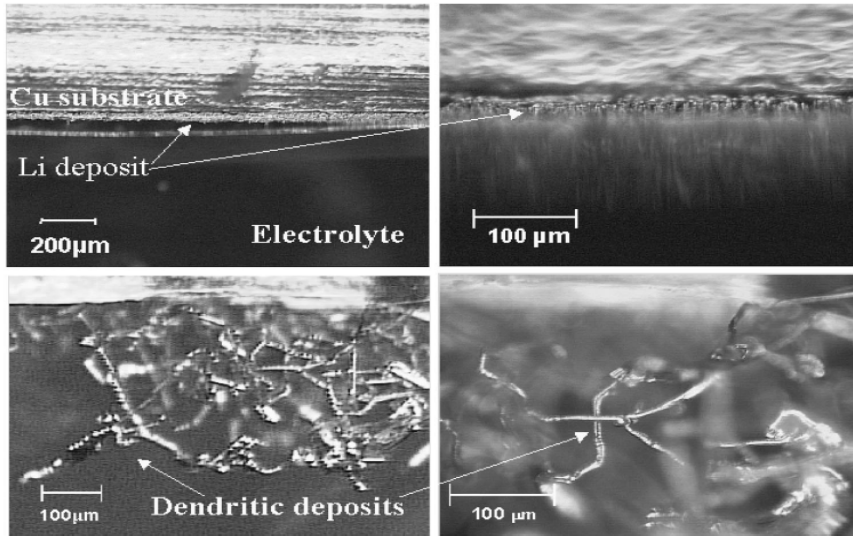
Figure 1-1: dendrite growth in C_3mpyrNTf$_2$ and C_4mpyrNTf$_2$, from Howlett, *et al*. 2004[24]
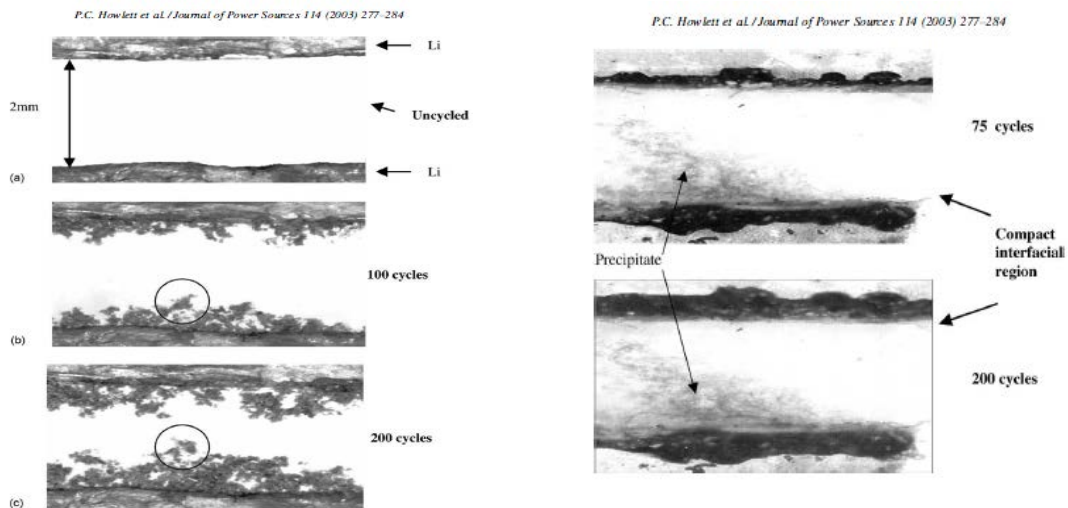
Figure 1-2: Comparison of lithium dendrite growth with 1M LiPF$_6$ in PC (left) and with 20 mol% Li NTf$_2$ in C_2mimNTf$_2$ (right), from Howlett, *et al*. [22]

Recently, Bhatt, *et al*.[25] also reported the effect of Li NTf$_2$ in C_2mimFSI on lithium dendrite formation in a Li|Li symmetrical cell study. This report also presents a pre-deposition effect on the metal electrode including lithium, which was demonstrated by Howlett, *et al*. in a

different electrolyte system previously.[24] The mechanism of lithium dendrite formation has been explained in many ways with modelling, mainly involving a crystal growth mechanism during electro-deposition due to the function of current or gradient of driving forces and salt concentration.[26-27,28] Lane, *et al.* also reported no detectable lithium dendrite formation during 100 cycles with a DCA based IL. Nonetheless, the main mechanism of suppression of dendrite growth in ionic liquids has not yet clearly been identified.[16]

Table 1-4 to 1-7 summarises some selected results of research on RTILs as electrolytes for lithium metal batteries.

Table 1-4: Selected results on RTIL researches for lithium metal batteries using $LiCoO_2$ cathode

Year	Author	Electrolyte	Result	Remark*
2003	Nakagawa[29]	C_2mimBF_4 with $LiBF_4$	94% capacity retention for 50 cycles (0.2C rate).	$Li_{1/3}Ti_{5/3}O_4$ | $LiCoO_2$
2003	Sakaebe[30]	$C_2mimNTf_2$, $C_3mpyrNTf_2$, $C_3mpipNTf_2$, $N_{1113}NTf_2$	The cathodic stability: C_2mim < N_{1113} < C_3mpyr < C_3mpip. $C_3mpipNTf_2$: (Initial) 120 $mAh.g^{-1}$, 85% capacity retention for 50 cycles (0.5C).	
2004	Garcia[31]	$C_2mimNTf_2$, C_2mimBF_4	$C_2mimNTf_2$: 90% capacity retention for 200 cycles (1C)	$Li_4Ti_5O_{12}$| $LiCoO_2$
2004	Howlett[32]	$C_4mpyrNTf_2$ with 0.5 $mol.kg^{-1}$ $LiNTf_2$	Coulombic efficiency reaches 100% for 350 cycles on Pt electrode	
2005	Chagnes[33]	$C_4mimBF_4^-$ + γ-BL	Initial : 157 $mAh.g^{-1}$, 90% capacity retention for 19 cycles (1/15C)	$Li_4Ti_5O_{12}$ | $LiCoO_2$
2005	Hayashi[34]	*1,2*-diethyl-3,4(5)-dimethylimidazolium NTf_2 with 0.8M $LiNTf_2$	Initial : 100 $mAh.g^{-1}$, 3 cycles	
2005	Holzapfel[35]	$C_2mimNTf_2$ with 1M $LiPF_6$ + 5% VC	120 $mAh.g^{-1}$ after 200 cycles	
2005	Sakaebe[36]	Combinations of cations and anions, Cation: C_3mpip, N_{5555}, N_{2222}, C_2mim	$C_3mpipNTf_2$ with 0.4M Li NTf_2 : Initial 140 $mAh.g^{-1}$, 120 $mAh.g^{-1}$ after 50 cycles (1/10C) Rate capability : $C_3mpipNTf_2$ >	

			Anion : NTf$_2$,TSAC, C1C2	C$_2$mimNTf$_2$ > C$_3$mpipNTf$_2$	
2005	Seki[37]		*N,N*-diethyl-*N*-methyl-*N*-(2-methoxyethyl)ammonium NTf$_2$ with 0.32M LiNTf$_2$	Initial : 145 mAh.g^{-1}, 81% capacity retention for 100 cycles (1/8C)	
2005	Xu[38]		C$_4$pipNTf$_2$ with LiNTf$_2$	Initial: 150 mAh.g^{-1}	
2006	Egashira[39]		C$_2$mimNTf$_2$ with LiNTf$_2$ + 10 v% additive (Cyanomethyl trimethyl ammonium bis(trifluoromethanesulfonyl)imide or Cyanoethyl trimethyl ammonium bis(trifluoromethanesulfonyl)imide)	Initial: 110 mAh.g^{-1}. 80% capacity retention for 30 cycles. This study was focused on the additives which increases the thermal stability.	
2006	Matsumoto[12]		C$_2$mimFSI, C$_3$mpipFSI, C$_3$mpyrFSI	Introduction of FSI anion as a fast charging / discharging ionic liquid electrolyte. Initial : 140 mAh.g^{-1}(0.1C) over 50 mAh.g^{-1} (5C)	
2006	Seki[40]		C$_2$mimNTf$_2$, *1,2*-dimethyl-*3*-propylimidazoliumNTf$_2$ with 0.32M LiNTf$_2$	Initial : 120 mAh.g^{-1} 100 mAh.g^{-1} after 50 cycles (0.5C)	
2006	Seki[41]		C$_2$mimNTf$_2$, *N,N*-diethyl-*N*-methyl-*N*-(*2*-methoxyethyl)-ammonium NTf$_2$ with 0.32M LiNTf$_2$	Initial : 180 mAh.g^{-1} (3.0V – 4.6V high voltage cell) 120 mAh.g^{-1} after 60 cycles (0.1C)	Zr coated LiCoO$_2$
2006	Xu[42]		C$_3$mpipNTf$_2$ with 0.4M LiNTf$_2$ and organic carbonate additives	Initial : 160 mAh.g^{-1} (2.5V – 4.5V high voltage cell) Cycle-ability (100 cycle) is not from the Li cell but electrochemical deposition / stripping data.	
2007	Sakaebe[43]		C$_3$mpipNTf$_2$ with 0.32 mol.kg^{-1} LiNTf$_2$	Initial : 140 mAh.g^{-1} 120 mAh.g^{-1} after 50 cycles	
2007	Seki[44]		C$_6$mimNTf$_2$,(comparative study of CxmimNTf$_2$)	Longer imidazolium cation chain is better for capacity retention. C$_6$mimNTf$_2$: initial 145 mAh.g^{-1} 110 mAh.g^{-1} after 120 cycles	
2007	Seki[45]		*1,2*-Dimethyl-*3*-propylimidazolium NTf$_2$, with different salt concentration of LiNTf$_2$	0.3 to 0.4 mol.kg^{-1} LiNTf$_2$ concentration showed the best capacity and rate capability. 140 mAh.g^{-1} (1/8C) , 110 mAh.g^{-1} (1C)	
2008	Seki[46]		*N,N*-diethyl-*N*-methyl-*N*-(*2*-methoxyethyl)ammonium NTf$_2$ with 0.32 mol.kg^{-1} LiNTf$_2$	4.2V charging initial: 140 mAh.g^{-1}, 120 mAh.g^{-1} at 100th cycle. 4.5V charging initial: 200 mAh.g^{-1}, 100 mAh.g^{-1} at 100th	
2009	Fang[47]		guanidinium-based ILs 1g13NTf$_2$ and 1g22NTf$_2$ with 0.3mol.kg^{-1} LiNTf$_2$	Initial : 160 mAh.g^{-1}, No significant capacity reduction for 50 cycles with 0.2C rate.	
2011	Fang[48]		guanidinium ILs (1g13 or 1g22) NTf$_2$ with different concentrated LiNTf$_2$	0.9 mol.kg^{-1} LiNTf$_2$ in 1g1(2o1)NTf$_2$: 140 mAh.g^{-1} for initial and 130 mAh.g^{-1} after 50	

			cycles, 0.2C, 25 ^{o}C.	
2013	Unemoto[49]	C_2mimNTf$_2$, *N,N*-diethyl-*N*-methyl-N-(*2*-methoxyethyl)ammonium NTf$_2$, C_3mpipNTf$_2$ with 1M LiNTf$_2$	120 to 130 mAh.g^{-1} for 0.05C rate	

Table 1-5: Selected results on RTIL researches for lithium metal batteries using LiMnO$_2$

cathode

Year	1st Author	Electrolyte	Result	Remark
1996	Xu[50]	$CH_3SO_2AlCl_4$	Initial : 130 mAh.g^{-1} 80% capacity retention for 60 cycles	
2000	Caja[51]	DMFPBF$_4$ (*1,2*-dimethyl-*4*-fluoropyrazolium tetrafluoroborate)	5V (vs. Li | Li) range high voltage Li battery. DMFPBF$_4$ | LiMn$_2$O$_4$ cell : 96% of coulombic efficiency and 27% of theoretical capacity.	
2008	Saint[52]	C_3mpyrNTf$_2$ with 0.5 mol.kg^{-1} LiNTf$_2$, C_3mpipFSI with 0.5 mol.kg^{-1} LiNTf$_2$	80 mAh.g^{-1} for C$_3$mpyrNTf$_2$, 120 mAh.g^{-1} for C$_3$mpyrFSI at 5th cycle	
2010	Saruwatari[53]	C_2mimBF$_4$ with 1M LiBOB	Initial : 225 mAh.g^{-1} (0.1mA.cm^{-2}, 20 ^{o}C)	
2011	Egashira[54]	*1*-cyanomethyl-*3*-methylimidazolium(CmMI) NTf$_2$ with C$_2$mimNTf$_2$ and LiNTf$_2$	100 mAh.g^{-1} after 30 cycles, 3.0 – 4.5V (high V), 0.02mA.cm^{-2}	

Table 1-6: Selected results on RTIL researches for lithium metal batteries using LiFePO$_4$

Year	Author	Electrolyte	Result	Remark
2007	Fernicola[55]	C_4mpyrNTf$_2$ with 0.2 mol.kg^{-1} LiNTf$_2$	Initial : 110 mAh.g^{-1} (0.2C), 60 mAh.g^{-1} (1.0C)	
2007	Kobayashi[56]	*N,N*-diethyl-*N*-methyl-N-(*2*-methoxyethyl)ammonium NTf$_2$	Initial : 160 mAh.g^{-1} (0.5C) 94% capacity retention for 200 cycles (0.5C)	
2008	Guerfi[57]	C_2mimFSI with 0.7 M LiFSI, C_3mpyrFSI with 0.7 M LiFSI	164 mAh.g^{-1} for C$_2$mimFSI, and 151 mAh.g^{-1} for C$_3$mpyrFSI (25 ^{o}C) No capacity reduction over 40 cycles at 60 ^{o}C (1/24C)	
2008	Watarai[58]	Li$_{20}$–K$_{10}$–Cs$_{70}$ NTf$_2$ at 150 ^{o}C	Initial : 160 mAh.g^{-1},	

			No significant capacity reduction for 50 cycles at 150 ^{o}C	
2009	Guerfi[59]	C_3mpyrFSI with 0.7M LiFSI, C_2mimFSI with 0.7M LiFSI	Initial capacity : C_3mpyrFSI with 0.7M LiFSI : 151 mAh.g^{-1} C_2mimFSI with 0.7M LiFSI : 164 mAh.g^{-1}	
2010	Guerfi[60]	C_2mimNTf$_2$ with 1M LiPF$_6$ + OL (EC:DEC:VC)	IL 100% with salt : initial 120 mAh.g^{-1}, 50% IL to 0% IL (full OL) does not show significant difference. (50% IL : 50% OL ratio is optimum for rate, capacity without reducing safety.)	
2010	Lane[61]	C_3mpyrNTf$_2$ with 0.25 mol.kg^{-1} 2-oxo-3,9-dioxa-6-azonia-spiro[5,5]undecane NTf$_2$ (or SMK NTf$_2$) + 0.25 mol.kg^{-1} LiNTf$_2$	Initial : 130 mAh.g^{-1} No capacity reduction for 100 cycles	
2011	Egashira[54]	*1*-cyanomethyl-*3*-methylimidazolium(CmMI) NTf$_2$ with C_2mimNTf$_2$ and LiNTf$_2$	Initial : 120 mAh.g^{-1}, 30 cycles, 3.0–4.0V(high V) 0.02mA.cm^{-2}	
2011	Fang[62]	Various N$_{a,(2o1)b,c}$NTf$_2$ (a:2-5, b:1-2, c:2-4 or (2o1))	N$_{(2o1)2,(2o2)2}$NTf$_2$: initial 140 mAh.g^{-1}, no capacity reduction for 100 cycles, 0.1C rate, 25 ^{o}C.	
2011	Fang[63]	Pyr$_{(2o1)2}$NTf$_2$, Pyr$_{(2o1)(2o2)}$NTf$_2$ with 0.6mol.kg^{-1} LiNTf$_2$	140 mAh.g^{-1} for initial max and over 100 cycles, 0.1C, 25 ^{o}C.	
2011	Seki[64]	LiTetraglymeFSI	150 mAh.g^{-1} initial and no capacity reduction for 100 cycles, 0.2C 30 ^{o}C	
2012	Chai[65]	1-(2-Methoxyethyl)-2,3,5-trimethylpyrazolium NTf$_2$ with 0.4 mol.kg^{-1} LiNTf$_2$	Initial 140 mAh.g^{-1} at 0.1C, 120 mAh.g^{-1} at 0.2C for all 50 cycles.	
2012	Kim[66]	C_3mpyrNTf$_2$: LiNTf$_2$ = 9 : 1 mol ratio	Initial: 167 mAh.g^{-1}. No significant capacity reduction for 1,000 cycles was claimed but the y axis (capacity) of the figure used a log scale so the capacity reduction trend is not clear. (0.05C)	

Table 1-7: Selected results on RTIL researches for lithium metal batteries using other electrode materials than LiCoO$_2$, LiMnO$_2$ or LiFePO$_4$ cathode

Year	1st Author	Electrode	Electrolyte	Result
2000	Caja[51]	Li |LiAsF$_6$	DMFPBF$_4$ (1,2-dimethyl-4-fluoropyrazolium tetrafluoroborate)	5V (vs. Li | Li) range high voltage Li battery with DMFPBF$_4$
2004	Holzapfel[67]	Li | graphite	C$_2$mimNTf$_2$ with 1M LiNTf$_2$ + 5% VC	Initial : 350 mAh.g^{-1}
2004	Howlett[32]	Li | Li	C$_4$mpyrNTf$_2$ with 0.5 mol.kg^{-1} LiNTf$_2$	Coulombic efficiency reaches 100% for 350 cycles on Pt electrode
2006	Markevich[68]	Mo$_6$S$_8$| LiNi$_{0.5}$Mn$_{1.5}$O$_4$	C$_2$mimBF$_4$ and C$_4$mimBF$_4$ with 1M LiBF$_4$	Attempt to make 5V cell with IL. Initial: 110 mAh.g^{-1}, 50 mAh.g^{-1} after 80 cycles, but this results were based on 3.8V voltage range.
2006	Yuan[69]	Li |S	C$_4$mpipNTf$_2$ with 1M LiNTf$_2$	Initial : 1000 mAh.g^{-1}, 80% capacity retention for 10 cycles
2007	Baranchugov[70]	Si |Li, Si | LiCoO$_2$	C$_3$mpipNTf$_2$	Initial : 3000 mAh.g^{-1}, No cyclic fading for 40 cycles
2007	Lewandowski[71]	Li | graphite	C$_3$mpipNTf$_2$ with 0.4M LiNTf$_2$ + 10% VC	Initial : 340 mAh.g^{-1} 90% of capacity for 100 cycles
2007	Sivakkumar[72]	Li | Polyaniline Carbon nanotube	C$_2$mimBF$_4$ with 1M LiBF$_4$	10th cycle: 140 mAh.g^{-1} 100th cycle : 120 mAh.g^{-1}
2008	Chou[73]	Li | V$_2$O$_5$ nanowire	C$_3$mpyrNTf$_2$ with 1 M LiNTf$_2$	Initial : 400 mAh.g^{-1} 270 mAh.g^{-1} after 50 cycles
2008	Kim[74]	Li | Polyaniline Carbon nanotube	C$_2$mimBF$_4$ with 1M LiBF$_4$ + 10 wt% VC	Initial capacity : 100 mAh.g^{-1} 100th cycle : 60 mAh.g^{-1}
2008	Seki[75]	Li | graphite	C$_3$mpyrNTf$_2$ with 0.32 mol.kg^{-1} LiNTf$_2$, C$_3$mpyrFSI with 0.32 mol.kg^{-1} LiNTf$_2$	340 mAh.g^{-1} for C$_3$mpyrFSI , no capacity reduction for 150 cycles. 220 mAh.g^{-1} initial discharge capacity for C$_3$mpyrNTf$_2$ at but reached over 300 mAh.g^{-1} at 120th cycle.
2008	Shin[76]	Li | S	C$_4$mpyrNTf$_2$ + Poly(ethylene glycol) dimethyl ether (IL + OL mixture) with 0.5M LiNTf$_2$	Initial : 500 mAh.g^{-1} 200 mAh.g^{-1} after 100 cycles
2008	Shin[77]	Li | S	C$_4$mpyrNTf$_2$ + Poly(ethylene glycol) dimethyl ether (IL + OL mixture) with 0.2M LiNTf$_2$	Initial : 270 mAh.g^{-1} 250 mAh.g^{-1} after 20 cycles
2008	Wang[78]	Li | NiS–Ni$_7$S$_6$	C$_3$mpyrNTf$_2$ with 1M LiNTf$_2$	Initial : 640 mAh.g^{-1}, 400 mAh.g^{-1} capacity retention for 20 cycles
2009	Borgel[79]	Li | LiMn$_{1.5}$Ni$_{0.5}$O$_4$	C$_4$mpyrNTf$_2$ with 0.5M LiNTf$_2$, C$_3$mpipNTf$_2$ with 0.5M LiNTf$_2$, N-ethyl-N,N-dimethyl-2-methoxyethylammonium	C$_4$mpyrNTf$_2$ with 0.5M Li NTf$_2$: Initial 100 mAh.g^{-1}, No significant capacity reduction for 40 cycles. C$_3$mpipNTf$_2$ with 0.5M Li

			(DEME)NTf$_2$ with 0.5M LiNTf$_2$, C$_6$mimNTf$_2$ with 0.5M LiNTf$_2$	NTf$_2$: Initial 140 mAh.g^{-1}, No significant capacity reduction for 40 cycles. DEMENTf$_2$ and C$_6$mimNTf$_2$: 4.8V cycles for 4 cycles at 30°C.
2009	Tsunashima [80]	Li |LiNi$_{0.8}$Co$_{0.1}$Mn$_{0.1}$O$_2$	P$_{222(2O1)}$NTf$_2$ with 1M LiNTf$_2$, P$_{2225}$NTf$_2$ with 1M LiNTf$_2$	P$_{222(2O1)}$NTf$_2$ with 1M LiNTf$_2$: initial 150 mAh.g^{-1}, no significant capacity reduction for 30 cycles P$_{2225}$NTf$_2$ with 1M LiNTf$_2$: initial 120 mAh.g^{-1}, 80 mAh.g^{-1}capacity retention after 30 cycles
2011	Balducci [81]	Li | silicon+graphite	C$_4$mpyrNTf$_2$ 50% + OL(EC:DEC:DMC, 1:1.1, w/w) 50% with 0.3M LiNTf$_2$	Initial : 600 mAh.g^{-1} 500 mAh.g^{-1} after 100 cycles 0.1C rate at r.t.
2011	Chou [82]	Li | Fe$_2$O$_3$+carbon composite	C$_2$mimFSI, C$_3$mpyrFSI	Initial : 425 mAh.g^{-1} No capacity reduction for 50 cycles with 50 mA.g^{-1} current density at 50 ^{o}C
2011	Lee [83]	Li | TiO$_2$	C$_3$mpyrNTf$_2$ with 1M LiNTf$_2$, C$_3$mpyrNTf$_2$ 50: EMC 50 (v%) with 0.5M LiNTf$_2$	Initial : 240 mAh.g^{-1} for IL and salt, 260 mAh.g^{-1} for IL:OL = 50:50 + salt
2011	Plashnitsa [84]	Li | LiVPO$_4$F	C$_2$mimBF$_4$ with 1M LiBF$_4$	The cathode showed 150 mAh.g^{-1} for 1M LiPF$_6$ in EC:DMC electrolyte, but only showed 100 mAh.g^{-1} for initial and less than 70 mAh.g^{-1} for IL electrolyte. (5V cell)

* Some results cannot be said as lithium metal batteries but were included in this table for their importance.

The majority of research using LiCoO$_2$ cathode materials have used quaternary ammonium and phosphonium NTf$_2$ based electrolytes for their high anodic electrochemical stabilities.[85-86] With relatively low viscosity and high cathodic stability than the aliphatic cations, cyclic

pyrrolidinium and piperidinium NTf_2 ILs were shown to efficient lithium cycling.[87] The reported initial capacities do not vary widely, most of them ranging from 140 mAh.g^{-1} to 150 mAh.g^{-1}, which correspond to the theoretical capacity of $LiCoO_2$ from 3.0V to 4.2V, the conventional charge / discharge voltage range. The highest cycle life retention reported was 200 cycles at 1C charge and discharge current rate using 1 M $LiNTf_2$ in $C_2mimNTf_2$ and a $Li_4Ti_5O_{12}$ anode.[31]

Recent trends in using this cathode material are to make high voltage cells (i.e., charging above 4.5V) to maximise its capacity. Many reports on high voltage Li metal batteries still use NTf_2 based electrolytes with various cations, salts or cathode materials. Research on FSI electrolytes was first reported by Matsumoto, *et al*, [12] showing significantly high rate charging capability compared to other electrolyte materials. This and the following research on the FSI anion also showed that the surface layer formed with the FSI anion without additives prevents irreversible intercalation of IL cations in graphite anode electrodes.[88-89] However, due to its relatively low anodic electrochemical stability, this FSI based electrolyte has not been reported for any high voltage cell applications.

More studies using FSI based electrolytes with $LiFePO_4$ cathode materials have been reported, even though the majority of studies still use NTf_2 based electrolytes. This may be because the relatively low operating voltage range, typically from 3.0V to 3.8V for $LiFePO_4$ cathodes, provides a wider range of opportunities for ionic liquid based electrolyte candidates. Studies using other cathode materials such as $LiNi_{0.8}Co_{0.1}Mn_{0.1}O_2$,[90] $LiMn_{1.5}Ni_{0.5}O_4$,[79] or $LiVPO_4F$[91] are more focused on the performance of the cathode materials themselves. It was shown that most of the new cathode materials still use NTf_2 based electrolytes and no other IL candidates were reported for high voltage battery

applications. One of the reasons that the number of publications on 'RTIL + Lithium metal batteries' (search using ISI Web of Knowledge in April 2013) peaked in 2009 and 2010, but decreased thereafter may be that NTf_2 based electrolytes have already reached its best possible performance on many electrode materials and no significant, promising candidate for replacing NTf_2 based electrolytes or conventional organic liquid electrolytes has yet been found. Therefore, research trends in ILs for lithium battery applications are on designing of both the cation and anion functionality and the use of additives and diluents.[92-96] The role of IL to the structure and formation mechanism of SEI (solid electrolyte interphase)[87, 97] including the charge transfer mechanism has also became an important research subject.[98-99]

However, there is no commercially available application of lithium batteries using IL electrolyte yet, in spite of these extensive reports. One of the main reasons seems to be due to the relatively high cost of ILs compared to the organic solvent based electrolytes. Hence, it is important to find alternative IL based electrolytes which have intrinsically lower cost. Another limiting factor of IL based electrolytes is their lower rate capability, especially at low temperatures, mainly due to their high viscosity, particularly when Li salts are added. FSI anion based IL electrolytes have been shown to address this problem.[100] However, reduced electrochemical stability and safety detract from the suitability of these ILs and require further investigation.[101-102]

1-5. Research Aim

This work further investigates two different room temperature ionic liquids for use as an electrolyte for lithium metal batteries: *bis*(fluorosulfonyl)imide (or FSI) ILs for a fluorinated ionic liquid and dicyanamide (or DCA) ILs for a non-fluorinated ionic liquid. A number of electrochemical, physical and spectroscopic methods have been used to increase the understanding of the properties of these ILs in combination with lithium salts with respect to their application in lithium metal batteries. The effect of lithium salt concentration and different lithium salt species is investigated for their performance of lithium metal batteries. The characteristics and performance of DCA based ILs and the effect of moisture content is also investigated.

The specific aims of this Ph.D. project are:

- Electrochemical characterisation of ionic liquids for lithium metal battery electrolytes

- Investigation of lithium metal battery cycling and rate capability with IL electrolytes

- Investigation of lithium transport mechanisms in IL electrolytes

- Demonstration of promising electrolytes in prototype lithium metal batteries.

References

1.   Aurbach, D., A review on new solutions, new measurements procedures and new materials for rechargeable Li batteries. *Journal of Power Sources* **2005,** *146* (1-2), 71-78.
2.   Sanyo, *http://battery.sanyo.com/en/product/lithiumion_2.html*.
3.   LGChem., *http://www.lgchem.com/*.
4.   Goodenough, J. B.; Kim, Y., Challenges for Rechargeable Li Batteries. *Chemistry of Materials* **2010,** *22* (3), 587-603.
5.   Merck, *http://www.merck-chemicals.com.au/ionic-liquids/*.

6.   Yamaki, J.; Baba, Y.; Katayama, N.; Takatsuji, H.; Egashira, M.; Okada, S., Thermal stability of electrolytes with LixCoO2 cathode or lithiated carbon anode. *Journal of Power Sources* **2003,** *119*, 789-793.

7.   Garcia, B.; Lavallee, S.; Perron, G.; Michot, C.; Armand, M., Room temperature molten salts as lithium battery electrolyte. *Electrochimica Acta* **2004,** *49* (26), 4583-4588.

8.   Seddon, K. R., Ionic liquids - A taste of the future. *Nature Materials* **2003,** *2* (6), 363-365.

9.   Ohno, H., Importance and Possibility of Ionic Liquids. In *Electrochemical Aspects of Ionic Liquids*, Hiroyuki, O., Ed. 2005; pp 1-3.

10.   Sakaebe, H.; Matsumoto, H., Application of Ionic Liquids to Li Batteries. In *Electrochemical Aspects of Ionic Liquids*, Hiroyuki, O., Ed. 2005; pp 171-186.

11.   MacFarlane, D. R.; Huang, J. H.; Forsyth, M., Lithium-doped plastic crystal electrolytes exhibiting fast ion conduction for secondary batteries. *Nature* **1999,** *402* (6763), 792-794.

12.   Matsumoto, H.; Sakaebe, H.; Tatsumi, K.; Kikuta, M.; Ishiko, E.; Kono, M., Fast cycling of Li/LiCoO2 cell with low-viscosity ionic liquids based on bis(fluorosulfonyl)imide [FSI]. *Journal of Power Sources* **2006,** *160* (2), 1308-1313.

13.   Guerfi, A.; Duchesne, S.; Kobayashi, Y.; Vijh, A.; Zaghib, K., LiFePO4 and graphite electrodes with ionic liquids based on bis(fluorosulfonyl)imide (FSI)(-) for Li-ion batteries. *Journal of Power Sources* **2008,** *175* (2), 866-873.

14.   MacFarlane, D. R.; Golding, J.; Forsyth, S.; Forsyth, M.; Deacon, G. B., Low viscosity ionic liquids based on organic salts of the dicyanamide anion. *Chemical Communications* **2001,** (16), 1430-1431.

15.   Aupiais, J., Electrophoretic Mobilities of the Isotopes of Chloride and Bromide Ions in Aqueous Solution at 25 degrees C and Infinite Dilution. *Journal of Solution Chemistry* **2011,** *40* (9), 1629-1644.

16.   Lane, G.; Best, A.; MacFarlane, D.; Forsyth, M.; Hollenkamp, T.; Begic, S., Lithium battery electrolytes based on the ionic liquid N-methyl-N-butylpyrrolidinium dicyanamide:compatibility with different electrode materials including lithium metal, Li4Ti5O12, LiFePO4 and LiCoO2. CSIRO, Monash University: Clayton, VIC, 2010.

17.   Wilkes, J. S.; Zaworotko, M. J., Air and water stable 1-ethyl-3-methylimidazolium based ionic liquids. *Journal of the Chemical Society-Chemical Communications* **1992,** (13), 965-967.

18.   Koch, V. R.; Nanjundiah, C.; Appetecchi, G. B.; Scrosati, B., The interfacial stability of Li with 2 new solvent-free ionic liquids - 1,2-dimethyl-3-propylimidazolium imide and methide. *Journal of the Electrochemical Society* **1995,** *142* (7), L116-L118.

19.   Bonhote, P.; Dias, A. P.; Papageorgiou, N.; Kalyanasundaram, K.; Gratzel, M., Hydrophobic, highly conductive ambient-temperature molten salts. *Inorganic Chemistry* **1996,** *35* (5), 1168-1178.

20.   Fuller, J.; Carlin, R. T.; Osteryoung, R. A., The room temperature ionic liquid 1-ethyl-3-methylimidazolium tetrafluoroborate: Electrochemical couples and physical properties. *Journal of the Electrochemical Society* **1997,** *144* (11), 3881-3886.

21.   MacFarlane, D. R.; Meakin, P.; Sun, J.; Amini, N.; Forsyth, M., Pyrrolidinium imides: A new family of molten salts and conductive plastic crystal phases. *Journal of Physical Chemistry B* **1999,** *103* (20), 4164-4170.

22.   Howlett, P. C.; MacFarlane, D. R.; Hollenkamp, A. F., A sealed optical cell for the study of lithium-electrode electrolyte interfaces. *Journal of Power Sources* **2003,** *114* (2), 277-284.

23.   Tatsuma, T.; Taguchi, M.; Oyama, N., Inhibition effect of covalently cross-linked gel electrolytes on lithium dendrite formation. *Electrochimica Acta* **2001,** *46* (8), 1201-1205.

24.   Howlett, P. C.; MacFarlane, D. R.; Hollenkamp, A. F.; Forsyth, M., High lithium metal cycling efficiency in a room temperature ionic liquid. *Abstracts of Papers of the American Chemical Society* **2003,** *226*, 166-IEC.

25.   Bhatt, A. I.; Best, A. S.; Huang, J. H.; Hollenkamp, A. F., Application of the N-propyl-N-methyl-pyrrolidinium Bis(fluorosulfonyl)imide RTIL Containing Lithium Bis(fluorosulfonyl)imide in Ionic Liquid Based Lithium Batteries. *Journal of the Electrochemical Society* **2010,** *157* (1), A66-A74.

26.   Chen, C.-P.; Jorne, J., Fractal Analysis of Zinc Electrodeposition. *Journal of the Electrochemical Society* **1990,** *137* (7), 2047-2051.

27.   Monroe, C.; Newman, J., Dendrite growth in lithium/polymer systems - A propagation model for liquid electrolytes under galvanostatic conditions. *Journal of the Electrochemical Society* **2003,** *150* (10), A1377-A1384.

28.   MacFarlane, D. R.; Forsyth, S. A.; Golding, J.; Deacon, G. B., Ionic liquids based on imidazolium, ammonium and pyrrolidinium salts of the dicyanamide anion. *Green Chemistry* **2002,** *4* (5), 444-448.

29.   Nakagawa, H.; Izuchi, S.; Kuwana, K.; Nukuda, T.; Aihara, Y., Liquid and Polymer Gel Electrolytes for Lithium Batteries Composed of Room-Temperature Molten Salt Doped by Lithium Salt. *Journal of the Electrochemical Society* **2003,** *150* (6), A695-A700.

30.   Sakaebe, H.; Matsumoto, H., N-Methyl-N-propylpiperidinium bis(trifluoromethanesulfonyl)imide (PP13-TFSI) - novel electrolyte base for Li battery. *Electrochemistry Communications* **2003,** *5* (7), 594-598.

31.   Garcia, B.; Lavallée, S.; Perron, G.; Michot, C.; Armand, M., Room temperature molten salts as lithium battery electrolyte. *Electrochimica Acta* **2004,** *49* (26), 4583-4588.

32.   Howlett, P. C.; MacFarlane, D. R.; Hollenkamp, A. F., High lithium metal cycling efficiency in a room-temperature ionic liquid. *Electrochemical and Solid State Letters* **2004,** *7* (5), A97-A101.

33.   Chagnes, A.; Diaw, M.; Carré, B.; Willmann, P.; Lemordant, D., Imidazolium-organic solvent mixtures as electrolytes for lithium batteries. *Journal of Power Sources* **2005,** *145* (1), 82-88.

34.   Hayashi, K.; Nemoto, Y.; Akuto, K.; Sakurai, Y., Alkylated imidazolium salt electrolyte for lithium cells. *Journal of Power Sources* **2005,** *146* (1-2), 689-692.

35.   Holzapfel, M.; Jost, C.; Prodi-Schwab, A.; Krumeich, F.; Würsig, A.; Buqa, H.; Novák, P., Stabilisation of lithiated graphite in an electrolyte based on ionic liquids: an electrochemical and scanning electron microscopy study. *Carbon* **2005,** *43* (7), 1488-1498.

36.   Sakaebe, H.; Matsumoto, H.; Tatsumi, K., Discharge-charge properties of Li/LiCoO2 cell using room temperature ionic liquids (RTILs) based on quaternary ammonium cation - Effect of the structure. *Journal of Power Sources* **2005,** *146* (1-2), 693-697.

37.   Seki, S.; Kobayashi, Y.; Miyashiro, H.; Ohno, Y.; Mita, Y.; Usami, A.; Terada, N.; Watanabe, M., Reversibility of lithium secondary batteries using a room-temperature ionic liquid mixture and lithium metal. *Electrochemical and Solid State Letters* **2005,** *8* (11), A577-A578.

38.   Xu, J. Q.; Yang, J.; Nuli, Y. N.; Zhang, W. B., Study of ionic liquid electrolytes for secondary lithium batteries. *Acta Chimica Sinica* **2005,** *63* (18), 1733-1738.

39.   Egashira, M.; Tanaka-Nakagawa, M.; Watanabe, I.; Okada, S.; Yamaki, J.-i., Charge-discharge and high temperature reaction of LiCoO2 in ionic liquid electrolytes based on cyano-substituted quaternary ammonium cation. *Journal of Power Sources* **2006,** *160* (2), 1387-1390.

40.   Seki, S.; Kobayashi, Y.; Miyashiro, H.; Ohno, Y.; Usami, A.; Mita, Y.; Kihira, N.; Watanabe, M.; Terada, N., Lithium Secondary Batteries Using Modified-Imidazolium Room-Temperature Ionic Liquid. *The Journal of Physical Chemistry B* **2006,** *110* (21), 10228-10230.

41.   Seki, S.; Kobayashi, Y.; Miyashiro, H.; Ohno, Y.; Usami, A.; Mita, Y.; Watanabe, M.; Terada, N., Highly reversible lithium metal secondary battery using a room temperature ionic liquid/lithium salt mixture and a surface-coated cathode active material. *Chemical Communications* **2006,** (5), 544-545.

42.   Xu, J.; Yang, J.; NuLi, Y.; Wang, J.; Zhang, Z., Additive-containing ionic liquid electrolytes for secondary lithium battery. *Journal of Power Sources* **2006,** *160* (1), 621-626.

43.   Sakaebe, H.; Matsumoto, H.; Tatsumi, K., Application of room temperature ionic liquids to Li batteries. *Electrochimica Acta* **2007,** *53* (3), 1048-1054.

44.   Seki, S.; Mita, Y.; Tokuda, H.; Ohno, Y.; Kobayashi, Y.; Usami, A.; Watanabe, M.; Terada, N.; Miyashiro, H., Effects of Alkyl Chain in Imidazolium-Type Room-Temperature Ionic Liquids as Lithium Secondary Battery Electrolytes. *Electrochemical and Solid-State Letters* **2007,** *10* (10), A237-A240.

45.   Seki, S.; Ohno, Y.; Kobayashi, Y.; Miyashiro, H.; Usami, A.; Mita, Y.; Tokuda, H.; Watanabe, M.; Hayamizu, K.; Tsuzuki, S.; Hattori, M.; Terada, N., Imidazolium-based room-temperature ionic liquid

for lithium secondary batteries - Effects of lithium salt concentration. *Journal of the Electrochemical Society* **2007,** *154* (3), A173-A177.

46.   Seki, S.; Ohno, Y.; Miyashiro, H.; Kobayashi, Y.; Usami, A.; Mita, Y.; Terada, N.; Hayamizu, K.; Tsuzuki, S.; Watanabe, M., Quaternary ammonium room-temperature ionic liquid/lithium salt binary electrolytes: Electrochemical study. *Journal of the Electrochemical Society* **2008,** *155* (6), A421-A427.

47.   Fang, S.; Yang, L.; Wang, J.; Zhang, H.; Tachibana, K.; Kamijima, K., Guanidinium-based ionic liquids as new electrolytes for lithium battery. *Journal of Power Sources* **2009,** *191* (2), 619-622.

48.   Fang, S.; Tang, Y.; Tai, X.; Yang, L.; Tachibana, K.; Kamijima, K., One ether-functionalized guanidinium ionic liquid as new electrolyte for lithium battery. *Journal of Power Sources* **2011,** *196* (3), 1433-1441.

49.   Unemoto, A.; Ogawa, H.; Ito, S.; Honma, I., Electrical Conductivity, Self-Diffusivity and Electrolyte Performance of a Quasi-Solid-State Pseudo-Ternary System, Bis(trifluoromethanesulfonyl) amide-Based Room Temperature Ionic Liquid-Lithium Bis(trifluoromethanesulfonyl) amide-Fumed Silica Nanoparticles. *Journal of the Electrochemical Society* **2013,** *160* (1), A138-A147.

50.   Xu, K.; Zhang, S.; Angell, C. A., Room temperature inorganic ''quasi-molten salts'' as alkali-metal electrolytes. *Journal of the Electrochemical Society* **1996,** *143* (11), 3548-3554.

51.   Caja, J.; Don, T.; Dunstan, J.; Ryan, D. M.; Katovic, V., Application of ionic liquids as electrolytes in lithium rechargeable cells. *Molten Salts Xii, Proceedings* **2000,** *99* (41), 150-160.

52.   Saint, J.; Best, A. S.; Hollenkamp, A. F.; Kerr, J.; Shin, J. H.; Doeff, M. M., Compatibility of LixTiyMn1-yO2 (y=0, 0.11) electrode materials with pyrrolidinium-based ionic liquid electrolyte systems. *Journal of the Electrochemical Society* **2008,** *155* (2), A172-A180.

53.   Saruwatari, H.; Kuboki, T.; Kishi, T.; Mikoshiba, S.; Takami, N., Imidazolium ionic liquids containing LiBOB electrolyte for lithium battery. *Journal of Power Sources* **2010,** *195* (5), 1495-1499.

54.   Egashira, M.; Kanetomo, A.; Yoshimoto, N.; Morita, M., Charge-discharge rate of spinel lithium manganese oxide and olivine lithium iron phosphate in ionic liquid-based electrolytes. *Journal of Power Sources* **2011,** *196* (15), 6419-6424.

55.   Fernicola, A.; Croce, F.; Scrosati, B.; Watanabe, T.; Ohno, H., LiTFSI-BEPyTFSI as an improved ionic liquid electrolyte for rechargeable lithium batteries. *Journal of Power Sources* **2007,** *174* (1), 342-348.

56.   Kobayashi, Y.; Mita, Y.; Seki, S.; Ohno, Y.; Miyashiro, H.; Terada, N., Comparative study of lithium secondary batteries using nonvolatile safety electrolytes. *Journal of the Electrochemical Society* **2007,** *154* (7), A677-A681.

57.   Guerfi, A.; Duchesne, S.; Kobayashi, Y.; Vijh, A.; Zaghib, K., LiFePO4 and graphite electrodes with ionic liquids based on bis(fluorosulfonyl)imide (FSI)- for Li-ion batteries. *Journal of Power Sources* **2008,** *175* (2), 866-873.

58.   Watarai, A.; Kubota, K.; Yamagata, M.; Goto, T.; Nohira, T.; Hagiwara, R.; Ui, K.; Kumagai, N., A rechargeable lithium metal battery operating at intermediate temperatures using molten alkali bis(trifluoromethylsulfonyl)amide mixture as an electrolyte. *Journal of Power Sources* **2008,** *183* (2), 724-729.

59.   Guerfi, A.; Dontigny, M.; Kobayashi, Y.; Vijh, A.; Zaghib, K., Investigations on some electrochemical aspects of lithium-ion ionic liquid/gel polymer battery systems. *Journal of Solid State Electrochemistry* **2009,** *13* (7), 1003-1014.

60.   Guerfi, A.; Dontigny, M.; Charest, P.; Petitclerc, M.; Lagace, M.; Vijh, A.; Zaghib, K., Improved electrolytes for Li-ion batteries: Mixtures of ionic liquid and organic electrolyte with enhanced safety and electrochemical performance. *Journal of Power Sources* **2010,** *195* (3), 845-852.

61.   Lane, G. H.; Best, A. S.; MacFarlane, D. R.; Hollenkamp, A. F.; Forsyth, M., An Azo-Spiro Mixed Ionic Liquid Electrolyte for Lithium Metal-LiFePO4 Batteries. *Journal of the Electrochemical Society* **2010,** *157* (7), A876-A884.

62.   Fang, S.; Jin, Y.; Yang, L.; Hirano, S.-i.; Tachibana, K.; Katayama, S., Functionalized ionic liquids based on quaternary ammonium cations with three or four ether groups as new electrolytes for lithium battery. *Electrochimica Acta* **2011,** *56* (12), 4663-4671.

63.   Fang, S.; Zhang, Z.; Jin, Y.; Yang, L.; Hirano, S.-i.; Tachibana, K.; Katayama, S., New functionalized ionic liquids based on pyrrolidinium and piperidinium cations with two ether groups as electrolytes for lithium battery. *Journal of Power Sources* **2011,** *196* (13), 5637-5644.

64.   Seki, S.; Takei, K.; Miyashiro, H.; Watanabe, M., Physicochemical and Electrochemical Properties of Glyme-LiN(SO2F)(2) Complex for Safe Lithium-ion Secondary Battery Electrolyte. *Journal of the Electrochemical Society* **2011,** *158* (6), A769-A774.

65.   Chai, M.; Jin, Y.; Fang, S.; Yang, L.; Hirano, S.-i.; Tachibana, K., Ether-functionalized pyrazolium ionic liquids as new electrolytes for lithium battery. *Electrochimica Acta* **2012,** *66*, 67-74.

66.   Kim, G. T.; Jeong, S. S.; Xue, M. Z.; Balducci, A.; Winter, M.; Passerini, S.; Alessandrini, F.; Appetecchi, G. B., Development of ionic liquid-based lithium battery prototypes. *Journal of Power Sources* **2012,** *199*, 239-246.

67.   Holzapfel, M.; Jost, C.; Novak, P., Stable cycling of graphite in an ionic liquid based electrolyte. *Chemical Communications* **2004,** (18), 2098-2099.

68.   Markevich, E.; Baranchugov, V.; Aurbach, D., On the possibility of using ionic liquids as electrolyte solutions for rechargeable 5 V Li ion batteries. *Electrochemistry Communications* **2006,** *8* (8), 1331-1334.

69.   Yuan, L. X.; Feng, J. K.; Ai, X. P.; Cao, Y. L.; Chen, S. L.; Yang, H. X., Improved dischargeability and reversibility of sulfur cathode in a novel ionic liquid electrolyte. *Electrochemistry Communications* **2006,** *8* (4), 610-614.

70.   Baranchugov, V.; Markevich, E.; Pollak, E.; Salitra, G.; Aurbach, D., Amorphous silicon thin films as a high capacity anodes for Li-ion batteries in ionic liquid electrolytes. *Electrochemistry Communications* **2007,** *9* (4), 796-800.

71.   Lewandowski, A.; Swiderska-Mocek, A., Properties of the graphite-lithium anode in N-methyl-N-propylpiperidinium bis(trifluoromethanesulfonyl)imide as an electrolyte. *Journal of Power Sources* **2007,** *171* (2), 938-943.

72.   Sivakkumar, S. R.; MacFarlane, D. R.; Forsyth, M.; Kim, D. W., Ionic liquid-based rechargeable lithium metal-polymer cells assembled with Polyaniline/Carbon nanotube composite cathode. *Journal of the Electrochemical Society* **2007,** *154* (9), A834-A838.

73.   Chou, S.-L.; Wang, J.-Z.; Sun, J.-Z.; Wexler, D.; Forsyth, M.; Liu, H.-K.; MacFarlane, D. R.; Dou, S.-X., High Capacity, Safety, and Enhanced Cyclability of Lithium Metal Battery Using a V2O5 Nanomaterial Cathode and Room Temperature Ionic Liquid Electrolyte. *Chemistry of Materials* **2008,** *20* (22), 7044-7051.

74.   Kim, D.-W.; Sivakkumar, S. R.; MacFarlane, D. R.; Forsyth, M.; Sun, Y.-K., Cycling performance of lithium metal polymer cells assembled with ionic liquid and poly(3-methyl thiophene)/carbon nanotube composite cathode. *Journal of Power Sources* **2008,** *180* (1), 591-596.

75.   Seki, S.; Kobayashi, Y.; Miyashiro, H.; Ohno, Y.; Mita, Y.; Terada, N.; Charest, P.; Guerfi, A.; Zaghib, K., Compatibility of N-Methyl-N-propylpyrrolidinium Cation Room-Temperature Ionic Liquid Electrolytes and Graphite Electrodes. *Journal of Physical Chemistry C* **2008,** *112* (42), 16708-16713.

76.   Shin, J. H.; Cairns, E. J., N-Methyl-(n-butyl)pyrrolidinium bis(trifluoromethanesulfonyl)imide-LiTFSI-poly(ethylene glycol) dimethyl ether mixture as a Li/S cell electrolyte. *Journal of Power Sources* **2008,** *177* (2), 537-545.

77.   Shin, J. H.; Cairns, E. J., Characterization of N-methyl-N-butylpyrrolidinium Bis(trifluoromethanesulfonyl)imide-LiTFSI-Tetra(ethylene glycol) dimethyl ether mixtures as a li metal cell electrolyte. *Journal of the Electrochemical Society* **2008,** *155* (5), A368-A373.

78.   Wang, J. Z.; Chou, S. L.; Chew, S. Y.; Sun, J. Z.; Forsyth, M.; MacFarlane, D. R.; Liu, H. K., Nickel sulfide cathode in combination with an ionic liquid-based electrolyte for rechargeable lithium batteries. *Solid State Ionics* **2008,** *179* (40), 2379-2382.

79.   Borgel, V.; Markevich, E.; Aurbach, D.; Semrau, G.; Schmidt, M., On the application of ionic liquids for rechargeable Li batteries: High voltage systems. *Journal of Power Sources* **2009,** *189* (1), 331-336.

80.   Tsunashima, K.; Yonekawa, F.; Sugiya, M., Lithium Secondary Batteries Using a Lithium Nickelate-Based Cathode and Phosphonium Ionic Liquid Electrolytes. *Electrochemical and Solid State Letters* **2009,** *12* (3), A54-A57.

81.   Balducci, A.; Jeong, S. S.; Kim, G. T.; Passerini, S.; Winter, M.; Schmuck, M.; Appetecchi, G. B.; Marcilla, R.; Mecerreyes, D.; Barsukov, V.; Khomenko, V.; Cantero, I.; De Meatza, I.; Holzapfel, M.; Tran, N., Development of safe, green and high performance ionic liquids-based batteries (ILLIBATT project). *Journal of Power Sources* **2011,** *196* (22), 9719-9730.

82.   Chou, S.-L.; Lu, L.; Wang, J.-Z.; Rahman, M. M.; Zhong, C.; Liu, H.-K., The compatibility of transition metal oxide/carbon composite anode and ionic liquid electrolyte for the lithium-ion battery. *Journal of Applied Electrochemistry* **2011,** *41* (11), 1261-1267.

83.   Lee, K.-H.; Song, S.-W., One-Step Hydrothermal Synthesis of Mesoporous Anatase TiO2 Microsphere and Interfacial Control for Enhanced Lithium Storage Performance. *Acs Applied Materials & Interfaces* **2011,** *3* (9), 3697-3703.

84.   Plashnitsa, L. S.; Kobayashi, E.; Okada, S.; Yamaki, J.-i., Symmetric lithium-ion cell based on lithium vanadium fluorophosphate with ionic liquid electrolyte. *Electrochimica Acta* **2011,** *56* (3), 1344-1351.

85.   Matsumoto, H.; Yanagida, M.; Tanimoto, K.; Nomura, M.; Kitagawa, Y.; Miyazaki, Y., Highly conductive room temperature molten salts based on small trimethylalkylammonium cations and bis (trifluoromethylsulfonyl) imide. *Chemistry Letters* **2000,** *29* (8), 922-923.

86.   Bhatt, A. I.; May, I.; Volkovich, V. A.; Hetherington, M. E.; Lewin, B.; Thied, R. C.; Ertok, N., Group 15 quaternary alkyl bistriflimides: ionic liquids with potential application in electropositive metal deposition and as supporting electrolytes. *Journal of the Chemical Society, Dalton Transactions* **2002,** (24), 4532-4534.

87.   Howlett, P. C.; MacFarlane, D. R.; Hollenkamp, A. F., High lithium metal cycling efficiency in a room-temperature ionic liquid. *Electrochemical and solid-state letters* **2004,** *7* (5), A97-A101.

88.   Ishikawa, M.; Sugimoto, T.; Kikuta, M.; Ishiko, E.; Kono, M., Pure ionic liquid electrolytes compatible with a graphitized carbon negative electrode in rechargeable lithium-ion batteries. *Journal of Power Sources* **2006,** *162* (1), 658-662.

89.   Holzapfel, M.; Jost, C.; Novak, P., Stable cycling of graphite in an ionic liquid based electrolyte. *Chemical Communications* **2004,** (18), 2098-2099.

90.   Tsunashima, K.; Yonekawa, F.; Sugiya, M., Lithium Secondary Batteries Using a Lithium Nickelate-Based Cathode and Phosphonium Ionic Liquid Electrolytes. *Electrochemical and solid-state letters* **2009,** *12* (3), A54-A57.

91.   Plashnitsa, L. S.; Kobayashi, E.; Okada, S.; Yamaki, J.-i., Symmetric lithium-ion cell based on lithium vanadium fluorophosphate with ionic liquid electrolyte. *Electrochimica Acta* **2011,** *56* (3), 1344-1351.

92.   Seki, S.; Kobayashi, Y.; Miyashiro, H.; Ohno, Y.; Mita, Y.; Usami, A.; Terada, N.; Watanabe, M., Reversibility of lithium secondary batteries using a room-temperature ionic liquid mixture and lithium metal. *Electrochemical and solid-state letters* **2005,** *8* (11), A577-A578.

93.   Egashira, M.; Tanaka-Nakagawa, M.; Watanabe, I.; Okada, S.; Yamaki, J.-i., Charge‚Äìdischarge and high temperature reaction of LiCoO2 in ionic liquid electrolytes based on cyano-substituted quaternary ammonium cation. *Journal of Power Sources* **2006,** *160* (2), 1387-1390.

94.   Sato, T.; Maruo, T.; Marukane, S.; Takagi, K., Ionic liquids containing carbonate solvent as electrolytes for lithium ion cells. *Journal of Power Sources* **2004,** *138* (1), 253-261.

95.   Lane, G. H.; Best, A. S.; MacFarlane, D. R.; Forsyth, M.; Bayley, P. M.; Hollenkamp, A. F., The electrochemistry of lithium in ionic liquid/organic diluent mixtures. *Electrochimica Acta* **2010,** *55* (28), 8947-8952.

96.   Bayley, P. M.; Lane, G. H.; Rocher, N. M.; Clare, B. R.; Best, A. S.; MacFarlane, D. R.; Forsyth, M., Transport properties of ionic liquid electrolytes with organic diluents. *Physical Chemistry Chemical Physics* **2009,** *11* (33), 7202-7208.

97.   Yoshizawa-Fujita, M.; MacFarlane, D. R.; Howlett, P. C.; Forsyth, M., A new Lewis-base ionic liquid comprising a mono-charged diamine structure: A highly stable electrolyte for lithium electrochemistry. *Electrochemistry Communications* **2006,** *8* (3), 445-449.

98.   Macfarlane, D. R.; Forsyth, M.; Howlett, P. C.; Pringle, J. M.; Sun, J.; Annat, G.; Neil, W.; Izgorodina, E. I., Ionic liquids in electrochemical devices and processes: managing interfacial Electrochemistry. *Accounts of Chemical Research* **2007,** *40* (11), 1165-1173.

99.   MacFarlane, D. R.; Pringle, J. M.; Howlett, P. C.; Forsyth, M., Ionic liquids and reactions at the electrochemical interface. *Physical Chemistry Chemical Physics* **2010,** *12* (8), 1659-1669.

100.   Matsumoto, H.; Sakaebe, H.; Tatsumi, K.; Kikuta, M.; Ishiko, E.; Kono, M., Fast cycling of Li/LiCoO2 cell with low-viscosity ionic liquids based on bis(fluorosulfonyl)imide [FSI]. *Journal of Power Sources* **2006,** *160* (2), 1308-1313.

101.   Wang, Y.; Zaghib, K.; Guerfi, A.; Bazito, F. F.; Torresi, R. M.; Dahn, J., Accelerating rate calorimetry studies of the reactions between ionic liquids and charged lithium ion battery electrode materials. *Electrochimica Acta* **2007,** *52* (22), 6346-6352.

102.   Vijayaraghavan, R.; Surianarayanan, M.; Armel, V.; MacFarlane, D.; Sridhar, V., Exothermic and thermal runaway behaviour of some ionic liquids at elevated temperatures. *Chemical Communications* **2009,** (41), 6297-6299.

Chapter 2. Experimental

2-1 Cyclic Voltammetry (CV)

Among the many important physical and chemical properties, characterising the electrochemical window (EW), diffusivity of each ion and the ionic conductivity are especially important for battery electrolyte applications. The EW is usually obtained by cyclic voltammetry and consideration of IR drop caused by electrode, scanning rate and cut off current density is important. Moisture content in ILs is also very important and needs to be considered when comparing ILs, in fact, the sensitivity of CV to moisture can be used to determine moisture content of ILs.[1]

Reference electrode

A pseudo-reference electrode (or a quasi-reference electrode) is a reference electrode for which electrochemical reaction is not specifically known. When a pseudo-reference is used for electrochemical measurement, the real potential of an electrochemical reaction cannot be determined without comparing to a standard reference electrode. Furthermore, the pseudo-reference metal may be sensitive to, and has the potential to generate, unwanted side reactions in the target solution.[2]

Snook, *et al.*[3] reported a Ag |Ag$^+$ reference electrode in a C$_4$mpyrNTf$_2$ ionic liquid which showed stable and reproducible performance. A number of ionic liquids were studied and junction potentials were determined and compared with the theoretical value obtained from Laity's formula.[3]

$$\Delta Ej = \left(\frac{RT}{F}\right) \left(\frac{\Lambda_{13} - \Lambda_{23}}{z_1 \Lambda_{13} - z_2 \Lambda_{23}}\right) \ln\left(\frac{z_1 \Lambda_{13}}{z_2 \Lambda_{23}}\right) \quad \text{(2-1)}$$

Where Λ is an equivalent conductivity (S.cm^{-1}), z is ionic charge number, the subscripts 1 and 2 denote the ions of the target ionic liquid and the reference electrode respectively and 3 is the common ion, R is the gas constant (in J.mol^{-1}.K^{-1}), T is the temperature (K) and F is the Faraday constant as A.sec.mol^{-1}. [3]

It was found that the measured junction potential value of the ionic liquids were lower than the calculated values. It was postulated that when an ionic liquid is used as a reference

electrode, the ionic mobility of an ion of the reference electrode solution and of the target liquid are similar at the liquid junction, where mixtures are formed, while Laity's formula assumed that ionic mobility remains that of the bulk electrolyte.[3]

 To develop a stable and reproducible reference electrode for further research, a part of Snook, *et al*.'s investigation was duplicated and adapted for the DCA system to determine if using a DCA based reference electrode in this research was possible. The junction potential between DCA and NTf$_2$ was also measured and compared with the calculated value.

Preparation

The basic methodology followed was similar to the method suggested by Snook, et al [3] except for the detailed size of the reference electrode. All preparation and electrochemical measurements were performed in an Argon filled glove box. As received C$_4$mpyrNTf$_2$ and C$_4$mpyrDCA (purchased from Merck™) was mixed with 10mM of silver trifluoromethanesulfonate (AgTf, Aldrich™) at 50 ^{o}C for 3 hours and used as a solution in the reference electrode. Glass compartments with an ultra-fine glass frit saltbridge at one end were filled with these solutions to prepare a reference electrode as shown in figure 2-1.
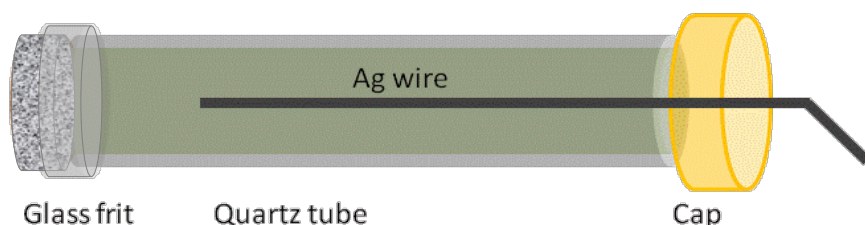

Figure2-1 Shape of the reference electrode

A Bis(cyclopentadienyl)iron(II) (ferrocene, Aldrich™) was dissolved into each IL (C$_4$mpyrNTf$_2$ and C$_4$mpyrDCA) at 50mM concentration and stirred for 3 hours at 50 ^{o}C to measure the Fc |Fc$^+$ standard potential in each IL environment. All electrochemical measurements used the µAutolab type III potentiostat/galvanostat (Ecochemie, Netherlands) with GPES manager v4.9 program at room temperature. The scan rate was 20 mV.s^{-1} unless otherwise stated. The conductivity measurement to calculate the junction potential was performed with a two-electrode platinum wire 'dip' cell using a Agilent 4284A impedance analyser and HP impedance analyser Labview 7.1 software (National Instruments) from 20 Hz ~ 400 KHz.
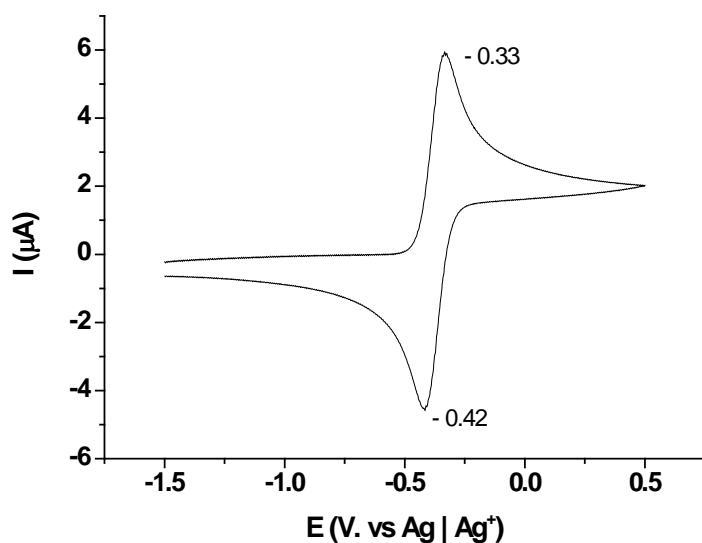
Junction Potential

Figure 2-2 Fc |Fc$^+$ redox couple in C$_4$mpyrNTf$_2$

 Figure 2-2 shows a Fc |Fc$^+$ redox couple CV at the room temperature. Since Fc |Fc$^+$ redox potential is affected by the type of IL,[4-5] the measured potential was adjusted by the reported value as per Torriero *et al.*[4] The Ag |Ag$^+$ redox potential E$_0$ (which is the average of the potential of the forward peak and the reverse peak) in 10mM AgTf : C$_4$mpyrNTf$_2$ is 0.37V vs. Fc |Fc$^+$. This result deviates by 4% from the result reported by Snook, *et al.*[3] which may be due to the accuracy of the concentration and the temperature control in these experiments.
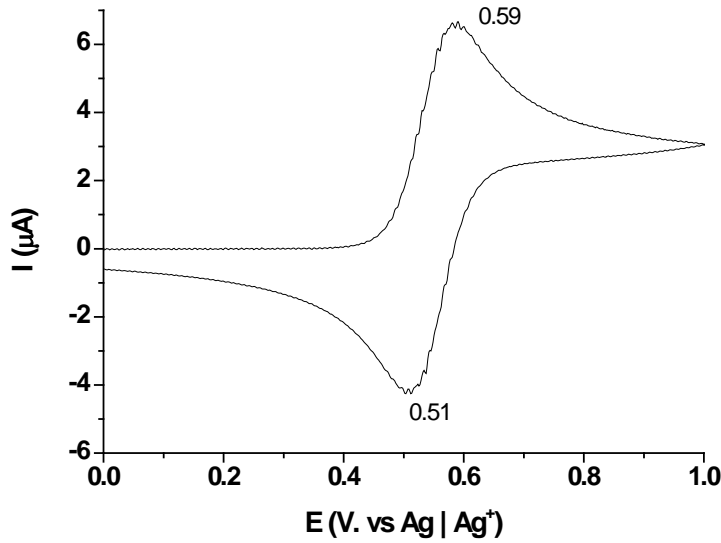
Figure 2-3 Fc |Fc⁺ redox couple in C$_4$mpyrDCA

When C$_4$mpyrDCA is used as the reference electrode solution and bulk electrolyte, the Fc |Fc⁺ reversible CV shows a Ag | Ag⁺ redox potential of E_0 = -0.55 vs. Fc | Fc⁺.

If both ionic liquids in the reference electrode and the target IL have the same cation or the same anion, then the junction potential ΔEj between the salt bridge can be calculated directly from the molar conductivity (Equation 2-1).

The ionic charges of both cation and anion in C$_4$mpyrNTf$_2$ and C$_4$mpyrDCA are unity so equation (2-1) can be simplified to equation (2-2) below and the junction potential of the two different ILs becomes only the function of the ionic conductivities.

$$\Delta Ej = \left(\frac{RT}{F}\right) \ln\left(\frac{\Lambda_{13}}{\Lambda_{23}}\right) \quad (2\text{-}2)$$

The measured conductivity of C$_4$mpyrNTf$_2$ and C$_4$mpyrDCA at 25 °C is 3 mS.cm⁻¹ and 10 mS.cm⁻¹ respectively. Thus, the calculated junction potential is around 30 mV.

$$\left(\Delta Ej = \left(\frac{RT}{F}\right) \ln\left(\frac{\Lambda_{13}}{\Lambda_{23}}\right) = \left(\frac{8.3145 \ (J.sec/mol.K) * \ 298 \ (K)}{96485 \ (A.sec/mol)}\right) \ln\left(\frac{10}{3}\right) = 0.030 \ V \quad (2\text{-}3)\right.$$

The junction potential measurement was performed in two ways. First using an NTf_2 based reference electrode to measure DCA and then vice versa and the results are shown in figure 2-4 and figure 2-5.

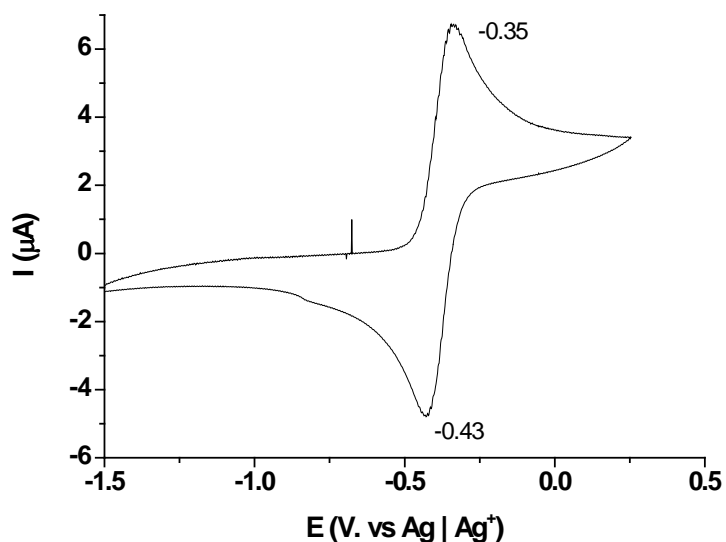**Figure 2-4** Fc |Fc$^+$ CV in C$_4$mpyrDCA using Ag |Ag$^+$ reference electrode in C$_4$mpyrNTf$_2$

E_0 (vs. Fc |Fc$^+$) = 0.39V

ΔEj = 0.39V - 0.37V = 20mV
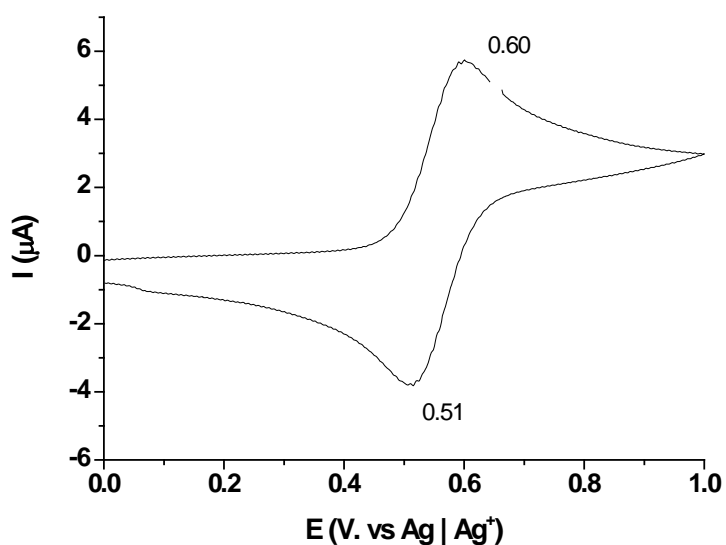
Figure 2-5 Fc |Fc$^+$ CV in C$_4$mpyrNTf$_2$ using Ag |Ag$^+$ reference electrode in C$_4$mpyrDCA

E_0 (vs. Fc | Fc$^+$) = - 0.56V

ΔEj = - 0.56V – (- 0.55V) = 10 mV

In both cases (each case measured twice) the measured junction potential value was not more than 20 mV, which is lower than the calculated value of 30 mV and is similar to the value reported by Snook, *et al.* [3] for a C$_4$mpyrBOB: C$_4$mpyrNTf$_2$ system. The similar junction potential between C$_4$mpyrNTf$_2$:C$_4$mpyrDCA and the C$_4$mpyrBOB: C$_4$mpyrNTf$_2$ system[3], even though the DCA anion is smaller than the BOB anion, suggests that the surrounding environment of the solvated Fc in different ILs alters the E_0 values of the Fc | Fc$^+$ redox couple, as recently reported. [4-5] If soluble in the IL system, decamethylferrocene (DmFc) has been shown to be less susceptible to solvent effects than Fc. [4-5]

2-2 Symmetric coin cell

Li symmetrical cells (2032 coin cells) were used to study the cell cycling ability and to investigate the Li metal surface. Li metal was cleaned with n-Hexane or n-Pentane to remove impurities and oxides, and cut into 10mm diameter discs. A separator and a Ni plate and a Ni flat spring were used for the symmetrical cell. The structure of the coin cell is presented in Figure 2-6. In most cases, 800 µL of electrolyte was used in all cells. All coin cells were placed in an oven at 50 ^{o}C to insure wetting of the separator and electrodes. Cell cycling and electrochemical impedance spectroscopy (EIS) measurements were performed using a Solartron™ 1470 and a Solartron™ 1255 frequency response analyser. The cycling conditions were typically 0.1 mA.cm^{-2} constant current for 16 minutes charge and discharge (i.e., 0.096 C.cm^{-2} per polarisation step). Z-plot (ver. 3.2c)/Z-view (ver. 2.9b) software was used to acquire and fit the EIS data. The data showed 4 to 28% fitting errors for each assigned resistance.

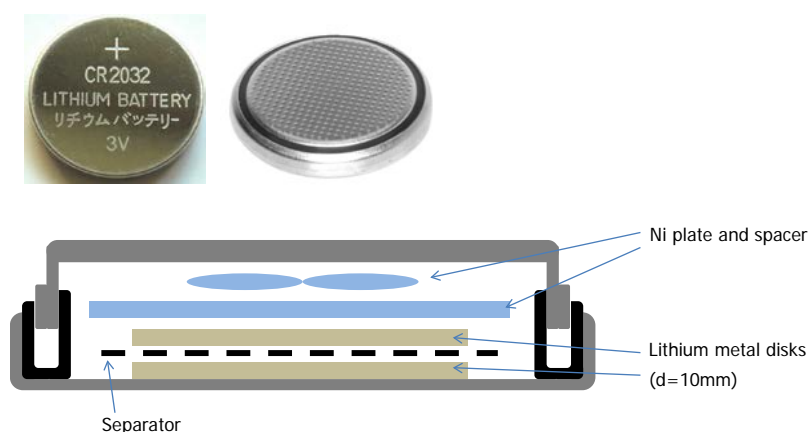**Figure 2-6** Coincell used for this research (upper) and the internal structure (lower)

A number of EIS models were applied in this research. Figure 2-7 shows the fitting results obtained for various equivalent circuits applied to EIS data acquired from a typical Li symmetrical cell.
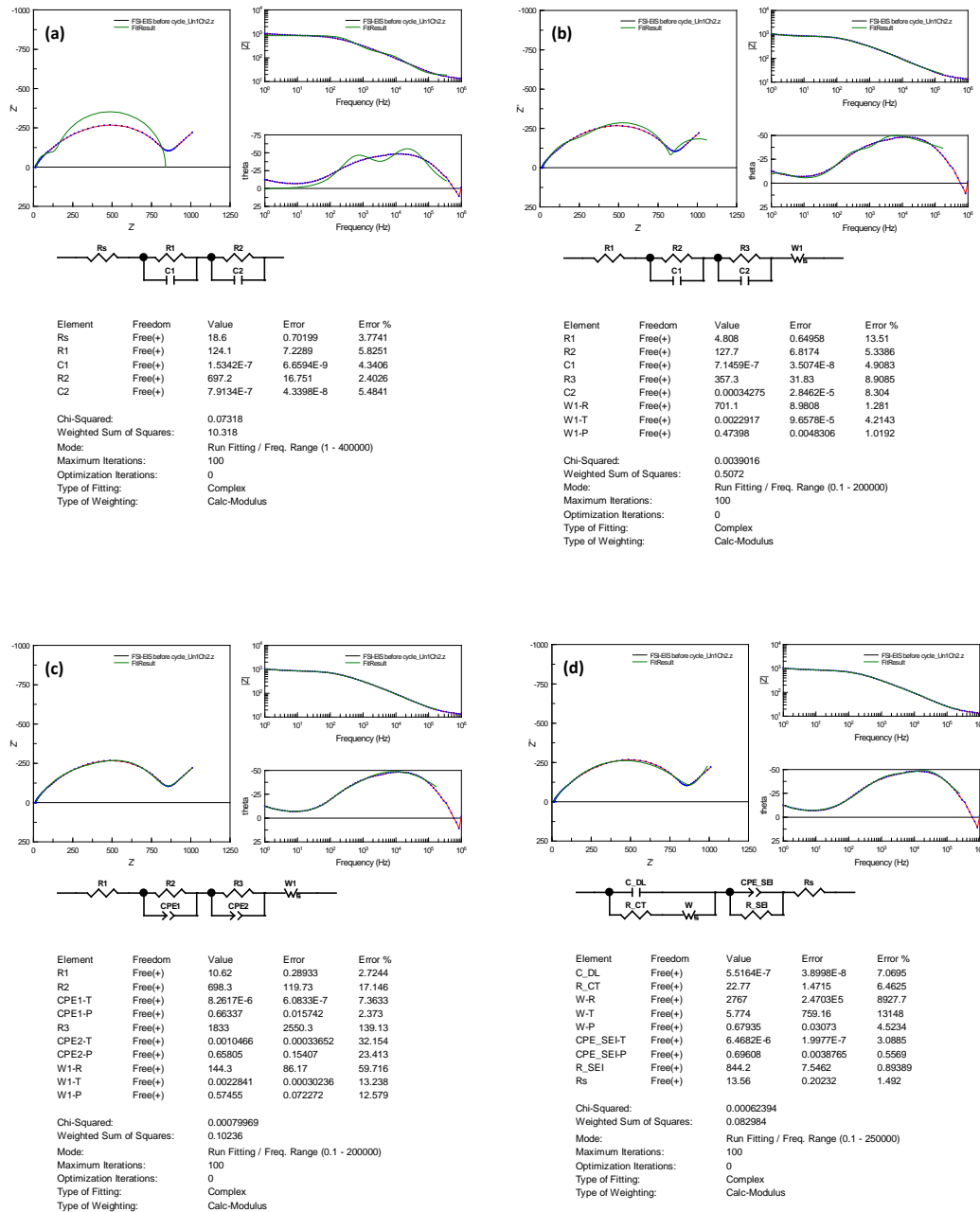

Figure 2-7 Different fitting results for EIS data acquired from a Lithium symmetrical cell with a LiFSI and C$_3$mpyrFSI electrolyte.

Figure 2-7 (a) consists of simplest RC model. Since it only consists of solution resistance and surface impedances, it is easy to apply each fitting component to the conceptual physical status in the cell. However, since the real cell has diffusion effects and the surface is not ideal, the fitting result does not match the EIS data well.

Figure 2-7(b) incorporates a Warburg diffusion component to fit the low frequency region and the fitting results are better than (a). Figure 2-7(c) uses constant phase elements instead of capacitors and shows quite nice fitting results.

Figure 2-7(d) was used to model the data to determine the charge transfer resistance and SEI resistance, as reported by Lewandowski et al. [6] and Lane et al. [7] This model assumes an evenly distributed SEI is formed on the surface of the lithium metal. The benefit of this model is that it is simple to determine the resistances by simplifying the SEI behaviour using a constant phase element. The element C-DL is double layer capacitance, R_CT is for the charge transfer resistance, W is a Warburg diffusion element, R_SEI is the bulk resistance of the SEI, CPE_SEI is a constant phase element denoting the pseudo-capacitance of the SEI, and Rs is the resistance of the solution. [7-8] In this research, specific models were chosen for each case.

2-3 Spectroscopy

Characterisation of the RTIL interactions with the electrode surface including surface analysis requires different techniques such as X-ray diffraction (XRD), X-ray photoelectron spectroscopy (XPS) or Fourier transform infrared spectroscopy (FT-IR) /Raman spectroscopy. Sutto, et al., [9] demonstrated the intercalation of imidazolium cations and lithium ion into a graphite electrode using XRD. C_2mim cation does not intercalate into graphite layers while the C_4mim and C_3dmim cations do intercalate. In their report, comparing the 2θ position of C_2mim with graphite, C_4mim and C_3dmim exhibit a different peak at lower 2θ values, which indicates cation intercalation into graphite. The theoretical volumetric expansion of graphite during intercalation of lithium or other ion can be obtained from the d (100 plane). [9]

Recently, Hashimoto, et al. [10] investigated $C_4mimDCA$ using XPS and the results. With depth profiling research, they suggest that the surface of $C_4mimDCA$ is covered by ~1.7 x 10^{14} molecules.cm^{-2} of esters and/or carboxylic acids. [10]

In this study a Perkin Elmer™ Spectrum 400 FT-IR/FT-NIR Spectrometer with Spectrum ver. 6.3.4 software was used to record FT-IR spectra and a Perkin Elmer™ Ramanstation 400F with Spectrum ver. 10.03.06.0100 was used to acquire Raman spectra. An ATR cell under argon was used for FT-IR prepared in an argon filled glove box.

2-4 Diffusion NMR (Nuclear Magnetic Resonance)

The ion self-diffusion properties of each species including the dissolved salt ion can be determined using diffusion NMR when each ion has different exclusive atoms. For example, in C_2mimFSI, hydrogen and carbon atoms are only located in the C_2mim cations while fluoride atoms are only present in the FSI anion, which makes the diffusivity determination for each ionic species possible. For the case of C_2mimDCA, the absence of protons in the DCA anion can be used to determine the diffusivity of each ion species.

Since conductivity depends on the temperature, it should ideally follow the Arrhenius equation, however, sometimes conductivity temperature dependency follows a modified Arrhenius equation, or Vogel-Tamann-Fulcher (VTF) – equation as follows:

$$\sigma(T) = A\, T^{-\frac{1}{2}}\, e^{-\frac{B}{T_0 - T}} \qquad\qquad (2\text{-}4)$$

where A is proportional to the ion concentration and B is called the pseudo activation energy. T_0 is usually close to Tg.

When the information is combined with ion self-diffusivity and bulk conductivity, the contribution of each ion to the conductivity can be calculated and the degree of ion dissociation in the RTIL can be estimated from the Nernst–Einstein equation:

$$\Lambda = \frac{N_A e^2 (D_+ + D_-)}{kT} = \frac{F^2 (D_+ + D_-)}{RT} \qquad\qquad (2\text{-}5)$$

where N_A is Avogadro's number, e is the electric charge on each ionic carrier, D is the self-diffusion coefficient of the anion (-) and cation (+), k is Boltzmann's constant, F is Faraday's constant, R the universal gas constant and T is the absolute temperature. In salt mixed system, the D values are contributed the weight averages of each ion species and can be modified into the equation below;

$$\Lambda = \frac{F^2}{RT}\left(2\sum D_i x_i\right) \qquad\qquad (2\text{-}6)$$

Where D_i is the self-diffusion coefficient of each ion and x_i is the mol fraction of each ion.

Comparing the molar conductivity calculated with this equation and bulk ionic conductivity, the dissociation degree of the RTIL can be obtained. Because the measured ion dissociation degree is a key property indicating the overall conductivity contributed by each ion, Bayley,

et al. [11] calculated the dissociation parameter for $C_3mpyrNTf_2$ containing LiTFSI with different additive environments.[11]

 In this study, pulse-field gradient stimulated echo (PFG-STE) diffusion measurements for ^{1}H, [7]Li and ^{19}F were performed on a Bruker 300 MHz Ultrashield with Avance I console utilizing a Diff30 diffusion probe and GREAT60 amplifier for ^{1}H for C_4mpyr^+, [7]Li and ^{19}F, following the method described by Bayley *et al.*[11] A Bruker 500 MHz Ultrashield with Avance I console was used for ^{13}C diffusion measurements.

References

1.   Ohno, H.; Yoshizawa, M.; Mizumo, T., Ionic Conductivity. In *Electrochemical Aspects of Ionic Liquids*, Hiroyuki, O., Ed. 2005; pp 75-81.

2.   Katayama, Y., General Techniques. In *Electrochemical Aspects of Ionic Liquids*, Hiroyuki, O., Ed. 2005; pp 25-34.

3.   Snook, G. A.; Best, A. S.; Pandolfo, A. G.; Hollenkamp, A. F., Evaluation of a Ag vertical bar Ag+ reference electrode for use in room temperature ionic liquids. *Electrochemistry Communications* **2006,** *8* (9), 1405-1411.

4.   Torriero, A. A. J.; Sunarso, J.; Howlett, P. C., Critical evaluation of reference systems for voltammetric measurements in ionic liquids. *Electrochimica Acta* **2012,** *82*, 60-68.

5.   Torriero, A. A. J.; Howlett, P. C., Ionic liquid effects on the redox potential of ferrocene. *Electrochemistry Communications* **2012,** *16* (1), 84-87.

6.   Lane, G. H.; Best, A. S.; MacFarlane, D. R.; Forsyth, M.; Bayley, P. M.; Hollenkamp, A. F., The electrochemistry of lithium in ionic liquid/organic diluent mixtures. *Electrochimica Acta* **2010,** *55* (28), 8947-8952.

7.   Lewandowski, A.; Swiderska-Mocek, A., Properties of the lithium and graphite-lithium anodes in N-methyl-N-propylpyrrolidinium bis(trifluoromethanesulfonyl)imide. *Journal of Power Sources* **2009,** *194* (1), 502-507.

8.   Lane, G.; Best, A.; MacFarlane, D.; Forsyth, M.; Hollenkamp, T.; Begic, S., Lithium battery electrolytes based on the ionic liquid N-methyl-N-butylpyrrolidinium dicyanamide:compatibility with different electrode materials including lithium metal, Li4Ti5O12, LiFePO4 and LiCoO2. CSIRO, Monash University: Clayton, VIC, 2010.

9.   Sutto, T. E.; Duncan, T. T.; Wong, T. C., X-ray diffraction studies of electrochemical graphite intercalation compounds of ionic liquids. *Electrochimica Acta* **2009,** *54* (24), 5648-5655.

10.   Hashimoto, H.; Ohno, A.; Nakajima, K.; Suzuki, M.; Tsuji, H.; Kimura, K., Surface characterization of imidazolium ionic liquids by high-resolution Rutherford backscattering spectroscopy and X-ray photoelectron spectroscopy. *Surface Science* **2010,** *604* (3-4), 464-469.

11.   Bayley, P. M.; Lane, G. H.; Rocher, N. M.; Clare, B. R.; Best, A. S.; MacFarlane, D. R.; Forsyth, M., Transport properties of ionic liquid electrolytes with organic diluents. *Physical Chemistry Chemical Physics* **2009,** *11* (33), 7202-8.

Chapter 3. Studies of *bis*(fluorosulfonyl)imide (FSI) ionic liquids

Introduction:

This chapter describes the properties and performance of Li metal batteries incorporating pyrrolidinium FSI ionic liquid electrolytes. These ionic liquids exhibit higher conductivities and diffusivities than the corresponding *bis*(trifluoromethanesulfonyl)imide (TFSI or NTf$_2$) compounds, and have been regarded as potential electrolytes for lithium metal batteries. A number of publications have reported on its performance on LiCoO$_2$ or LiFePO$_4$, or other cathode materials.

Due to its high viscosity and reduced conductivity a relatively low Li salt concentration has typically been employed as an optimal composition for lithium cycle-ability, including rate capability, in organic liquid based electrolytes. It is also well known that most commercial lithium ion batteries use about 0.8 to 1.2 M Li salt concentration (in a carbonate based organic liquid electrolyte) to maximise cell performance by optimising the electrolyte conductivity and viscosity. However, the optimal Li salt concentration in an ionic liquid electrolyte, its influence on the lithium transport mechanism and, ultimately, cell performance is not yet fully understood.

One interesting aspect of this FSI anion is, like TFSI or other asymmetric anions, it exhibits conformational cis- and trans-isomerism. A number of publications have described the conformational equilibrium of TFSI or FSI anions in ionic liquids and reported its temperature dependence. However, there are no reports of its conformational isomerism in the presence of the lithium ion.

In this chapter, one publication investigates the performance of varying Li salt concentration in a pyrrolidinium FSI ionic liquid electrolytes in Li | LiCoO$_2$ cells, determining rate capability, cycling stability and the lithium transference number. The dependency of the electrochemical performance of the electrolyte on the Li salt concentration is investigated to determine the optimal salt concentration and its relationship to cell performance.

Another publication demonstrates the conformational change of the FSI anion in pyrrolidinium FSI ionic liquids in the presence of varying lithium salt concentrations, using spectroscopic and physical measurements to understand its influence on the Li ion transport mechanism.

Monash University

Declaration for Thesis Chapter 3

Declaration by candidate

In the case of Chapter 3, the nature and extent of my contribution to the work was the following:

Nature of contribution	Extent of contribution (%)
Cyclic Voltammetry, transference number test, electrochemical impedance spectroscopy, coincell cycling, conductivity, viscosity, density, DSC, 1D and diffusion NMR, FT-IR and Raman spectroscopy, solution preparation and electrode manufacture. Data analysis, manuscript writing.	90

The following co-authors contributed to the work. Co-authors who are students at Monash University must also indicate the extent of their contribution in percentage terms:

Name	Nature of contribution	Extent of contribution (%) for student co-authors only
Douglas MacFarlane	Publication 3.1, 3.2: Project initiation, key ideas, editing, experiment planning.	
Maria Forsyth	Publication 3.1, 3.2: Project initiation, key ideas, editing, experiment planning.	
Patrick Howlett	Publication 3.1, 3.2: Project initiation, key ideas, editing, experiment planning.	
Adam Best	Publication 3.1, 3.2: Project initiation, key ideas, editing, experiment planning.	

Candidate's Signature	Hyungook (Martin) Yoon	Date 2/06/2013

Declaration by co-authors

The undersigned hereby certify that:

(1) the above declaration correctly reflects the nature and extent of the candidate's contribution to this work, and the nature of the contribution of each of the co-authors.

(2) they meet the criteria for authorship in that they have participated in the conception, execution, or interpretation, of at least that part of the publication in their field of expertise;

(3) they take public responsibility for their part of the publication, except for the responsible author who accepts overall responsibility for the publication;

(4) there are no other authors of the publication according to these criteria;

(5) potential conflicts of interest have been disclosed to (a) granting bodies, (b) the editor or publisher of journals or other publications, and (c) the head of the responsible academic unit; and

(6) the original data are stored at the following location(s) and will be held for at least five years from the date indicated below:

Location(s) | **CSIRO Energy Technology, Clayton, Victoria, Australia**

[Please note that the location(s) must be institutional in nature, and should be indicated here as a department, centre or institute, with specific campus identification where relevant.]

Signature 1	D.R.MacFarlane		**Date** 21/6/13
Signature 2	M.Forsyth		24/6/13
Signature 3	P.C.Howlett		24/6/13
Signature 4	A.S.Best		27/06/13

Fast charge/discharge of Li metal batteries using an ionic liquid electrolyte

*H. Yoon,[a,b] P. C. Howlett,[c] A. S. Best,[*b] M. Forsyth,[c] and D. R. MacFarlane[a]*

[a]School of Chemistry, Monash University, Victoria 3800, Australia

[b]Commonwealth Scientific and Industrial Research Organisation (CSIRO), Division of Energy Technology, Bayview Ave., Clayton, Victoria 3169, Australia

E-mail: ▮▮▮▮▮▮▮▮▮▮

[c]ARC Centre of Excellence for Electromaterials Science (ACES), Institute for Frontier Materials (IFM), Deakin University, Burwood, Victoria 3125, Australia

Abstract

Because of their potentially superior safety characteristics, room temperature ionic liquids (RTILs or ILs) have been vigorously researched to replace current commercial lithium battery electrolytes, which are based on volatile and flammable organic carbonates. However, relatively poor battery performance, which is a consequence of the higher viscosity and lower conductivity of these materials, has prevented them becoming mainstream electrolytes for commercial lithium batteries.

Amongst various RTILs, those containing the bis(fluorosulfonyl)imide (FSI) anion exhibit high conductivities and diffusivities, making them interesting potential electrolytes for lithium metal batteries. Here, we evaluate the electrochemical stability, lithium electrochemistry, and Li^+ transference numbers of FSI-based ionic liquid electrolytes intended for use in rechargeable Li metal batteries. We show that ILs containing high concentrations of lithium, up to 3.2 mol.kg^{-1} in C_3mpyr FSI, have excellent rate capability (higher than that of standard battery electrolytes) with both the lithium metal electrode and $LiCoO_2$ cathode, in spite of their significantly higher viscosities and lower conductivities.

This unusual behaviour is ascribed to the concomitant increase in transference number with increasing Li-salt concentration.

1. Introduction

The challenge to develop suitable electrolytes having wide electrochemical windows and high Li^+ transference number for lithium-ion batteries has become increasingly important as applications require increases in capacity, charging rate and safety.[1] Room Temperature Ionic Liquids (RTILs or ILs) are potential candidates for electrolytes. These materials came to prominence in the late 1990's as solvents suitable for electrochemical reactions. Over the last 15 years, there have been many studies on ILs for battery applications, as evidenced by significant numbers of patents and publications.[2-3] These materials have numerous features that should lend themselves to use in high energy lithium batteries: negligible volatility, relatively high decomposition temperatures when compared to traditional lithium battery electrolytes, high ionic conductivity and wide electrochemical windows.[4-6]

Of all anions to date, the sulfonylimide family are the most studied, and show, in general, the best electrochemical performance. ILs containing the bis(fluorosulfonyl)imide (FSI) anion exhibit higher conductivities and diffusivities than the corresponding bis(trifluoromethanesulfonyl)imide (TFSI or NTf_2) compounds, thereby generating interest as potential electrolytes for lithium metal batteries.[7-16] However, there are several aspects of concern, including high temperature stability and corrosion.[17-19]

The Li salt concentration in an IL is important for charging and discharging of Li batteries, because in general, while increasing the Li salt concentration increases the viscosity and decreases the conductivity, it also increases the amount of lithium ion available in the IL.[20] Seki et al. studied the effect of LiTFSI salt concentrations (from 0 to 0.8 mol.kg^{-1}) on the performance of 1,2-dimethyl-3-propylimidazolium bis(trifluoromethylsulfonyl)imide

(DMPImTFSI). They measured conductivity, viscosity, cell electrochemical impedance spectra (EIS) and the rate capability of a LiCoO$_2$ cathode based cell, and found that the optimum salt concentration was 0.4 mol.kg^{-1}.[20]

In most commercial lithium-ion batteries, a concentration of 0.8 to 1.2 M Li salt in organic liquid electrolyte is used to maximise cell performance by achieving a balance between conductivity and viscosity. Nyman et al. confirmed this optimum concentration effect in an organic liquid electrolyte by measuring both conductivities and transference numbers.[21]

Following Zhou et al.'s electrochemical and physicochemical studies on *N*-propyl-*N*-methylpyrrolidinium bis(fluorosulfonyl)imide (C$_3$mpyr FSI) and *N*-butyl-*N*-methylpyrrolidinium bis(fluorosulfonyl)imide (C$_4$mpyr FSI),[13] Paillard et al. added different amounts of LiFSI salts (mole ratios from 0 to 0.6, where a mole ratio of 0.6 LiFSI : 0.4 C$_4$mpyr is equivalent to an LiFSI concentration of 4.9 mol.kg^{-1}) to C$_4$mpyr FSI and performed physical and electrochemical studies.[14] Unlike previous reports showing that additional lithium salts increased the cathodic electrochemical stability in imidazolium-based TFSI ILs,[22-23] increasing the amount of LiFSI salts in C$_4$mpyr FSI decreased the cathodic stability in their study; this was attributed to the high level of impurities in the commercial grade LiFSI salt used.[14] They also demonstrated that the FSI anion (in contrast to the TFSI anion) could establish a solid electrolyte interphase (SEI) on graphite anodes without the need for additives. FSI may also allow the exploitation of the high voltage plateaus of materials such as LiNi$_{0.5}$Mn$_{1.5}$O$_2$ and LiNi$_{0.33}$Mn$_{0.33}$Co$_{0.33}$O$_2$, leading to higher energy lithium-ion batteries.[24-26] However, they did not explain the effect of lithium concentration on electrochemical and battery properties (other than the increased electrochemical window).

Best and Bhatt studied various lithium salts in C$_3$mpyrFSI at concentrations ranging from 0.2 to 1 mol.kg^{-1}, and found that 0.5 mol.kg^{-1} LiBF$_4$ showed the widest electrochemical windows and Li symmetric cell stability.[15, 27] They also studied the lithium electrochemistry of the FSI

anion using cyclic voltammetry (CV) and EIS, and showed that these electrolytes can be used to cycle a Li metal anode.[15, 27]

In this work, we examine the effects of salt concentration on various electrochemical properties of C_3mpyrFSI. In cycling lithium-metal symmetric cells as a function of lithium salt concentration, we show remarkably low cycling over-potentials at various current densities. We demonstrate that because of the C_3mpyr FSI IL's stability against lithium metal, the Bruce and Vincent method for measuring transference numbers can be effectively used to determine t_{Li}^+ without complications from the SEI layer. Finally, we show that ionic liquids based on C_3mpyr FSI with especially high concentrations of LiFSI are able to effectively cycle batteries consisting of lithium anodes and $LiCoO_2$ cathodes at high charge-discharge rates.

2. Experimental

Materials:

N-propyl-*N*-methylpyrrolidinium bis(fluorosulfonyl)imide (C_3mpyrFSI, purity > 99.9%) and lithium bis(fluorosulfonyl)imide (LiFSI, purity > 99.5%) were both sourced from Suzhou Fluolyte Co., Ltd., China. Moisture contents of all electrolytes were (< 20 ppm, as determined via Karl Fisher titration (Metrohm). Lithium metal was sourced from China Energy Lithium Co., Ltd. (purity > 99.9%).

Electrolytes for these experiments were prepared by adding LiFSI to C_3mpyrFSI IL and stirring for 24 hours at room temperature in an Ar- filled glove box. Table 1 shows the concentration of each electrolyte and molar ratio of each ion in solution. The highest Li salt concentration used in these experiments was 3.2 mol.kg^{-1}, which has an ion ratio of 1 Li$^+$: 1 C_3mpyr$^+$: 2 FSI$^-$.

Table 1. Salt concentrations in each electrolyte

LiFSI conc. in IL (mol.kg^{-1})	Molar ratio of each ions		
	Li$^+$	C$_3$mpyr$^+$	FSI$^-$
0 (neat IL)	0	0.50	0.50
0.8	0.10	0.40	0.50
1.6	0.17	0.33	0.50
2.4	0.21	0.29	0.50
3.2	0.25	0.25	0.50

Cyclic Voltammetry:

A 1 mm diameter Pt working electrode and a Pt wire counter electrode were employed for cyclic voltammetry and a 3 mm diameter Ni working electrode was also employed for comparison. The surface area (0.009 cm^{-2}) of the Pt electrode was obtained by measuring a bis(cyclopentadienyl)iron(II) (ferrocene, or Fc) Fc | Fc$^+$ redox peak currents determined using 5 mM Fc at scanning rates of 20, 50, 100 and 200 mV.sec^{-1}, and then applying the Randles-Sevcik equation.[28] The surface area of Ni working electrode was not measured but just calculated from the diameter. The reference electrode consisted of a silver wire immersed in a solution of 10 mM silver triflate (AgTf, 99.95+% purity, Aldrich) in *N*-butyl-*N*-methylpyrrolidinium bis(trifluoromethanesulfonyl)imide (C$_4$mpyr TFSI, Merck high purity specification, <100 ppm water, <100 ppm chloride) and separated from the main solution by a glass frit, as reported by Snook et al..[29] Therefore, the CV measurements were performed against Ag | Ag$^+$ reference potential and converted into Li | Li$^+$ redox potential. The potential was checked with a Fc | Fc$^+$ internal reference. The scan rate was 20 mV.s^{-1}. Measurements were obtained at 23 ± 3 °C. Potentiostatic control was provided by an Autolab Pgstat302 (Eco Chimie, Netherlands) controlled with GPES (Version 4.9.005) software.

Coin cell preparation:

CR2032 size lithium symmetric cells were prepared with 2 10 mm^2 diameter lithium discs and a Solupor 7P03A^{TM} separator (Lydall, Inc., UK) in an Ar-filled glove box. Cells were then stored for 24 hours at 50 °C.

LiCoO$_2$ electrodes consisted of 90 wt% LiCoO$_2$ (Nippon Chemical Industrial, Japan), 5 wt% carbon black (Shawinigan) and 5 wt% PVdF binder. Dry ingredients were ball milled together for 72 h, prior to the addition of the binder (dissolved in *N*-methylpyrrolidone) to form a slurry. The slurry was ball milled for a further 72 h prior to being spread onto aluminium foil using a 60 µm graded roller. Coated foils were allowed to dry overnight in a fume hood and then dried further in a vacuum oven at 100 °C for 72 h. The final LiCoO$_2$ loading was approximately 4.5 mg.cm^{-2}. LiCoO$_2$ cells were prepared with the prepared LiCoO$_2$ electrodes, Li discs and Solupor 7P03A^{TM} separators (50 μm thick, micro-porous polyethylene). All cells were then stored for 24 hours at 50 °C before cycling to allow for wetting. The specific capacities of the prepared electrodes were checked by making cells with a standard battery electrolyte (1M LiPF$_6$, EC:DMC=50:50 vol.%, Mitsubishi Chemical Co.).

Transference number:

Lithium symmetrical cells were used to determine the Li$^+$ transference number with the method described by Evans, Bruce, and Vincent.[30-31]

Cells were polarized at 25 °C with a constant voltage of 1.0 mV for 5 min. 10 min. 20 min. or 2 hours and the currents during the polarization were measured. The EIS spectra were measured before and after the polarization using a 1 mV perturbation. 24 hours recovery was allowed between each experiment. All experiments were conducted using a Solartron™ 1470 Battery test unit connected to a 1255B Frequency response analyser with Corrwave ver. 3.1c and Zplot ver. 3.1c.

Coin cell cycling:

Li | $LiCoO_2$ cells were charged to 4.2 V and discharged to 2.75 V at 0.1 C, 0.5 C, 1.0 C, 1.5 C, 2.0 C, 3.0 C, 4.0 C or 5.0 C constant currents to measure charge and discharge rate capability, and then cycled at 0.1 C at 25 °C on a Maccor Series 4000 instrument.

3. Results and Discussion

Cyclic Voltammetry:

Cyclic voltammograms (20 mV.sec^{-1} scan rate) are presented for LiFSI dissolved in C_3mpyrFSI at room temperature using mainly a Pt working electrode in figure 1.It was known that a Pt working electrode forms an alloy with lithium during the reduction of lithium[32] while there is no alloy formation when using a Ni working electrode, the CVs when using a Ni working electrode were also embedded in the figure 1(a) and 1(d) for a comparison purpose. In figure 1(a), the Li$^+$ reduction peak for 0.8 mol.kg^{-1} solution was observed at -3.77 V vs. Ag | Ag$^+$, and two distinct oxidation peaks were observed at -3.08 V and -2.08 V with the main Li stripping occurring at -3.08 V and successive Li under-potential deposition stripping and residual H_2O oxidation at higher potentials.[33]

When the salt concentration is increased to 1.6 mol.kg^{-1} (figure 1(b)) the Li$^+$ deposition peak moves to more negative potential, -3.87 V, while the corresponding Li stripping peak moves to more positive potential, -2.91V, because of decreasing ionic conductivity and increasing viscosity of the electrolyte. This trend persists at even higher solution concentrations, as shown in figure 1(c) and 1(d). Unlike Paillard et al., we do not observe a large parasitic current prior to Li plating (which had been ascribed to the purity of the LiFSI salt).[14] Figure 1(d) and 1(e) show the electrochemistry at the highest salt concentration, 3.2 mol.kg^{-1}; in both cases, we do not observe a well-defined lithium deposition peak. We have first cycled the electrolyte to -5 V (figure 1(d)) then to -6.5 V (figure 1(e)) to find the lithium deposition peak.

After scanning reductively to -6.5V vs. Ag | Ag$^+$ (figure 1(e)) a stripping peak is observed on the first cycle, however, because of coincident electrolyte decomposition and lithium deposition, the stripping peak current decreases rapidly, and the peak is no longer observable after 5 cycles. Whilst we do not observe a lithium deposition peak in figure 1(d), the cycling efficiency is significantly higher when cycled in this narrower electrochemical window. These two experiments allow us to determine that the bulk IL reduction process occurs between -5 and -6.5 V in the 3.2 mol.kg^{-1} electrolyte. Figure 1(f) shows that in all the solutions prepared here, the cathodic stability is unchanged by the presence of various concentrations of lithium salt. Finally, we note that the shifts in the peak positions of the lithium deposition and stripping are also influenced by the speciation of Li in solution, as evidenced by the changing NMR ^{7}Li chemical shift. This effect will be described in more detail in a forthcoming paper.

Bhatt et al. reported that a salt concentration of 0.45 mol.kg^{-1} shows better cycling stability than 0.2 mol.kg^{-1}.[27] However, in this study, the lowest Li concentration in the IL is 0.8 mol.kg^{-1} and all electrolytes in figures 1(c) to 1(f) show essentially stable lithium deposition and stripping for 5 cycles. Moreover, and very significantly, the lithium deposition current densities for the highest salt concentrations start at -30 mA.cm^{-2} (figure 1(d)) and increases in magnitude to -80 mA.cm^{-2} (figure 1(e)), equivalent to a 27A charge rate (or 7.5C rate) in a 18650 cell having 3.6 Ah capacity with 4 mAh.cm^{-2} loading on both sides of the Al current collector.[34] This shows the potential use of these electrolytes for fast charging lithium batteries. In addition, this trend also remains when using Ni working electrode. Figure 2 shows the Li deposition and stripping efficiencies for the different salt concentrations studied in this work. The Coulombic efficiency is higher at concentrations such as 2.4 mol.kg^{-1} or 3.2 mol.kg^{-1}, which can be attributed to the high number of charge carriers in solution.
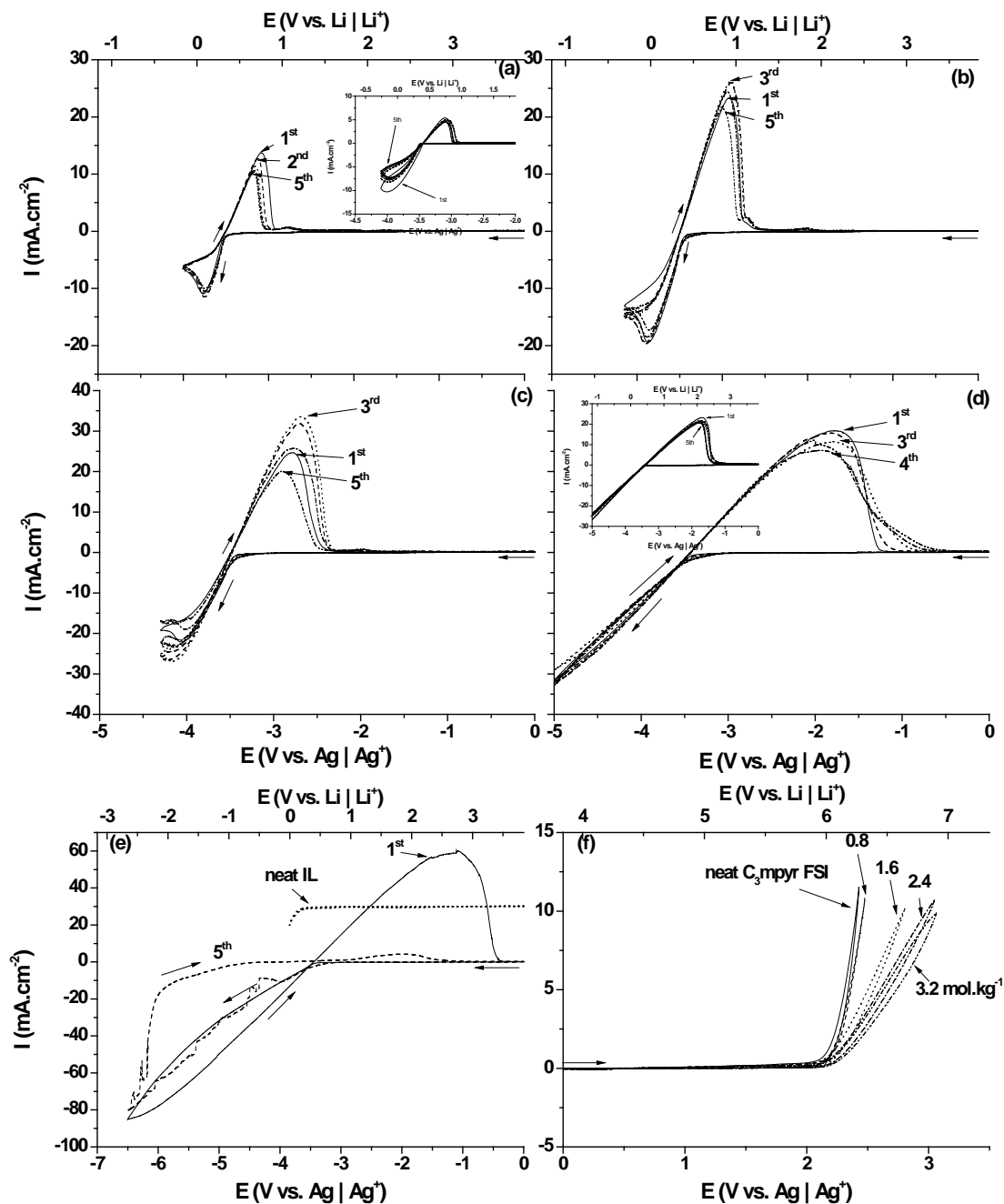
Figure 1. Cyclic voltammograms (Pt working electrode, 20 mV.sec^{-1}, room temperature) for concentrated LiFSI in C$_3$mpyrFSI ILs: a) 0.8 mol.kg^{-1}, b) 1.6 mol.kg^{-1}, c) 2.4 mol.kg^{-1},(d) 3.2 mol.kg^{-1} -5V cut-off, (e) 3.2 mol.kg^{-1}, -6.5V cut-off 1st cycle (solid line) and 5th cycle (dashed line) compared with the neat IL (dotted line, arbitrary current range) , (f) Anodic electrochemical limits. The embedded boxes in the figure (a) and (d) are the CV with Ni working electrode. Note: Top axis is converted to the Li | Li$^+$ redox potential from Ag | Ag$^+$ potential (bottom).
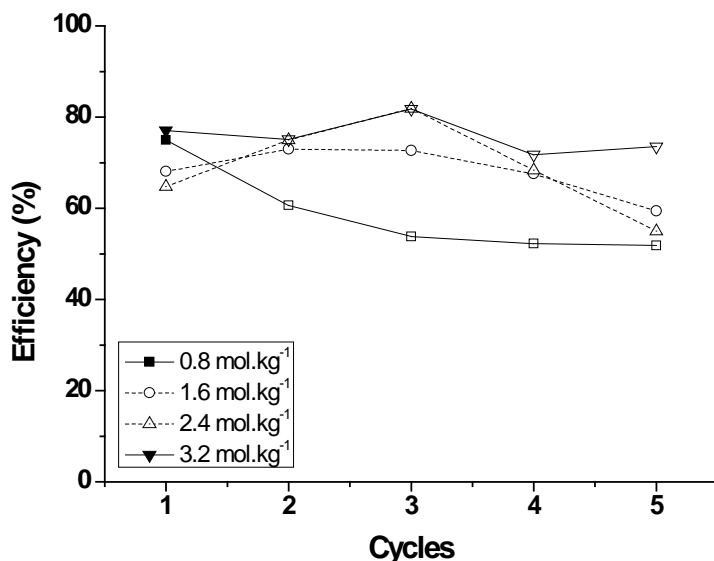
Figure 2. Li stripping/deposition columbic efficiency during the first 5cycles

Cycling performance of C_3mpyrFSI lithium symmetrical coin cells:

We have constructed Li symmetrical cells to determine if the stability of Li cycling depends on the lithium salt concentration. These cells have been cycled at different current densities from 0.01 mA.cm^{-2} to 1 mA.cm^{-2}, at room temperature. The voltage-time responses for the different salt concentrations are shown in Figure 3. Each cell shows that, for any given applied current density, the over-potential remains relatively stable; the most significant changes occur with changes in salt concentration. The cell resistance increases with increasing molar concentrations of Li salt up to 2.4 mol.kg^{-1}, and then decreases when the salt concentration reaches 3.2 mol.kg^{-1}. The internal resistance values calculated from the DC polarizations are several hundred Ω.cm^{-2}, as expected from the resistivities of the electrolytes obtained from EIS measurements. When the polarization current density was increased to 0.1 mA.cm^{-2}, (Figure 3(b)) the same trend was observed, however, a significant instantaneous over-potential was observed for every cell. Figure 3(c) shows the voltage-time response at 1 mA.cm^{-2} for the 2.4 mol.kg^{-1} electrolyte.
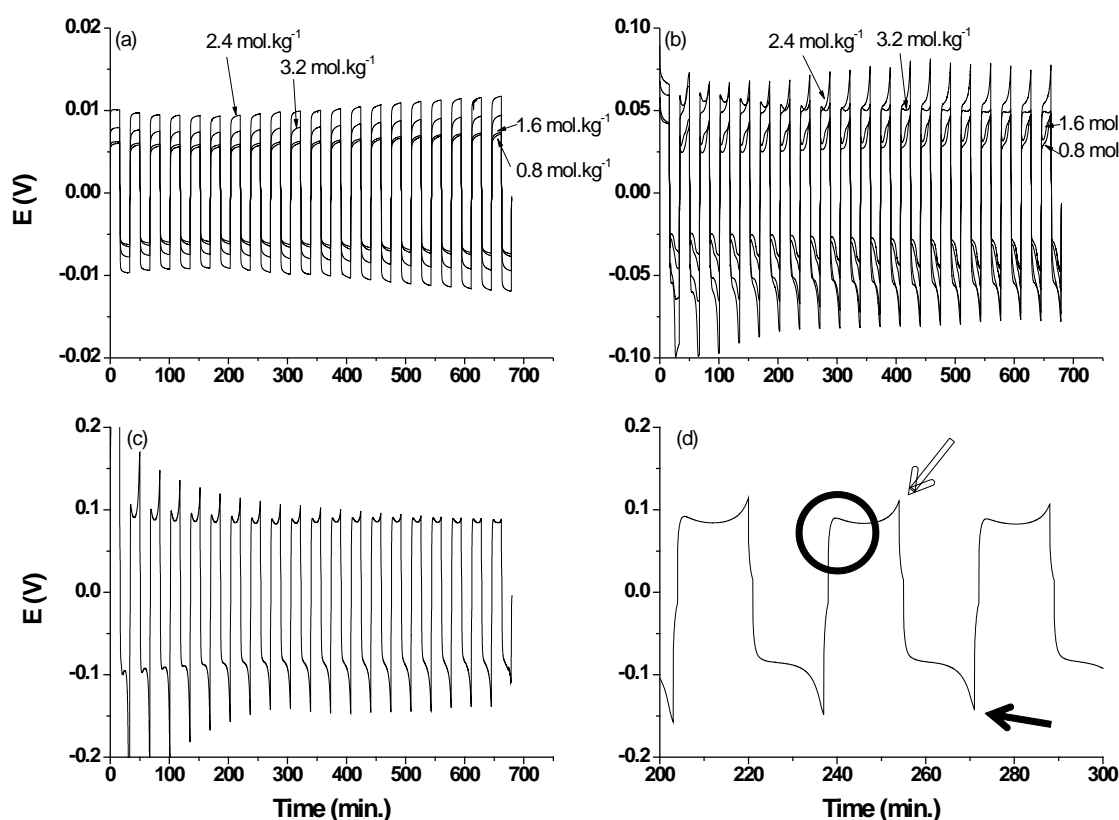
Figure 3. Voltage-time profiles for Li symmetric cells: a) 0.01 mA.cm^{-2} for 4 different electrolyte concentrations, b) 0.1 mA.cm^{-2} for 4 different electrolyte concentrations, c) 1.0 mA.cm^{-2} for 2.4 mol.kg^{-1} electrolyte, d) magnification of c)

There are 2 discrete over-potentials observed during the polarization: the over-potential in the initial polarization (circled) indicates the kinetic limit of the IL system, and the second one during the final polarization (arrow) indicates a dendritic lithium morphology.[15, 27] It should be noted that the over-potential decreases as the polarization continues this was also previously observed by Best and Bhatt and ascribed to the increasing geometric surface area of the electrode which meant that the actual applied current density is less than the apparent applied current density.[15, 27] In conclusion, we found no significant correlation between salt concentration and lithium symmetric cell cycling performance.

Lithium Transference numbers:

The transference number is the fraction of current transported by Li^+ in an electrolyte and, possibly, the most important quantity for lithium batteries.[35-37] It is desirable for electrolytes to have a transference number of unity.[1] The traditional method to determine a transference number is the Hittorf method.[38] In this method, constant current is applied, and the changes in voltage with time are used to compare the effective charge carried to the applied charge. However, this method cannot be directly applied to an electrolyte which consists of several ionic species, or where there is growing passivation film on the electrode which affects potential. Initially, when a symmetric cell is polarized, all positive ions (Li^+, C_3mpyr^+ in this experiment) migrate towards the negatively polarized electrode, while negative ions migrate towards the positively polarized electrode. However, after a certain time a steady state is reached for a charge concentration gradient established, where only Li^+ moves toward the opposite electrode. By measuring the initial and steady state currents, the portion of the charge carried by Li^+ can be obtained. Considering the solution concentration gradient and the increasing passivation layer, Bruce, Evans and Vincent demonstrated that an ion transference number in a symmetric cell can be calculated as:[30, 38]

$$t_{Li}^+ = \frac{I_S (\Delta V - I_0 R_0)}{I_0 (\Delta V - I_S R_S)} \tag{1}$$

where, ΔV is the potential applied across the cell, t_{Li}^+ is the lithium transference number, I_0 and I_S are the initial and steady state currents during the polarization, and R_0 and R_S are the initial and steady state resistances of the passivation layers. The authors applied this equation to polymer electrolyte systems, but subsequently, researchers have shown that the equation can be adapted to ionic liquids, where stable passivation layers form.[39-41] This equation may be used by applying a constant voltage, and measuring the initial and steady state currents, along with the resistance of the passivation film before and after the polarization. Due to the

stability of the IL electrolyte towards the Li metal electrode, we show that the impedance change of the bulk electrolyte before and after the polarization is negligible, which allows us to use this simplified approach with confidence.

To determine the resistances of passivation layers before and after polarization, an equivalent circuit proposed by Zugmann et al. was used (as shown in Figure 4(a)).[37]
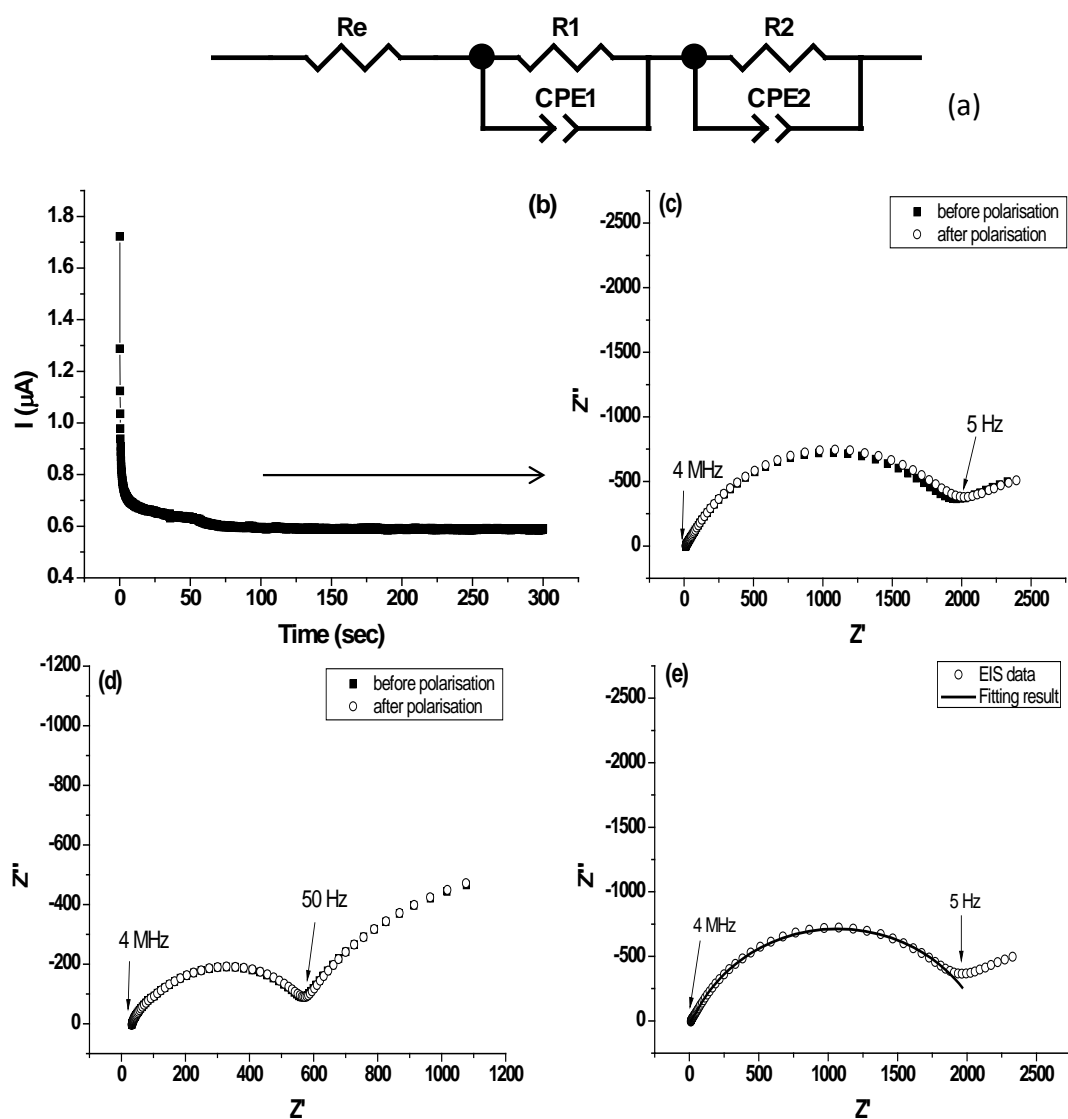

Figure 4. Polarisation and EIS of Li symmetric cells. (a) Equivalent circuit used to determine electrode resistances (b) a cell reaching a steady state current. (c) EIS of 0.8 mol.kg^{-1} LiFSI in C$_3$mpyrFSI (d) EIS of 3.2 mol.kg^{-1} LiFSI in C$_3$mpyrFSI. (e) EIS of the cell used in figure (b), taken before the cell was polarized; fit to equivalent circuit in (a) also shown.

Figure 4(b) is an example of the polarization of a symmetrical cell containing 0.8 mol.kg^{-1} LiFSI in C$_3$mpyr FSI for 300 seconds. In contrast with previous studies on PEO or plastic crystal electrolytes, which required several hours to reach steady state current, the cells reached steady state current within several minutes. In some cells, particularly those with lower Li salt concentration (0.8 mol.kg^{-1}), an increase in current was observed after the cell had been at steady state for some time (Figure 4(d)). This phenomenon was not observed in the cells with the highest lithium concentrations (3.2 mol.kg^{-1}). This may be due to the presence of an unexpected side reaction on the lithium surface when the concentration of Li$^+$ is not sufficient. To determine I$_0$ and I$_S$, any cells which showed increasing current after steady state, did not reach steady state or showed short circuit behavior were eliminated, and the remaining cells were used to calculating average values for each electrolyte concentration. Figure 4(c) is an example EIS of a Li symmetric cell containing 0.8 mol.kg^{-1} Li salt in the IL electrolyte, while 4(e) shows the EIS of a cell containing 3.2 mol.kg^{-1} Li salt. With increasing concentration, R$_e$ increases from 7–8 Ω in 0.8 mol.kg^{-1} to 28–32 Ω in 3.2 mol.kg^{-1}, while the R$_1$ + R$_2$ value decreases from approximately 2,000 Ω in 0.8 mol.kg^{-1} to 600 Ω in 3.2 mol.kg^{-1}. This implies that the passivation layer formed on the lithium electrodes depends strongly on the concentration of Li$^+$, and that an increase in Li$^+$ concentration reduces the surface impedance. The cells were polarized at 1.0 mV for 2 hours 3 times. It should also be noted that the EIS did not change significantly after these polarizations.

The calculated transference numbers for different salt concentrations are shown in Figure 5 (with error bars) and are collated in Table 2, along with conductivities, viscosities, and densities at 25 °C. The density and viscosity increase, and the ionic conductivity decreases, with increasing salt concentration. The transference numbers vary 0.1 to 0.2 as the LiFSI concentration changes. There is a general trend that increasing salt concentration increases transference number, although it is not clear if there is an optimum point between 2.4 mol.kg$^-$

[1] and 3.2 mol.kg^{-1}. This result corresponds with that previously reported by Ferrari et al. in their *N*-methoxyethyl-*N*-methylpyrrolidinium TFSI and LiTFSI systems.[42] However, they did not explain why this result was obtained. Our measured transference numbers are similar to the 0.13 value determined by Seki et al. for 0.32 mol.kg^{-1} LiTFSI in different ILs,[41] but are much lower than the 0.6 value reported by Han et al. for a LiFSI-ammoniumFSI equimolar system[43] or the 0.4 value reported by Fernicola et al. for a TFSI-based system.[40] It should be noted that most electrolyte research has been conducted in the 0.5 mol.kg^{-1} to 1.0 mol.kg^{-1} range of added Li salts, but in some cases the optimum concentration may be much higher, as we have demonstrated here for the FSI-based electrolyte.
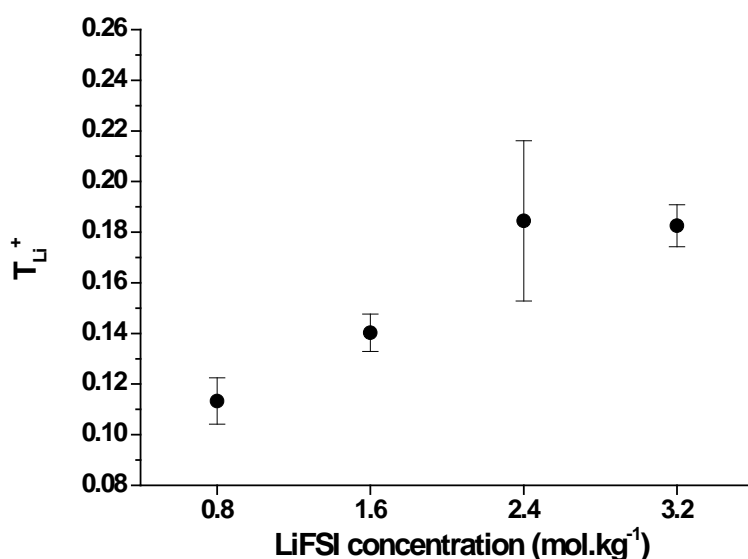
Figure 5. Li^{+} transference number for different LiFSI concentrations in C$_3$mpyr FSI, showing average values and standard deviations

Table 2. Transference numbers of each concentrated Li+ electrolyte at 25 °C

Salt concentration	δ (g.cm^{-3})	v (cP)	σ (mS.cm^{-1})	Ave t_{Li}^{+}
0.8 mol.kg^{-1}	1.413	49.4	3.40	0.113
1.6 mol.kg^{-1}	1.454	85.7	2.02	0.140
2.4 mol.kg^{-1}	1.495	136	1.23	0.185
3.2 mol.kg^{-1}	1.536	253	0.821	0.183

Li | LiCoO$_2$ cells:

First, the LiCoO$_2$ electrode pasted onto Al foil was characterized in combination with a commercial standard battery electrolyte. Cells were cycled from 2.75 V to 4.2 V at various rates between 0.1 C and 5.0 C followed by several additional cycles at 0.1 C. The initial 0.1 C charge capacity was 137 mAh.g^{-1} and discharge capacity was 131 mAh.g^{-1}, equating to 96% initial efficiency in figure 6(a), which is slightly lower than the known practical capacity of LiCoO$_2$.[1, 44] When the charge/discharge rate was over 1 C, a small distortion in the profile was observed in all cells, which became more noticeable at the higher rates. Of 6 replicate cells tested, only one cell allowed charging up to the 3 C rate (the remaining five couldn't be charged at this rate). No cells using this standard liquid electrolyte could be charged above 4 C. These cells recovered their initial capacity when a 0.1 C rate was applied. We confirmed that the standard liquid electrolyte can be a limiting factor for high rate charge and discharge, although the actual limiting rate will vary with different electrode formulations, separators and cell configurations. Thus, in these experiments, the 3 C charging rate was the limit for the organic liquid electrolyte used, 1M LiPF$_6$ in EC:DMC (50:50 vol.%).

Figure 6(b) to (e) presents the results of coin cells containing C$_3$mpyrFSI electrolyte with different lithium salt concentrations, from 0.8 to 3.2 mol.kg^{-1}. The initial 0.1 C capacity with 0.8 mol.kg^{-1} lithium salt was 118 mAh.g^{-1}, which is lower than the standard battery electrolyte reference (Figure 6(b)); this can be ascribed to the higher viscosity and lower conductivity of this ionic liquid electrolyte.[20] When the salt concentration is increased to 1.6 mol.kg^{-1} (Figure 6(c)), surprisingly, the capacity increased to 132 mAh.g^{-1} even though the viscosity is higher and the conductivity is lower than the 0.8 mol.kg^{-1} solution. This result is in agreement with the increased current observed in the CV data previously presented in Figure 1. A decrease in capacity to 120 mAh.g^{-1} at 2.4 mol.kg^{-1} and further increase to 135 mAh.g^{-1} at 3.2 mol.kg^{-1} (figure 6(d) and 6(e)) were also seen.
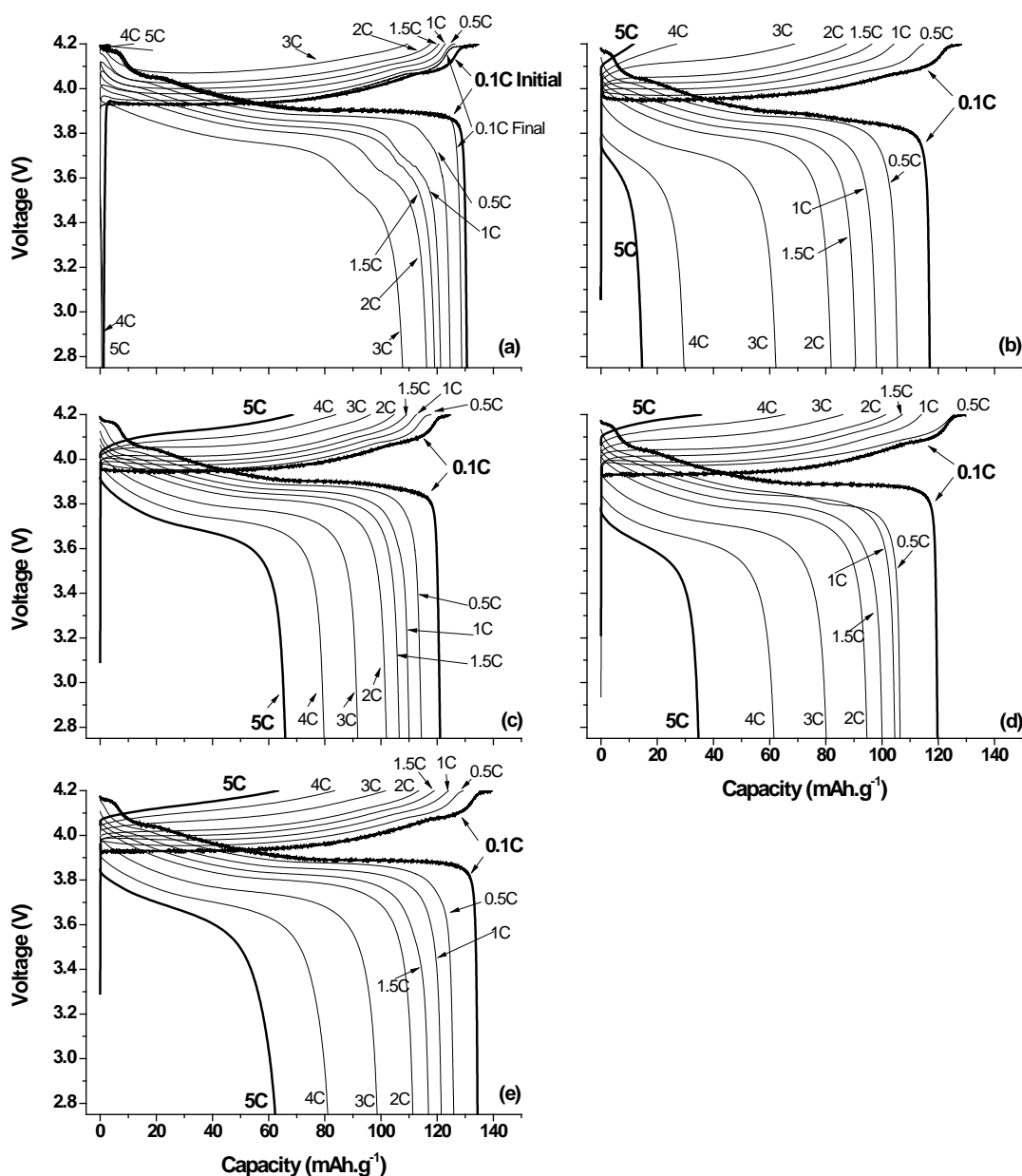
Figure 6. Charging and discharging rate capability results for Li | LiCoO$_2$ cells with Solupor 7P separator. The conditions were 0.1C, 0.2C, 0.5C, 1.0C, 1.5C, 2.0C, 3.0C, 4.0C and 5.0C rates consequently from 2.75V to 4.2V at room temperature. (a) 1M LiPF$_6$ in EC:DMC (50: 50 vol.%) for comparison, (b) 0.8 mol.kg^{-1},(c) 1.6 mol.kg^{-1}, (d) 2.4 mol.kg^{-1}, (e) 3.2 mol.kg^{-1} LiFSI in C$_3$mpyr FSI

The 2 C rate capacity in the 0.8 mol.kg^{-1} electrolyte was also inferior to that of the organic

liquid reference. However, the performance improved when the lithium salt concentration

was increased to 1.6 mol.kg^{-1} or higher. The capacity reached the same charge and discharge

57

capacity within a tolerance range at 3 C. A significant difference was observed at the higher charge/discharge rates of 4 C and 5 C. Whilst no cell successfully charged at 4 C with the standard electrolyte, all cells with FSI were successfully cycled at 4 C and 5 C charge/discharge rates. When the salt concentration is 3.2 mol.kg^{-1}, 50–60 mAh.g^{-1} (or approximately 40% of the initial 0.1 C discharge capacity) was observed, as shown in Figure 6(e). To put these results in perspective, Matsumoto et al. conducted similar experiments using a C$_3$mpyr FSI ionic liquid with 0.3 mol.kg^{-1} LiTFSI,[9] however, their results showed approximately 35 mAh.g^{-1} discharge capacity at the 3 C rate with a 1.0–1.5 mg.cm^{-2} LiCoO$_2$ loading (i.e., 3 C current density is 0.42 mA.cm^{-2} to 0.81 mA.cm^{-2})[9, 45] compared to the approximately 4.5 mg.cm^{-2} loading used in this work (i.e., 3 C current density is 2.43 mA.cm^{-2}). This clearly demonstrates the superior results of this work with significantly higher active material loading and salt concentrations.

The 1 C to 5 C charging profiles from figure 6(a) and 6(e) are presented in Figure 7 for comparative purposes. The cell with the standard organic electrolyte showed significantly higher over-voltage at the high charging rates at the initial stage; this over-voltage caused by the coin cell impedance, caused the cell voltage to reach 4.2V instantaneously, resulting in a premature end of the charging step. Additional cells were prepared and cycled with different charging method to verify the low rate capability of organic electrolyte at high current rate is only of the observed over-voltage.
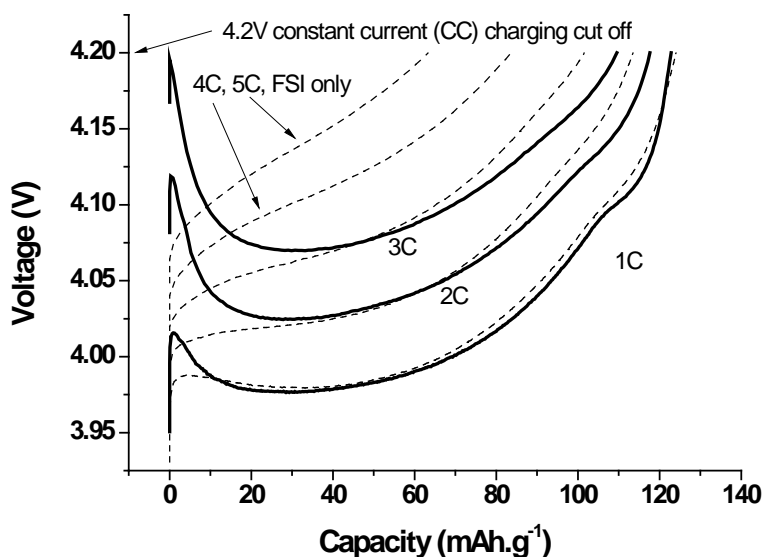
Figure 7.1 C to 5 C Charging profiles magnified from figure 8: Solid bold line : Organic liquid electrolyte (1M LiPF$_6$, EC:DMC=50:50 vol.%, from figure 8(a)), Dash line : 3.2 mol.kg^{-1} LiFSI in C$_3$mpyrFSI from figure 8(e).

The discharging rate capability of the cells with a fixed low current (0.1C) charging rate is presented in figure 8. Figure 8(a) is the discharging profiles with the standard organic electrolyte. It was shown that the charging profiles vary with cycles and the efficiency (discharging capacity / charging capacity) at the 5C rate charging and discharging is much greater than 100%, which was due to the remained capacity of the previous cycle (4C) discharge. It is interesting that the cell with the standard organic electrolyte shows relatively low discharging capability at high C rate over 4C than the cell having FSI IL based electrolyte (figure 8(b)). This implies that the relatively low discharging capability of the cell with standard organic electrolyte is not only the problem of over-voltage during high rate charging, but also of its intrinsic characteristics. Considering charging rate limit caused by over-voltage problem, since the cell impedance is high for the coin cells in this study, the charging rate limit in this study may be relatively low when compared to commercial lithium ion batteries. However, the cells using the FSI based electrolyte, which have the same

configuration as the cell with standard electrolyte, do not show this over-voltage behavior at the start of charging in spite of its higher viscosity. This indicates that the Li^+ transport mechanism may be different in the ionic liquid electrolyte compared to the standard organic electrolyte. We will elaborate on this further in our forthcoming paper.
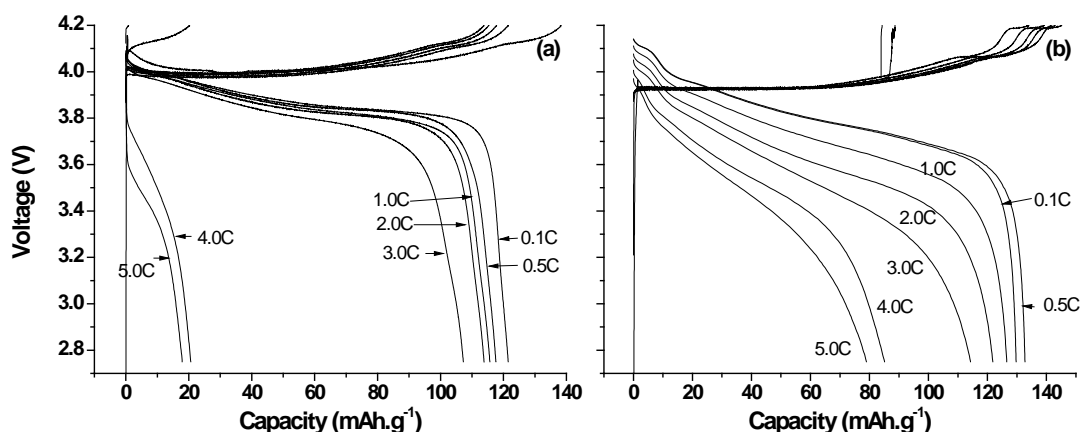

Figure 8. 0.1 C to 5 C discharging rate capability results with fixed 0.1C rate charging for Li | LiCoO$_2$ cells with Solupor 7P separator; (a) 1M LiPF$_6$ in EC:DMC (50: 50 vol.%) for comparison, (b) 3.2 mol.kg^{-1} LiFSI in C$_3$mpyr FSI

After the rate capacity measurement, the cell with 3.2 mol.kg^{-1} Li salt FSI electrolyte was cycled successfully, as shown in Figure 9(a). However, the cells with lower lithium concentrations show significant capacity fade during cycling. Most of the cells containing 0.8 mol.kg^{-1} to 2.4 mol.kg^{-1} Li salt did not survive beyond 5 cycles at 0.1 C after the tests at 5 C, but the 3.2 mol.kg^{-1} cycled more reliably as shown in Figure 9(b). The cells with lower lithium concentration electrolytes failed after cycling and could not be charged up to 4.2V. The cells with 3.2 mol.kg^{-1} Li salt also showed a continuous decrease in discharge capacity after 5 C cycling. This phenomenon may be due to consumption of lithium ions during the high rate charge and discharge, or may due to degradation of the prepared LiCoO$_2$ electrode in the presence of the IL.[46] Further investigations will be performed to understand this phenomenon. The important point here is that the barrier to high rate charging and

discharging because of transport limitations in the cell, as was observed when using a conventional organic liquid electrolyte system, is overcome in this FSI system. We expect this FSI system to show even better rate performance when combined with high rate cathode and anode materials.
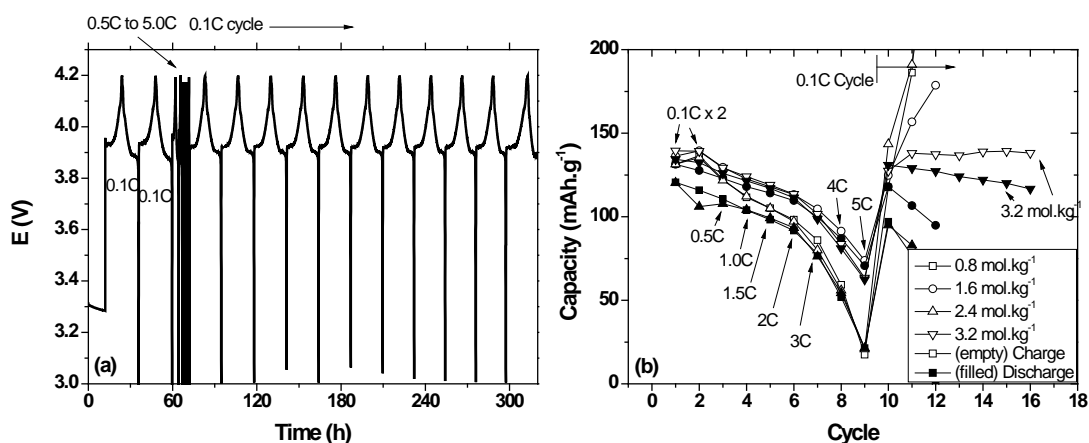

Figure 9.(a) A cycle profile of a Li | LiCoO$_2$ coin cell with 3.2 mol.kg^{-1} LiFSI in C$_3$mpyr FSI electrolyte, (b) Charge/discharge capacity of cells during cycling

4. Conclusion

We describe ionic liquid electrolytes, based on the bis(fluorosulfonyl)imide (FSI) anion with LiFSI salts, that show high rate charge and discharge characteristics. The C$_3$mpyrFSI ionic liquid can dissolve lithium salt up to a 1:1 IL:Li salt concentration ratio; this concentrated electrolyte then allows the Li metal electrode to be cycled at high current density. Transference numbers have also been measured in these cells to determine the lithium salt concentration effect on lithium cell performance. There is a concomitant increase in transference number from 0.1 to 0.2 with increasing salt concentration.

Li | LiCoO$_2$ batteries, prepared using this FSI electrolyte, show better rate capability than those made with 1M LiPF$_6$ in EC:DMC organic liquid electrolyte at higher than 3C charge and discharge rates, in spite of the significantly higher viscosity and lower conductivity of the

IL. Importantly, the electrolyte containing 3.2 mol.kg^{-1} Li salt (i.e., a 1:1 molar ratio of salt and IL) showed the best high-rate cycling performance. This implies that the lithium transport mechanism in these high lithium concentration IL electrolytes may be different, to allow high rate charge and discharge. Finally, we expect this FSI system to show better charge and discharge capability when combined with a fast-charging electrode material.

5. Acknowledgements

References

1.   Goodenough, J. B.; Kim, Y., Challenges for Rechargeable Li Batteries. *Chemistry of Materials* **2010,** *22* (3), 587-603.
2.   Ohno, H., Importance and Possibility of Ionic Liquids. In *Electrochemical Aspects of Ionic Liquids*, Hiroyuki, O., Ed. 2005; pp 1-3.
3.   Bhatt, A. I.; Snook, G. A.; Lane, G. H.; Rees, R. J.; Best, A. S., *Application of Room Temperature Ionic Liquids in Lithium Battery Technology*. Nova Science Publishers, inc: 2011.
4.   Appetecchi, G. B.; Kim, G. T.; Montanina, M.; Carewska, M.; Marcilla, R.; Mecerreyes, D.; De Meatza, I., Ternary polymer electrolytes containing pyrrolidinium-based polymeric ionic liquids for lithium batteries. *Journal of Power Sources* **2010,** *195* (11), 3668-3675.
5.   Lux, S. F.; Schmuck, M.; Jeong, S.; Passerini, S.; Winter, M.; Balducci, A., Li-ion anodes in air-stable and hydrophobic ionic liquid-based electrolyte for safer and greener batteries. *International Journal of Energy Research* **2010,** *34* (2), 97-106.
6.   Kim, G. T.; Jeong, S. S.; Xue, M. Z.; Balducci, A.; Winter, M.; Passerini, S.; Alessandrini, F.; Appetecchi, G. B., Development of ionic liquid-based lithium battery prototypes. *Journal of Power Sources* **2012,** *199*, 239-246.
7.   Zaghib, K.; Charest, P.; Guerfi, A.; Shim, J.; Perrier, M.; Striebel, K., Safe Li-ion polymer batteries for HEV applications. *Journal of Power Sources* **2004,** *134* (1), 124-129.
8.   Ishikawa, M.; Sugimoto, T.; Kikuta, M.; Ishiko, E.; Kono, M., Pure ionic liquid electrolytes compatible with a graphitized carbon negative electrode in rechargeable lithium-ion batteries. *Journal of Power Sources* **2006,** *162* (1), 658-662.

9.   Matsumoto, H.; Sakaebe, H.; Tatsumi, K.; Kikuta, M.; Ishiko, E.; Kono, M., Fast cycling of Li/LiCoO2 cell with low-viscosity ionic liquids based on bis(fluorosulfonyl)imide FSI (-). *Journal of Power Sources* **2006,** *160* (2), 1308-1313.

10.   Guerfi, A.; Duchesne, S.; Kobayashi, Y.; Vijh, A.; Zaghib, K., LiFePO4 and graphite electrodes with ionic liquids based on bis(fluorosulfonyl)imide (FSI)(-) for Li-ion batteries. *Journal of Power Sources* **2008,** *175* (2), 866-873.

11.   Saint, J.; Best, A. S.; Hollenkamp, A. F.; Kerr, J.; Shin, J. H.; Doeff, M. M., Compatibility of LixTiyMn1-yO2 (y=0, 0.11) electrode materials with pyrrolidinium-based ionic liquid electrolyte systems. *Journal of the Electrochemical Society* **2008,** *155* (2), A172-A180.

12.   Seki, S.; Kobayashi, Y.; Miyashiro, H.; Ohno, Y.; Mita, Y.; Terada, N.; Charest, P.; Guerfi, A.; Zaghib, K., Compatibility of N-Methyl-N-propylpyrrolidinium Cation Room-Temperature Ionic Liquid Electrolytes and Graphite Electrodes. *Journal of Physical Chemistry C* **2008,** *112* (42), 16708-16713.

13.   Zhou, Q.; Henderson, W. A.; Appetecchi, G. B.; Montanino, M.; Passerini, S., Physical and Electrochemical Properties of N-Alkyl-N-methylpyrrolidinium Bis(fluorosulfonyl)imide Ionic Liquids: PY13FSI and PY14FSI. *Journal of Physical Chemistry B* **2008,** *112* (43), 13577-13580.

14.   Paillard, E.; Zhou, Q.; Henderson, W. A.; Appetecchi, G. B.; Montanino, M.; Passerini, S., Electrochemical and Physicochemical Properties of PY(14)FSI-Based Electrolytes with LiFSI. *Journal of the Electrochemical Society* **2009,** *156* (11), A891-A895.

15.   Best, A. S.; Bhatt, A. I.; Hollenkamp, A. F., Ionic Liquids with the Bis(fluorosulfonyl) imide Anion: Electrochemical Properties and Applications in Battery Technology. *Journal of the Electrochemical Society* **2010,** *157* (8), A903-A911.

16.   Lewandowski, A.; Acznik, I., Impedance study of protecting film formation on lithium and lithiated graphite induced by bis(fluorosulfonyl) imide anion. *Electrochimica Acta* **2010,** *56* (1), 211-214.

17.   Wang, Y. D.; Zaghib, K.; Guerfi, A.; Bazito, F. F. C.; Torresi, R. M.; Dahn, J. R., Accelerating rate calorimetry studies of the reactions between ionic liquids and charged lithium ion battery electrode materials. *Electrochimica Acta* **2007,** *52* (22), 6346-6352.

18.   Abouimrane, A.; Ding, J.; Davidson, I. J., Liquid electrolyte based on lithium bis-fluorosulfonyl imide salt: Aluminum corrosion studies and lithium ion battery investigations. *Journal of Power Sources* **2009,** *189* (1), 693-696.

19.   Vijayaraghavan, R.; Surianarayanan, M.; Armel, V.; MacFarlane, D. R.; Sridhar, V. P., Exothermic and thermal runaway behaviour of some ionic liquids at elevated temperatures. *Chemical Communications* **2009,** (41), 6297-6299.

20.   Seki, S.; Ohno, Y.; Kobayashi, Y.; Miyashiro, H.; Usami, A.; Mita, Y.; Tokuda, H.; Watanabe, M.; Hayamizu, K.; Tsuzuki, S.; Hattori, M.; Terada, N., Imidazolium-based room-temperature ionic liquid for lithium secondary batteries - Effects of lithium salt concentration. *Journal of the Electrochemical Society* **2007,** *154* (3), A173-A177.

21.   Nyman, A.; Behm, M.; Lindbergh, G., Electrochemical characterisation and modelling of the mass transport phenomena in LiPF6-EC-EMC electrolyte. *Electrochimica Acta* **2008,** *53* (22), 6356-6365.

22.   Shin, J. H.; Henderson, W. A.; Appetecchi, G. B.; Alessandrini, F.; Passerini, S., Recent developments in the ENEA lithium metal battery project. *Electrochimica Acta* **2005,** *50* (19), 3859-3865.

23.   Randstroem, S.; Appetecchi, G. B.; Lagergren, C.; Moreno, A.; Passerini, S., The influence of air and its components on the cathodic stability of N-butyl-N-methylpyffolidinium bis(trifluoromethanesulfonyl)imide. *Electrochimica Acta* **2007,** *53* (4), 1837-1842.

24.   Aklalouch, M.; Manuel Amarilla, J.; Rojas, R. M.; Saadoune, I.; Maria Rojo, J., Chromium doping as a new approach to improve the cycling performance at high temperature of 5 VLiNi0.5Mn1.5O4-based positive electrode. *Journal of Power Sources* **2008,** *185* (1), 501-511.

25.   Abouimrane, A.; Belharouak, I.; Amine, K., Sulfone-based electrolytes for high-voltage Li-ion batteries. *Electrochemistry Communications* **2009,** *11* (5), 1073-1076.

26.   Marom, R.; Amalraj, S. F.; Leifer, N.; Jacob, D.; Aurbach, D., A review of advanced and practical lithium battery materials. *Journal of Materials Chemistry* **2011,** *21* (27), 9938-9954.

27.   Bhatt, A. I.; Best, A. S.; Huang, J.; Hollenkamp, A. F., Application of the N-propyl-N-methyl-pyrrolidinium Bis(fluorosulfonyl)imide RTIL Containing Lithium Bis(fluorosulfonyl)imide in Ionic Liquid Based Lithium Batteries. *Journal of the Electrochemical Society* **2010,** *157* (1), A66-A74.

28.   Girault, H. H., *Analytical and physical electrochemistry*. 2004; p xiii + 431 pp.-xiii + 431 pp.

29.   Snook, G. A.; Best, A. S.; Pandolfo, A. G.; Hollenkamp, A. F., Evaluation of a Ag vertical bar Ag+ reference electrode for use in room temperature ionic liquids. *Electrochemistry Communications* **2006,** *8* (9), 1405-1411.

30.   Evans, J.; Vincent, C. A.; Bruce, P. G., Electrochemical measurement of transference numbers in polymer electrolytes. *Polymer* **1987,** *28* (13), 2324-2328.

31.   Bruce, P. G.; Vincent, C. A., Polymer electrolytes. *Journal of the Chemical Society-Faraday Transactions* **1993,** *89* (17), 3187-3203.

32.   Wibowo, R.; Jones, S. E. W.; Compton, R. G., Kinetic and Thermodynamic Parameters of the Li/Li+ Couple in the Room Temperature Ionic Liquid N-Butyl-N-methylpyrrolidinium Bis(trifluoromethylsulfonyl) Imide in the Temperature Range 298-318 K: A Theoretical and Experimental Study Using Pt and Ni Electrodes. *Journal of Physical Chemistry B* **2009,** *113* (36), 12293-12298.

33.   Howlett, P. C.; Izgorodina, E. I.; Forsyth, M.; MacFarlane, D. R., Electrochemistry at negative potentials in bis(trifluoromethanesulfonyl)amide ionic liquids. *Zeitschrift Fur Physikalische Chemie-International Journal of Research in Physical Chemistry & Chemical Physics* **2006,** *220* (10-11), 1483-1498.

34.   Nagasubramanian, G., Fabrication and testing capabilities for 18650 Li/(CF(x))(n) cells. *International Journal of Electrochemical Science* **2007,** *2* (12), 913-922.

35.   Atkins, P. W., *Physical chemistry*. 6th ed.; Oxford University Press: Oxford, 1998.

36.   Hafezi, H.; Newman, J., Verification and analysis of transference number measurements by the galvanostatic polarization method. *Journal of the Electrochemical Society* **2000,** *147* (8), 3036-3042.

37.   Zugmann, S.; Fleischmann, M.; Amereller, M.; Gschwind, R. M.; Wiemhoefer, H. D.; Gores, H. J., Measurement of transference numbers for lithium ion electrolytes via four different methods, a comparative study. *Electrochimica Acta* **2011,** *56* (11), 3926-3933.

38.   Bruce, P. G.; Hardgrave, M. T.; Vincent, C. A., The determination of transference numbers in solid polymer electrolytes using the Hittorf method. *Solid State Ionics* **1992,** *53*, 1087-1094.

39.   Abraham, K. M.; Jiang, Z.; Carroll, B., Highly conductive PEO-like polymer electrolytes. *Chemistry of Materials* **1997,** *9* (9), 1978-1988.

40.   Fernicola, A.; Croce, F.; Scrosati, B.; Watanabe, T.; Ohno, H., LiTFSI-BEPyTFSI as an improved ionic liquid electrolyte for rechargeable lithium batteries. *Journal of Power Sources* **2007,** *174* (1), 342-348.

41.   Seki, S.; Ohno, Y.; Miyashiro, H.; Kobayashi, Y.; Usami, A.; Mita, Y.; Terada, N.; Hayamizu, K.; Tsuzuki, S.; Watanabe, M., Quaternary ammonium room-temperature ionic liquid/lithium salt binary electrolytes: Electrochemical study. *Journal of the Electrochemical Society* **2008,** *155* (6), A421-A427.

42.   Ferrari, S.; Quartarone, E.; Mustarelli, P.; Magistris, A.; Protti, S.; Lazzaroni, S.; Fagnoni, M.; Albini, A., A binary ionic liquid system composed of N-methoxyethyl-N-methylpyrrolidinium bis(trifluoromethanesulfonyl)-imide and lithium bis(trifluoromethanesulfonyl)imide: A new promising electrolyte for lithium batteries. *Journal of Power Sources* **2009,** *194* (1), 45-50.

43.   Han, H.-B.; Liu, K.; Feng, S.-W.; Zhou, S.-S.; Feng, W.-F.; Nie, J.; Li, H.; Huang, X.-J.; Matsumoto, H.; Armand, M.; Zhou, Z.-B., Ionic liquid electrolytes based on multi-methoxyethyl substituted ammoniums and perfluorinated sulfonimides: Preparation, characterization, and properties. *Electrochimica Acta* **2010,** *55* (23), 7134-7144.

44.   Mizushima, K.; Jones, P. C.; Wiseman, P. J.; Goodenough, J. B., A new cathode material for batteries of high-energy density. *Materials Research Bulletin* **1980,** *15* (6), 783-789.

45.   Sakaebe, H.; Matsumoto, H., N-Methyl-N-propylpiperidinium bis(trifluoromethanesulfonyl)imide (PP13-TFSI) - novel electrolyte base for Li battery. *Electrochemistry Communications* **2003,** *5* (7), 594-598.

46.   Snook, G. A.; Huynh, T. D.; Hollenkamp, A. F.; Best, A. S., Rapid SECM probing of dissolution of LiCoO2 battery materials in an ionic liquid. *Journal of Electroanalytical Chemistry* **2012,** *687* (0), 30-34.

Physical properties of *N*-propyl-*N*-methylpyrrolidinium bis(fluorosulfonyl)imide in high LiFSI concentration

Hyungook Yoon,[†,‡,§] Adam S. Best,[*,‡] Maria Forsyth,[§] and Douglas R. MacFarlane [†] and Patrick C. Howlett[§]

[†] School of Chemistry, Monash University, 3800 Victoria, Australia

[*,‡] Commonwealth Scientific and Industrial Research Organisation (CSIRO), Division of Energy Technology, Bayview Ave., Clayton, 3169 Victoria, Australia; Tel: ▉▉▉▉▉▉▉▉ E-mail: ▉▉▉▉▉▉▉▉

[§] ARC Centre of Excellence for Electromaterials Science (ACES), Institute for Frontier Materials (IFM), Deakin University, Burwood, Victoria 3125, Australia

KEYWORDS : Ionic liquids, FSI, lithium, concentration, conformation, diffusivity

ABSTRACT: Electrolytes of bis(fluorosulfonyl)imide (FSI) with a range of LiFSI salt concentrations were characterized using physical property measurements, as well as NMR, FT-IR and Raman spectroscopy. Different from the behavior at lower concentrations, the FSI electrolyte containing the highest salt concentration (1:1 salt to IL molar ratio) showed less deviation from the KCl line in the Walden plot, suggesting greater ionic dissociation. Diffusion measurements show higher mobility of lithium ions compared to the other ions, which suggests that the partial conductivity of Li^+ is higher at higher concentration. Changes in the FT-IR and Raman peaks indicate that the cis-FSI conformation is preferred with increasing Li salt concentration.

INTRODUCTION

Because of their negligible vapor pressure and wide electrochemical windows, ionic liquids (ILs) have been considered viable replacements for current organic-liquid based electrolytes for lithium batteries.[1] Of the various ILs studied, those which include the bis(fluorosulfonyl)imide (FSI) anion have gained significant attention for their relatively low viscosity and high conductivity.[2] This anion was first introduced by Armand et al.,[3] and organic liquids containing lithium FSI were successfully used as lithium battery electrolytes by Zaghib et al.[4]. Matsumoto et al.[2] reported that FSI-based ILs show fast charging ability with $LiCoO_2$ cathodes, and Ishikawa et al.[5] demonstrated stable cycling ability with graphite anodes, with no organic diluents or additives.[5] There have also been many subsequent studies applying this FSI based electrolyte in lithium batteries.[6-13] Some drawbacks of this IL have also been reported, including concerns about high temperature stability and its corrosive properties.[14-16]

To understand the superior qualities of FSI-based ILs - in particular low viscosity and high conductivity, there have been many investigations of their physicochemical and electro-chemical properties, including comparative studies with ILs based on the similar bis(trifluoromethylsulfonyl)imide (TFSI) anion. Zhou et al. and Paillard et al. investigated the electrochemical and physicochemical properties of FSI-based ILs and their solutions containing Li salts, and demonstrated their superiority compared to the respective TFSI counterparts.[9-10]

One interesting aspect of this anion is its conformational equilibrium, and since the conformational structure of FSI is similar to that of TFSI, most of this research was originally performed on TFSI, and subsequently similar approaches were taken to see if FSI showed different behavior. For example, Johansson et al. estimated, using ab-initio theoretical calculations, that the TFSI anion can adopt 2 different conformers in liquids.[17] Fujii et al. confirmed, using Raman spectroscopy and molecular dynamics (MD), that TFSI has 2 conformers: C1 (cis-) and C2 (trans-) which are in equilibrium in the liquid state.[18] They then showed that the C1(cis-) form is dominant at higher temperatures, and claimed that the low melting point of TFSI-based ILs is related to this behavior.[18] Umebayashi et al. extended this research to ILs containing Li salts, and showed that TFSI ILs prefer cis- conformations and coordinate Li^+ to

66

form Li(TFSI)$_2^-$ or LiC$_2$mimTFSI$^+$ (1-ethyl-3-methylimidazolium TFSI). In Li(TFSI)$_2^-$, the Li$^+$ coordinates with 4 oxygen atoms in 2 TFSI anions.[19] Shirai et al. also studied the effects of LiTFSI salt concentration on speciation and coordination in *N,N*-diethyl-*N*-methyl-*N*-(2-methoxyethyl)ammonium TFSI by investigating the Raman and NMR shifts.[20] In their study, Li coordinates with 4 oxygen atoms within 2 TFSI anions to form Li(TFSI)$_2^-$ at low Li salt concentration, but forms a lithium oligomer at high Li concentrations.[20] In addition, Ishiguro et al. studied the temperature dependence of the speciation in a highly concentrated LiTFSI (0.171 mol fraction) in C$_2$mimTFSI solution, and showed that the cis-form of TFSI is more stable than the trans-form at high lithium salt concentration.[21] This research group also compared the coordination behavior of other metal ions such as Li$^+$, Na$^+$, K$^+$ and Cs$^+$ in solution of their TFSI salts in C$_2$mimTFSI..[22]

After Beran et al.'s report on the cis- form of the FSI anion in LiFSI salts, showing coordination of Li$^+$ and oxygen atoms in the FSI anion resulting in clustering around Li$^+$,[23] Fujii et al. extended their TFSI research to FSI, and demonstrated that FSI also behaves similarly to TFSI. FSI shows cis- and trans-equilibrium in the liquid state, and the low viscosity of FSI is also related to this conformational equilibrium.[24-25] The same conclusion was also reached separately by Lopes et al., based on Raman spectroscopy and MD calculations.[26] Recently, some interesting findings were reported by Huang et al., who noted from DSC studies that an exothermic reaction occurs when LiFSI is added into an FSI based IL, Raman spectroscopy was used to show that the Li cation is strongly associated with the FSI anion.[27]

Recently, we have shown that solutions containing a high Li salt concentration, up to 0.5 mol fraction (3.2 mol.kg^{-1}), in an FSI electrolyte can successfully cycle Li | LiCoO$_2$ cells, with fast charging and discharging rate capability (up to 5 C rate at 25 °C), in spite of the high viscosity and relatively low conductivity of these solutions.[28] This suggests that the Li transport mechanism at high lithium salt concentration (> 1.6 mol.kg^{-1}) is different from that at lower lithium concentration (< 1.6 mol.kg^{-1}).[28] In this present study, we now probe the intermolecular interactions to understand why this behavior occurs. We look at physical property changes across a range of Li salt concentrations in C$_3$mpyr FSI electrolyte, and use ionic conductivity, DSC, FT-IR, Raman and diffusion NMR measurements to elucidate the conduction mechanisms in these electrolytes.

EXPERIMENTAL

Materials:

N-propyl-*N*-methylpyrrolidinium bis(fluorosulfonyl)imide (C$_3$mpyrFSI, purity > 99.9%) and lithium bis(fluorosulfonyl)imide (LiFSI, purity > 99.5%) were both sourced from Suzhou Fluolyte Co., Ltd., China. Lithium metal was sourced from China Energy Lithium Co., Ltd. (purity > 99.9%).

Electrolytes in this work were prepared by adding LiFSI salts into C$_3$mpyrFSI IL and stirring for 24 hours at room tem-perature in an Ar-filled glove box. Moisture contents (< 20 ppm) and halides (Cl < 1 ppm) of all electrolytes were determined via Karl Fisher titrations (Metrohm) and ICP measurements, respectively. Table 1 lists the concentrations of each electrolyte and the molar ratio of each ion in solution. The highest Li salt concentration in this experiment was 3.2 mol.kg^{-1}, which has one Li$^+$ and one C$_3$mpyr$^+$ for every two FSI$^-$ ions in the solution (i.e., 0.5 mol fraction).

Conductivity, DSC, Viscosity and Density:

To measure ionic conductivity, samples were placed in a sealed glass conductivity dip-cell equipped with two porous platinum electrodes; all preparations took place inside an Ar-filled glove box. 0.01 M KCl solution was used to determine the cell constant, before and after each sample measurement. The ionic conductivity was measured from -50 to 100 °C and then back to 30 °C to check if there was any hysteresis.

Differential scanning calorimetry (DSC) was carried out on a TA instruments^{TM} DSC 2910. Samples (~10 mg) were sealed in Al hermetic pans (part numbers 900793.901, 900794.901) and then were cooled by liquid nitrogen at 10-20 °C.min^{-1} to -150 °C. The DSC traces were recorded during heating at 10 °C.min^{-1} to 100 °C.

An Anton Paar™ Automated Micro Viscometer with VisioLab ver. 1.0.1 was used to measure viscosity from 25 to 60 °C. An Anton Paar™ DMA 4500M was used to measure density over the same temperature range.

FT-IR:

A Perkin Elmer™ Spectrum 400 FT-IR/FT-NIR Spectrometer with Spectrum ver. 6.3.4 software was used to record FT-IR spectra. ATR mode was used at ambient temperature, after the sample was loaded into the ATR cell under argon.

Raman:

A Perkin Elmer™ Ramanstation 400F with Spectrum ver. 10.03.06.0100 was used to measure Raman spectra. All spectra were measured at ambient temperature. Baseline correction and normalization to the highest peak or area were applied to the spectra.

Diffusion NMR:

Pulse-field gradient stimulated echo (PFG-STE) diffusion measurements were performed on a Bruker 300 MHz Ultrashield with Avance I console utilizing a Diff30 diffusion probe and GREAT60 amplifier, following the method described by Bayley et al.[29] The diffusivities of ^{1}H and ^{19}F nuclei were measured for the C$_3$mpyr cation and FSI anion. ^{7}Li spectra and diffusivities were also measured; the chemical shifts are reported relative to a 2 M LiCl solution. Each sample was packed to a height of 50mm in a 5mm Schott E NMR tube in an Ar filled glove box and sealed with Teflon tape and a cap. Each sample was measured from 278 – 333 K.

RESULTS AND DISCUSSION

Conductivity and DSC:

Figure 2(a) shows the ionic conductivity data of LiFSI in C_3mpyrFSI at concentrations from the neat IL to 3.2 mol.kg^{-1}. The ionic conductivity values of the neat C_3mpyrFSI were 5.6 mS.cm^{-1}, 6.5 mS.cm^{-1}, and 7.4 mS.cm^{-1} at 20, 25 and 30 °C respectively, which is lower than the values reported by previous researchers,[2, 5-6, 8, 14, 30-31] but closer to more recently reported data.[32] We assume this difference arises from variations in the purity of the neat IL.

The neat IL changes into a solid or plastic crystal phase between -5 and -10 °C with a huge decrease in ionic conductivity. This phase transition shifts to more negative temperatures with increased salt concentration: it is between -15 and -20 °C for 0.4 mol.kg^{-1} solution and between -25 and -30 °C for 0.8 mol.kg^{-1} solution. This phase transition was not observed down to -50 °C when the salt concentration was 1.2 mol.kg^{-1} or greater. We note that the ionic conductivity of the 0.8 mol.kg^{-1} sample in the solid phase below -30 °C is higher than that of 0.4 mol.kg^{-1} in the solid phase or those for the electrolytes of higher salt concentrations (in their liquid state) at the same temperature. The ionic conductivity of the electrolytes in the solid phase has an optimum point, whilst in the liquid phase, conductivity appears to decrease as the salt concentration increases. A similar trend was also observed by Paillard et al. for LiFSI –C_4mpyrFSI electrolyte.[10] This suggests that the ionic conduction mechanism in the solid phase of the FSI electrolyte is quite different to that in the liquid phase. Figure 2(b) demonstrates the concentration dependence of ionic conductivity in C_3mpyrFSI electrolytes, from neat IL through to 3.2 mol.kg^{-1} at 25 °C, showing that the conductivity continuously decreases with increasing salt concentration in the liquid phase.

DSC heating traces from -120 to 100 °C are presented in figure 3 (a) and (b). There are several endothermic transitions in neat C_3mpyr FSI (fig 3(a) bottom curve), including a low energy solid-solid phase transition (phase III – II) with a peak at -78 °C, a combined endothermic-exothermic peak at -46 °C which was described as a mesostable phase transition by Zhou et al.,[9] a solid-solid phase transition (phase II-I) at -16 °C and a melting transition (phase I-liquid) at -6 °C. This DSC result is exactly the same as that reported previously by Zhou et al.,[9] and similar to those reported by Huang et al.[27], and Kunz et al.,[33-34] except for small peak temperature differences which are probably because of the different scan rate. When Li salt was added to C_3mpyr FSI to make a 0.4 mol.kg^{-1} solution, the melting point decreased to -15 °C, which correlates with the previous conductivity data. An exothermic crystallization peak was observed at -60 °C, and a glass transition at -95 °C. The glass transition temperature moved from -95 °C to -72 °C with the introduction of the lithium salt. The crystallization peak was not observed when the LiFSI salt concentration was 0.2 or 0.3 mol.kg^{-1} (not shown), but was observed when it was 0.5 mol.kg^{-1} or higher (figure 3 (b)). Huang et al has also described similar behaviour in solutions of LiTFSI in C_3mpyr FSI or C_3mpyr TFSI.[27] However, Paillard et al.[10] did not observe this peak for solutions of LiFSI (from 0 to 2.06 mol.kg^{-1}) in C_4mpyr FSI (which has one more methyl group in the chain attached to the pyrrolidinium ring). Instead they found that the IL solutions remained amorphous from neat IL up to a molar

ratio of LiFSI : C_4mpyr FSI of 0.4 : 0.6. This suggests that crystal formation in this FSI electrolyte system more readily occurs with the smaller C_3mpyr$^+$ cation.

At higher concentrations, we do note that there is evidence, in some cases, that multiple steps exist in the Tg shown in figure 3 (b). This may be not unexpected due to the high salt concentrations used here; while they are clearly miscible at room temperature there appears to be a phase separation in the glassy state as shown by the steps in Tg.

Density, Viscosity and Walden plots:

A Walden plot based on the Walden equation (eq. 1) described by Angell and co-workers is an effective qualitative method to characterise the properties of an IL.[35]

$$\Lambda\eta^\alpha = C \qquad , \qquad (1)$$

where Λ is the molar conductivity, η is the viscosity, α is an adjustable parameter and C is a temperature dependent constant.

Recently, MacFarlane et al. suggested and demonstrated a modified Walden plot including the effect of each ion in an IL, since the traditional Walden rule assumes all participating ions are of equal size.[36] The role of ion size can be deduced from the Stokes-Einstein equation (eq. 2) and combined with the Nernst-Einstein equation (eq. 3) to yield a modified Walden equation (eq. 4).[36]

$$D_i = \frac{K_b T}{6\pi\eta r_i} \qquad (2)$$

$$\Lambda = \frac{N_A e^2}{kT}(D^+ + D^-) \qquad (3)$$

$$\Lambda = C'\eta^\alpha \left(\frac{1}{r^+} + \frac{1}{r^-}\right) \qquad (4)$$

where r^+ and r^- are the respective effective cation and anion sizes. Since there are 2 different sized cations in the electrolyte, Li$^+$ and C_3mpyr$^+$, r^+ is the weight average radius of both cations. From equation 4, we can plot the log molar conductivity vs. log inverse adjusted viscosity (corrected for effective ion sizes) to get α and C'.

The Walden plots of each concentrated electrolyte are shown in figure 4. The slopes of the plots are from 0.9 to 0.95, which is similar to the values generally observed for other ILs.[35, 37-40] The C' values, which represent the distance from the ideal KCl line, change from -0.009 to -0.446 when going from the neat IL to 2.4 mol.kg^{-1} LIFSI. The trend then changes direction; at 3.2 mol.kg^{-1} LIFSI, $C' = -0.355$. A 'good IL' has a line close to the ideal line ($\alpha = 1$, $C' = 0$) in the Walden plot;[35-36] lines far from the ideal line ($C' \ll 0$) mean that more ions are associated in various forms.[41] Hence, the conductivity did not decrease as much as the viscosity increased when the salt concentration increased from 2.4 mol.kg^{-1} to 3.2 mol.kg^{-1},

which again implies that there may be a different conduction mechanism in the solution with the highest lithium concentration; this mechanism may be related to Li coordination with surrounding ions.

Diffusivity and Ionicity:

To understand the local environment surrounding Li^+ and its effects on ionic mobility and conductivity, 1D NMR spectra and PFG-STE NMR diffusion coefficients for ^7Li, ^1H, and ^{19}F were measured.

In order to set the pulse sequence for the PFG-STE experiment, we have measured the 1D NMR spectra, Figure 5, which shows that the ^7Li NMR peak position unexpectedly shifts to more negative values with increasing Li salt concentration in the electrolytes. This suggests that, as the number of Li^+ ions in the ionic liquid increases, its nearest neighbour environment (and possibly its coordination) changes, resulting in the observed chemical shift. We did not observer similar shifts in either the ^{19}F and ^1H spectra under the same experimental conditions, thereby allowing us to rule out magnetic susceptibility effects for the shift in the ^7Li spectra.[42] This is somewhat in contrast to work by Shirai et al. in their studies on the effect of LiTFSI concentration in N,N-diethyl-N-methyl-N-(2-methoxyethyl) ammonium TFSI; they observed a ^{19}F NMR peak shift to higher ppm, whilst the ^7Li peak did not move.[20] With the support of Raman data, they concluded that Li forms $Li(TFSI)_2^-$ in lower concentration solutions and forms a Li oligomer (as also observed in $Li_2emim(TFSI)_3$ ILs by Matsumoto et al.[43]) at higher salt concentrations. Given that our results for the FSI electrolytes presented here are the opposite of those found for the TFSI system, this suggests, somewhat surprisingly, that the coordination of Li in the FSI-based ILs is likely to be different.

The diffusivities of each ion in both the neat IL and the LiFSI solutions, as measured by PFG-STE NMR, are presented in figure 6. The diffusivities of all ions decreased as the Li^+ concentration in solution increased. Figure 6(a) shows the diffusivity plots for neat $C_3mpyrFSI$, where FSI^- is faster than C_3mpyr^+ at 25 °C. The difference in diffusivity between the two ions became smaller at 60 °C. When 0.8 mol.kg^{-1} of LiFSI salt was added into the neat IL (figure 6(b) and table 2), the order of diffusivities of the ions at 25 °C was $FSI^- > C_3mpyr^+ > Li^+$. As Li salt concentration is further increased up to 3.2 mol.kg^{-1}, the diffusivities of all ion species are decreased. Presumably the addition of Li^+ decreases the fluidity of the entire system and hence all ions show a decreased diffusivity, however, as seen from figure S1, the rate at which the diffusion coefficient decreases with increasing LiFSI concentration is greatest for the FSI ion, followed by C_3mpyr and finally the Li^+ diffusivity. Since a high Li^+ concentration means a relatively smaller amount of C_3mpyr^+ interacting with the FSI^-, this trends implies that the Li^+ ion has a much stronger influence on the FSI^- diffusion and thus possibly implies a more aggregated structure whereby the ions are not moving independently of one another but rather as a larger species. Interestingly, for all concentrations, the temperature dependence of the diffusion coefficients for both cations is almost identical, indicating similar activation energies, whereas the anion appears to have an apparently smaller activation energy for all compositions, even in the neat ionic liquid.

The diffusivity of each ion followed a simple Arrhenius equation:

$$D = D_0 \, exp(-\frac{E_A}{RT}), \qquad (5)$$

where, D is diffusivity at each temperature, D_0 is self diffusion constant, E_A is activation energy and R is the gas constant. The calculated D_0 and E_A values are presented in table 2. Both the self diffusion constants and activation energies of all ion species increased with increased Li salt concentration, hence the diffusivity decreased with increased salt concentration because of the increased activation energy, which is related to the strength of interaction between the ions.

According to Seki[44], who compared ILs containing imidazolium and phosphonium cations, a higher D_0 value results in lower viscosity and density, and higher ionic conductivity. However, in contrast to Seki's study with different ion species, our present system has the same cation and anion, and only differs in lithium concentration. In our case, the highest D_0 value occurs at the highest concentration, which is the sample with the highest viscosity and density and lowest ionic conductivity.

The diffusivity obtained by PFG-NMR does not distinguish between ion pairs and dissociated ions and is, rather, the average diffusivity over all possible species.[29] The NMR conductivity Λ_{NMR}, as calculated from the Nernst-Einstein equation (equation 3), assumes contributions from all individual ions, regardless of ion association. However, the molar conductivity obtained by impedance spectroscopy, Λ_{imp}, only includes conductivity due to dissociated ions or charged aggregates.[29] Hence, the ratio $\Lambda_{imp} / \Lambda_{NMR}$ is referred to as the ionicity, and represents the degree of ion correlation within the IL; if the ionicity is unity, all ions are assumed to be dissociated and no ion pairs or ionic clusters are present.[29, 44-47] The calculated ionicity values for each solution are presented in table 3. The ionicity increases as temperature increases, but decreases with increased salt concentration; consistent with the previous interpretation of the diffusivity data. One interesting point here is that the ionicity was lowest when the Li salt concentration was 2.4 mol.kg^{-1} and increased again at 3.2 mol.kg^{-1}, after the addition of more Li salt. This also correlates with the Walden plot (shown previously in figure 4). This may indicate that the increased Li^+ concentration enhances the ion pair association or clustering for the neat IL to the 2.4 mol.kg^{-1} solutions but adding more Li^+ up to 3.2 mol.kg^{-1} does not contribute to ion pairing or clustering; instead the additional Li may exist as free Li^+ on the time scales of the measurements here.

In addition, the Li^+ partial conductivity calculated from the NMR diffusivity data in figure 6 using the Nernst-Einstein equation (eq. 3) is presented in figure 7. While the actual total conductivity decreases with increased salt concentration, the Li^+ partial conductivity increases up to 1.6 mol.kg^{-1} salt concentration while the contributions of the C_3mpyr^+ and FSI^- conductivities, 0.72 and 1.13 mS.cm^{-1} respectively at 1.6

mol.kg^{-1}, decrease as the relative molar fraction of Li$^+$ increases.

FSI configuration with Li salts:

We have used FT-IR and Raman spectroscopy to study the interactions between Li$^+$, C$_3$mpyr$^+$, and FSI$^-$ The FT-IR and Raman spectra for each Li salt concentration are presented in figure 8. We have assigned the peaks based on the assignments for 0.5 mol.kg^{-1} LiTFSI in C$_3$mpyrFSI by Hardwick et al.[48]

Figure 8 (a) presents the FT-IR spectra for various LiFSI concentrations in the C$_3$mpyr FSI. The S-N-S stretching peaks at 730 and 830 cm^{-1} respectively, become restricted and shift to higher wavenumber, with S-F asymmetrical stretching (830 cm^{-1}) closer to the peak position in the pure LiFSI salt. These changes are anticipated as both symmetric and asymmetric bond stretching in FSI will be strongly associated with the Li ion.

Figure 8 (b) shows the FT-IR spectra for the asymmetric SO$_2$ bending that is located at 564 cm^{-1}. A shoulder appears at ~595 cm^{-1} which increases in intensity with increasing salt concentration, a phenomena was has also been reported by Huang et al.[27] Raman peaks in figure 8 (c) and 8 (d) were assigned according to the previous reports by Fujii et al.[18] and Castriota et al.[49]. The data show that the peaks at 1215 cm^{-1} (υ(SO$_2$)) and 720 cm^{-1} (υ_s(SNS)) are shifted toward higher frequency and peak broadening occurs as the LiFSI salt concentration increases. Together, these three spectra imply there are changes in the coordination between FSI$^-$ and Li$^+$ which we ascribe to ion-paring effects in the electrolyte. Due to the high salt concentrations, and the peaks in the spectra being quite broad in nature, we would also expect that there are higher levels of ion-pairing present such as doubles, triples and polymer-like aggregates. This observation is consistent with the ionicity data presented earlier. Hardwick et al. also reported that the Raman peaks shift to higher frequency for the TFSI system (figure 8 (c)) which indicates that Li$^+$ is bound to the TFSI anion[50]; this interpretation is consistent with our observations in the FSI system studied here.

Furthermore, Fujii et al. calculated theoretical Raman peak positions and compared them with experimental Raman spectra.[24-25] The peaks for the trans-form of FSI (or C2 conformer) were calculated in the liquid phase to be at 353, 316 and 275 cm^{-1} and the peaks for a cis-form (or C1 conformer) were calculated as 344, 315 and 278 cm^{-1}. While the absolute peak positions in this experiment are slightly different from these calculated values, Figure 9 clearly shows that the trans-form of the FSI conformer is changing into the cis-form with increasing Li$^+$ concentration.

The FT-IR and Raman spectra clearly show that a percentage of FSI anions are converted from the trans- to cis- conformer as increasing amounts of Li salt is added to the IL. Fujii et al. have shown, using Raman and ab-initio calculations, that the binding energy of Li$^+$ in the cis- conformer is lower than in the trans- conformer.[51] Such a change may allow Li ions to move via a site activation model, analogous to that observed in polymer electrolytes. One could therefore postulate that these changes could affect the transport mechanism of Li$^+$ at these high salt concentrations, going from being dominated by vehicular transport to a mixed conduction mechanism.

CONCLUSIONS

We have previously shown that high concentration FSI-based ionic liquid electrolytes display interesting electrochemical properties, exhibit high Li$^+$ transport number and excellent rate capability in lithium batteries. This work seeks to understand why this might be the case through the use of a number of different physical characterisation techniques. The conductivity, viscosity, density and DSC data for C$_3$mpyrFSI with different LiFSI salt concentrations from 0 to 3.2 mol.kg^{-1} (1 : 1 : 2 molar ratio of Li$^+$: C$_3$mpyr$^+$: FSI$^-$) are reported. The Walden plots and ionicity data show that these electrolytes exhibit behaviour closer to that of an ideal IL at the higher salt concentration of 3.2 mol.kg^{-1} (or 0.5 mol fraction). FT-IR and Raman spectra show two distinct behaviours; ion-paring with increasing salt concentration and a shift in the preferred conformation of the anion to a mixture of cis- / trans- FSI species. As the lithium concentration increases, the conformation of FSI$^-$ changes from largely trans- to a mostly cis- form. The changes in the local structure of the FSI based electrolytes leads us to postulate that this may be the origin of the enhanced transport properties.

^{7}Li NMR showed a shift to higher fields, consistent with a more electron-shielded environment as the Li$^+$ concentration increased. The NMR diffusivity measurements show that, at a high lithium concentration, the mobility of Li$^+$ relative to that of the other ionic species is greater than in solutions with lower lithium concentrations. These results imply that the coordination of the lithium ion in the FSI-based IL containing a high Li$^+$ concentration is different, and that the Li$^+$ transport mechanism may be different from that seen in TFSI-based ILs or FSI-based ILs at low Li salt concentrations.

REFERENCES

1.   Shin, J. H.; Henderson, W. A.; Passerini, S., *Electrochem. Commun.* **2003,** *5* (12), 1016-1020.
2.   Matsumoto, H.; Sakaebe, H.; Tatsumi, K.; Kikuta, M.; Ishiko, E.; Kono, M., *J. Power Sources* **2006,** *160* (2), 1308-1313.
3.   Armand, M.; Choquette, Y.; Gauthier, M.; Michot, C.; Chobuette, Y.; Kapfer, B. Salts of perfluorinated amides - useful materials with ionic and electronic conduction, as colourants and catalysts. EP850920-A; WO9829358-A; etc., Dec 30 1997.

4.   Zaghib, K.; Charest, P.; Guerfi, A.; Shim, J.; Perrier, M.; Striebel, K., *J. Power Sources* **2004,** *134* (1), 124-129.
5.   Ishikawa, M.; Sugimoto, T.; Kikuta, M.; Ishiko, E.; Kono, M., *J. Power Sources* **2006,** *162* (1), 658-662.
6.   Guerfi, A.; Duchesne, S.; Kobayashi, Y.; Vijh, A.; Zaghib, K., *J. Power Sources* **2008,** *175* (2), 866-873.
7.   Saint, J.; Best, A. S.; Hollenkamp, A. F.; Kerr, J.; Shin, J. H.; Doeff, M. M., *J. Electrochem. Soc.* **2008,** *155* (2), A172-A180.
8.   Seki, S.; Kobayashi, Y.; Miyashiro, H.; Ohno, Y.; Mita, Y.; Terada, N.; Charest, P.; Guerfi, A.; Zaghib, K., *J. Phys. Chem. C* **2008,** *112* (42), 16708-16713.
9.   Zhou, Q.; Henderson, W. A.; Appetecchi, G. B.; Montanino, M.; Passerini, S., *J. Phys. Chem. B* **2008,** *112* (43), 13577-13580.
10.   Paillard, E.; Zhou, Q.; Henderson, W. A.; Appetecchi, G. B.; Montanino, M.; Passerini, S., *J. Electrochem. Soc.* **2009,** *156* (11), A891-A895.
11.   Best, A. S.; Bhatt, A. I.; Hollenkamp, A. F., *J. Electrochem. Soc.* **2010,** *157* (8), A903-A911.
12.   Bhatt, A. I.; Best, A. S.; Huang, J.; Hollenkamp, A. F., *J. Electrochem. Soc.* **2010,** *157* (1), A66-A74.
13.   Lewandowski, A.; Acznik, I., *Electrochim. Acta* **2010,** *56* (1), 211-214.
14.   Wang, Y.; Zaghib, K.; Guerfi, A.; Bazito, F. F. C.; Torresi, R. M.; Dahn, J. R., *Electrochim. Acta* **2007,** *52* (22), 6346-6352.
15.   Abouimrane, A.; Ding, J.; Davidson, I. J., *J. Power Sources* **2009,** *189* (1), 693-696.
16.   Vijayaraghavan, R.; Surianarayanan, M.; Armel, V.; MacFarlane, D. R.; Sridhar, V. P., *Chemical Communications* **2009,** (41), 6297-6299.
17.   Johansson, P.; Gejji, S. P.; Tegenfeldt, J.; Lindgren, J., *Electrochim. Acta* **1998,** *43* (10-11), 1375-1379.
18.   Fujii, K.; Fujimori, T.; Takamuku, T.; Kanzaki, R.; Umebayashi, Y.; Ishiguro, S. I., *Journal of Physical Chemistry B* **2006,** *110* (16), 8179-8183.
19.   Umebayashi, Y.; Mitsugi, T.; Fukuda, S.; Fujimori, T.; Fujii, K.; Kanzaki, R.; Takeuchi, M.; Ishiguro, S.-I., *Journal of Physical Chemistry B* **2007,** *111* (45), 13028-13032.
20.   Shirai, A.; Fuji, K.; Seki, S.; Umebayashi, Y.; Ishiguro, S.-i.; Ikeda, Y., *Anal. Sci.* **2008,** *24* (10), 1291-1296.
21.   Ishiguro, S.-i.; Umebayashi, Y.; Kanzaki, R.; Fujii, K., *Pure and Applied Chemistry* **2010,** *82* (10), 1927-1941.
22.   Umebayashi, Y.; Yamaguchi, T.; Fukuda, S.; Mitsugi, T.; Takeuchi, M.; Fujii, K.; Ishiguro, S.-i., *Anal. Sci.* **2008,** *24* (10), 1297-1304.
23.   Beran, M.; Prihoda, J.; Zak, Z.; Cernik, M., *Polyhedron* **2006,** *25* (6), 1292-1298.
24.   Fujii, K.; Seki, S.; Fukuda, S.; Kanzaki, R.; Takamuku, T.; Ulmebayashi, Y.; Ishiguro, S.-i., *J. Phys. Chem. B* **2007,** *111* (44), 12829-12833.
25.   Fujii, K.; Seki, S.; Fukuda, S.; Takamuku, T.; Kohara, S.; Kameda, Y.; Umebayashi, Y.; Ishiguro, S., *Journal of Molecular Liquids* **2008,** *143* (1), 64-69.
26.   Lopes, J. N. C.; Shimizu, K.; Padua, A. A. H.; Umebayashi, Y.; Fukuda, S.; Fujii, K.; Ishiguro, S.-i., *J. Phys. Chem. B* **2008,** *112* (31), 9449-9455.
27.   Huang, J.; Hollenkamp, A. F., *J. Phys. Chem. C* **2010,** *114* (49), 21840-21847.

28.   Yoon, H.; Howlett, P. C.; Best, A. S.; Forsyth, M.; MacFarlane, D. R., *Journal of the Electrochemical Society* **2013,** *160* (10), A1629-A1637.
29.   Bayley, P. M.; Lane, G. H.; Rocher, N. M.; Clare, B. R.; Best, A. S.; MacFarlane, D. R.; Forsyth, M., *Phys. Chem. Chem. Phys.* **2009,** *11* (33), 7202-7208.
30.   Guerfi, A.; Dontigny, M.; Kobayashi, Y.; Vijh, A.; Zaghib, K., *J. Solid State Electrochem.* **2009,** *13* (7), 1003-1014.
31.   Hayamizu, K.; Tsuzuki, S.; Seki, S.; Fujii, K.; Suenaga, M.; Umebayashi, Y., *Journal of Chemical Physics* **2010,** *133* (19).
32.   Johansson, P.; Fast, L. E.; Matic, A.; Appetecchi, G. B.; Passerini, S., *Journal of Power Sources* **2010,** *195* (7), 2074-2076.
33.   Kunze, M.; Montanino, M.; Appetecchi, G. B.; Jeong, S.; Schoenhoff, M.; Winter, M.; Passerini, S., *J. Phys. Chem. A* **2010,** *114* (4), 1776-1782.
34.   Kunze, M.; Jeong, S.; Paillard, E.; Winter, M.; Passerini, S., *J. Phys. Chem. C* **2010,** *114* (28), 12364-12369.
35.   Angell, C. A.; Byrne, N.; Belieres, J.-P., *Accounts Chem. Res.* **2007,** *40* (11), 1228-1236.
36.   MacFarlane, D. R.; Forsyth, M.; Izgorodina, E. I.; Abbott, A. P.; Annat, G.; Fraser, K., *Phys. Chem. Chem. Phys.* **2009,** *11* (25), 4962-4967.
37.   Xu, W.; Cooper, E. I.; Angell, C. A., *J. Phys. Chem. B* **2003,** *107* (25), 6170-6178.
38.   Ferrari, S.; Quartarone, E.; Mustarelli, P.; Magistris, A.; Protti, S.; Lazzaroni, S.; Fagnoni, M.; Albini, A., *J. Power Sources* **2009,** *194* (1), 45-50.
39.   Ueno, K.; Tokuda, H.; Watanabe, M., *Phys. Chem. Chem. Phys.* **2010,** *12* (8), 1649-1658.
40.   Makino, T.; Kanakubo, M.; Umecky, T.; Suzuki, A.; Nishida, T.; Takano, J., *Journal of Chemical and Engineering Data* **2012,** *57* (3), 751-755.
41.   Fraser, K. J.; Izgorodina, E. I.; Forsyth, M.; Scott, J. L.; MacFarlane, D. R., *Chemical Communications* **2007,** (37), 3817-3819.
42.   Takamuku, T.; Kyoshoin, Y.; Shimomura, T.; Kittaka, S.; Yamaguchi, T., *Journal of Physical Chemistry B* **2009,** *113* (31), 10817-10824.
43.   Matsumoto, K.; Hagiwara, R.; Tamada, O., *Solid State Sci.* **2006,** *8* (9), 1103-1107.
44.   Seki, S.; Hayamizu, K.; Tsuzuki, S.; Fujii, K.; Umebayashi, Y.; Mitsugi, T.; Kobayashi, T.; Ohno, Y.; Kobayashi, Y.; Mita, Y.; Miyashiro, H.; Ishiguro, S.-i., *Phys. Chem. Chem. Phys.* **2009,** *11* (18), 3509-3514.
45.   Tokuda, H.; Hayamizu, K.; Ishii, K.; Abu Bin Hasan Susan, M.; Watanabe, M., *J. Phys. Chem. B* **2004,** *108* (42), 16593-16600.
46.   Tokuda, H.; Tsuzuki, S.; Susan, M.; Hayamizu, K.; Watanabe, M., *J. Phys. Chem. B* **2006,** *110* (39), 19593-19600.
47.   Fernicola, A.; Scrosati, B.; Ohno, H., *Ionics* **2006,** *12* (2), 95-102.
48.   Hardwick, L. J.; Saint, J. A.; Lucas, I. T.; Doeff, M. M.; Kostecki, R., *J. Electrochem. Soc.* **2009,** *156* (2), A120-A127.
49.   Castriota, M.; Caruso, T.; Agostino, R. G.; Cazzanelli, E.; Henderson, W. A.; Passerini, S., *Journal of Physical Chemistry A* **2005,** *109* (1), 92-96.

50.   Hardwick, L. J.; Hahn, M.; Ruch, P.; Holzapfel, M.; Scheifele, W.; Buqa, H.; Krumeich, F.; Novak, P.; Koetz, R., *Electrochim. Acta* **2006,** *52* (2), 675-680.
51.   Fujii, K.; Nonaka, T.; Akimoto, Y.; Umebayashi, Y.; Ishiguro, S.-i., *Anal. Sci.* **2008,** *24* (10), 1377-1380.
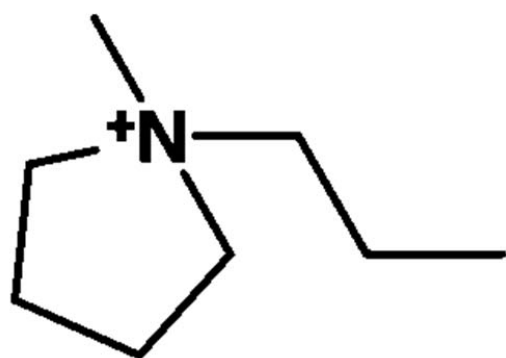
N-propyl-N-methylpyrrolidinium
(C_3mpyr$^+$)
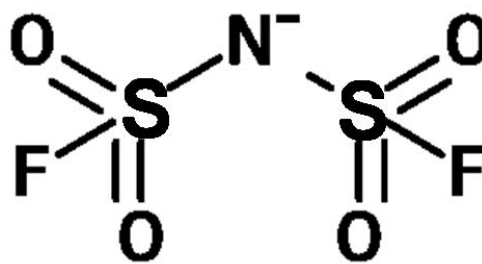
Bis(fluorosulfonyl)imide (FSI$^-$)

Figure 1 The structure of the ionic liquid

Table 1 Composition of electrolytes investigated.

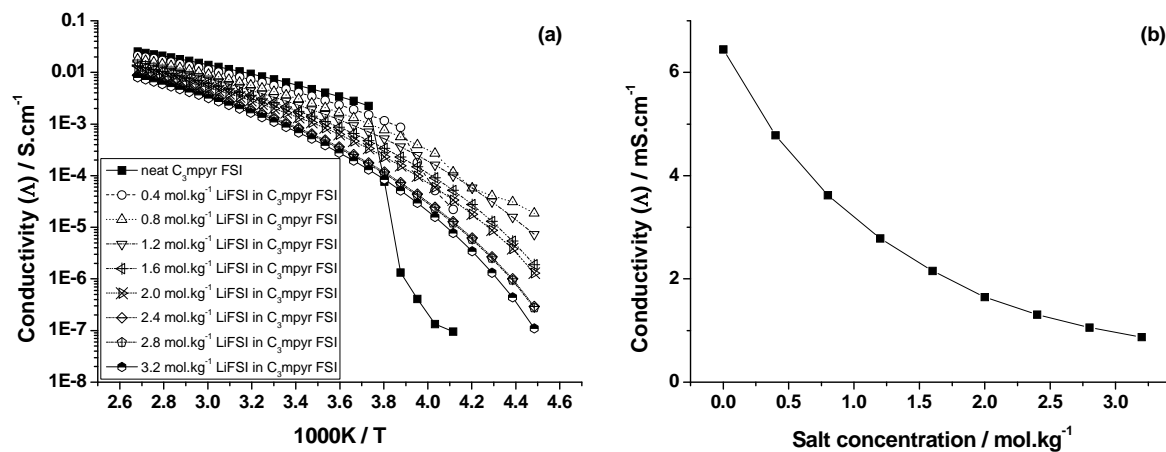| LiFSI conc.	Molar ratio of each ion		
(mol.kg^{-1})	Li$^+$	C$_3$mpyr$^+$	FSI$^-$
0 (neat IL)	0	0.50	0.50
0.4	0.06	0.44	0.50
0.8	0.10	0.40	0.50
1.2	0.14	0.36	0.50
1.6	0.17	0.33	0.50
2.0	0.19	0.31	0.50
2.4	0.21	0.29	0.50
2.8	0.23	0.27	0.50
3.2	0.25	0.25	0.50

Figure 2 (a) Temperature dependence of ionic conductivity of C_3mpyr FSI with different LiFSI concentrations, (b) Dependence of ionic conductivity on LiFSI concentration in C_3mpyr FSI at 25 °C
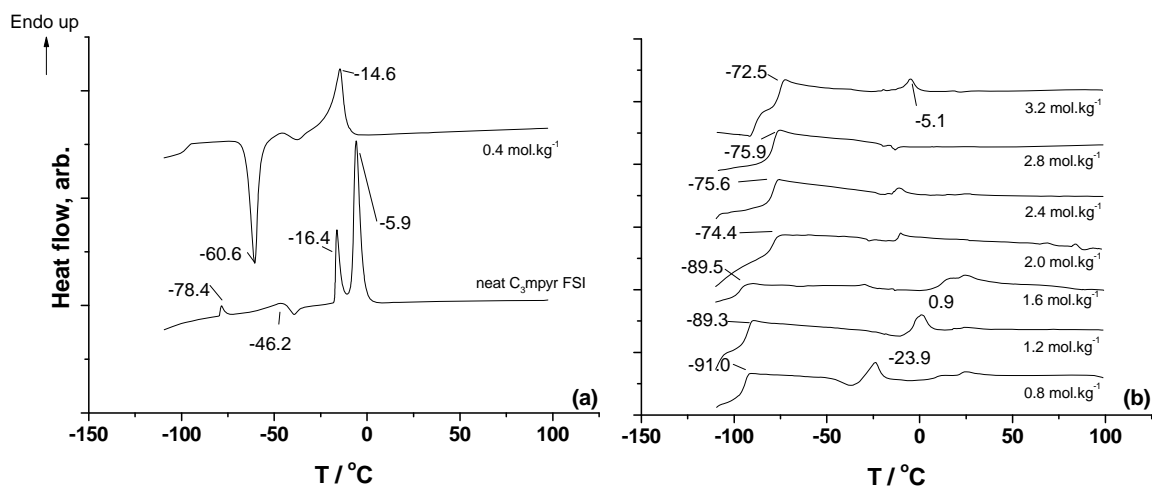
Figure 3 DSC traces for C$_3$mpyr FSI with LiFSI ionic liquids as a function of LiFSI concentration. a) neat C$_3$mpyrFSI and 0.4 mol.kg^{-1} LiFSI added C$_3$mpyrFSI, b) 0.8 to 3.2 mol.kg^{-1} LiFSI added C$_3$mpyrFSI. The numbers provided indicate the temperatures of the peak positions.
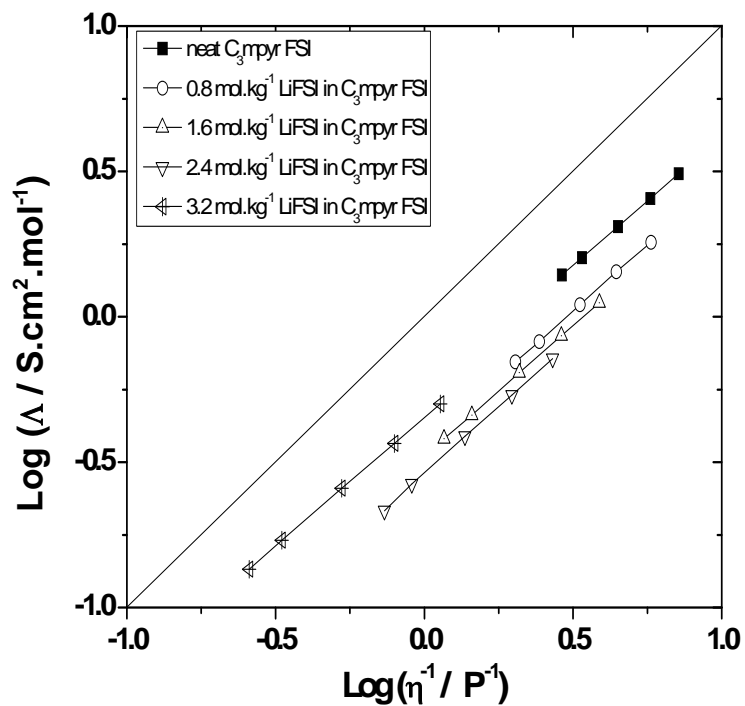
Figure 4 Walden plots showing relationships between inverse viscosity and molar conductivity for C$_3$mpyrFSI with different LiFSI concentrations and the neat IL

Figure 5 ^{7}Li NMR chemical shifts at 25 °C (2 M LiCl reference). Arrow indicates direction of increasing LiFSI concentration.

Figure 6 Diffusivities of Li^+, C_3mpyr^+ and FSI^- ions measured using PFG-STE NMR from 25 °C to 60 °C. (a) neat C_3mpyr FSI; (b) 0.8 mol.kg^{-1}, (c) 1.6 mol.kg^{-1}, (d) 2.4 mol.kg^{-1}, and (e) 3.2 mol.kg^{-1} LiFSI in C_3mpyr FSI.

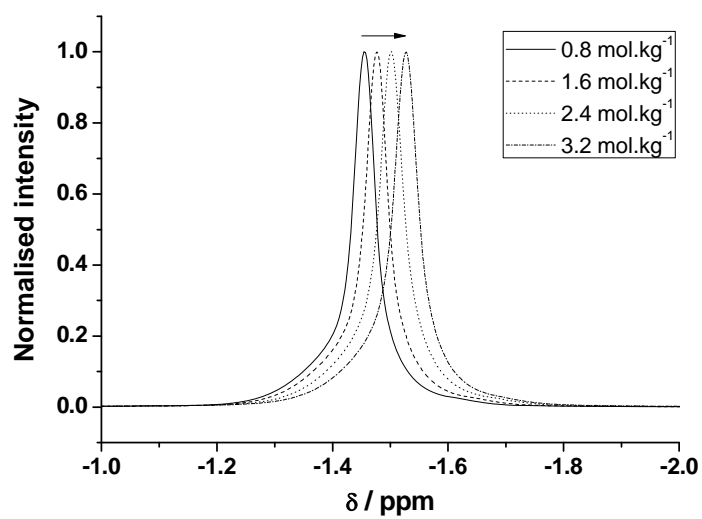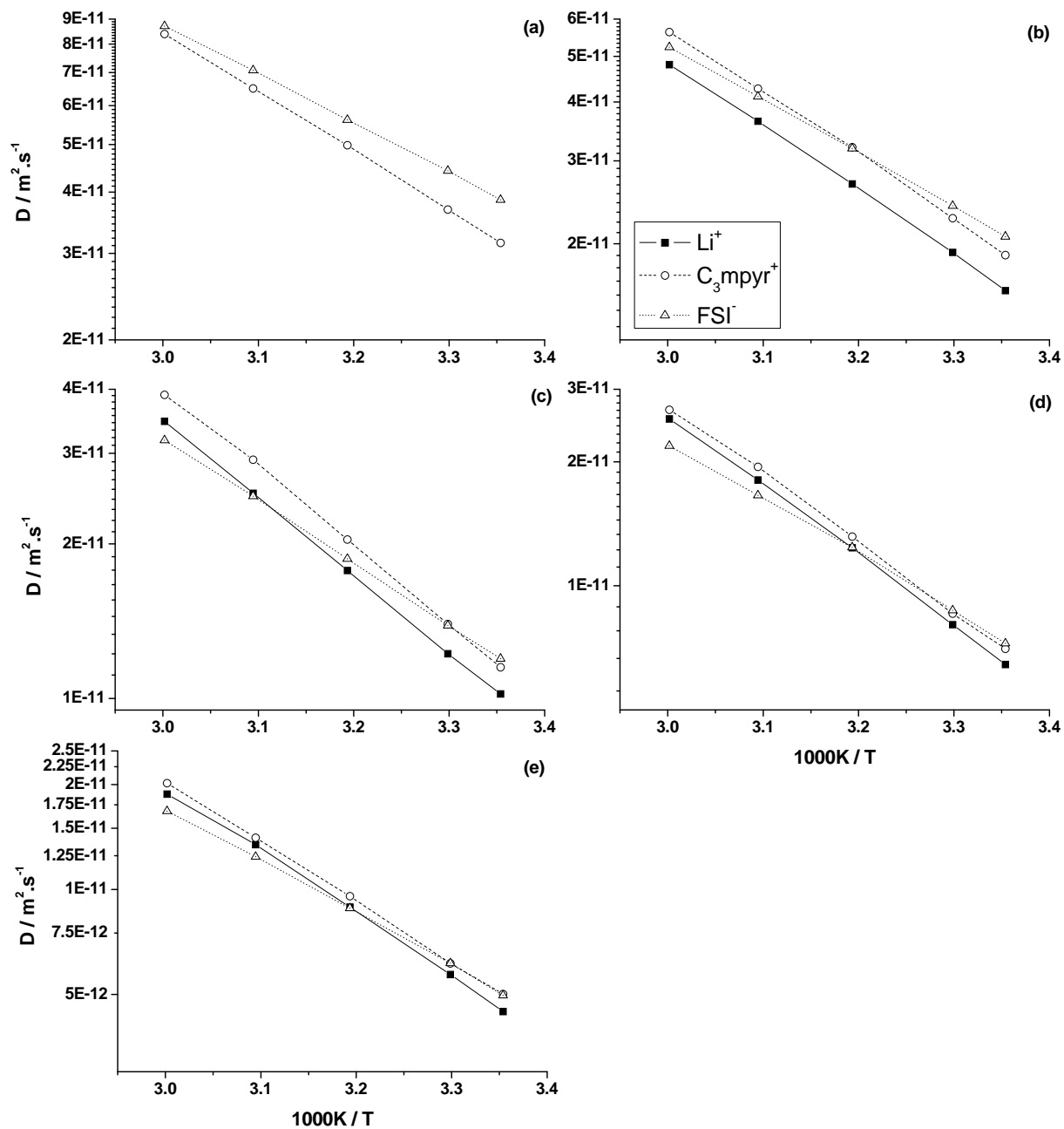**Table 2** Parameters from Arrhenius fits to diffusivity data: self diffusion constant, D_0 and activation energy, E_A for each ion in C$_3$mpyr FSI ionic liquid as a function of LiFSI concentration. ($< \pm 5\%$)

	Li$^+$		C$_3$mpyr$^+$		FSI$^-$	
	D_0 $(m^2.sec^{-1})$	E_A $(kJ.mol^{-1})$	D_0 $(m^2.sec^{-1})$	E_A $(kJ.mol^{-1})$	D_0 $(m^2.sec^{-1})$	E_A $(kJ.mol^{-1})$
Neat IL	-	-	$3.5e^{-7}$	23	$9.0e^{-8}$	19
0.8 mol.kg^{-1}	$5.9e^{-7}$	26	$6.2e^{-7}$	25	$1.4e^{-7}$	22
1.6 mol.kg^{-1}	$1.2e^{-6}$	29	$1.4e^{-6}$	29	$1.4e^{-7}$	23
2.4 mol.kg^{-1}	$3.2e^{-6}$	33	$2.8e^{-6}$	32	$2.7e^{-7}$	26
3.2 mol.kg^{-1}	$4.3e^{-6}$	34	$3.2e^{-6}$	33	$5.4e^{-7}$	29

Table 3 'Ionicity' of electrolytes indicating the degree of ion dissociation at each temperature and lithium salt concentration. ($< \pm 5\%$)

$\Lambda_{Imp} / \Lambda_{NMR}$	25 °C	30 °C	40 °C	50 °C	60 °C
Neat IL	0.56	0.57	0.57	0.58	0.58
0.8 mol.kg^{-1}	0.50	0.51	0.51	0.53	0.53
1.6 mol.kg^{-1}	0.46	0.48	0.49	0.50	0.50
2.4 mol.kg^{-1}	0.35	0.36	0.37	0.39	0.40
3.2 mol.kg^{-1}	0.39	0.40	0.42	0.43	0.43
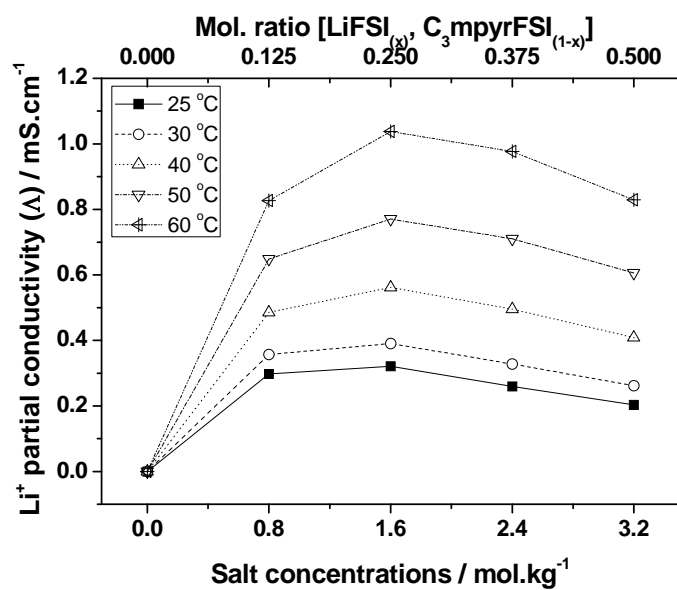
Figure 7 The partial conductivity of Li$^+$ in the solution, calculated from the ionic mobility data.
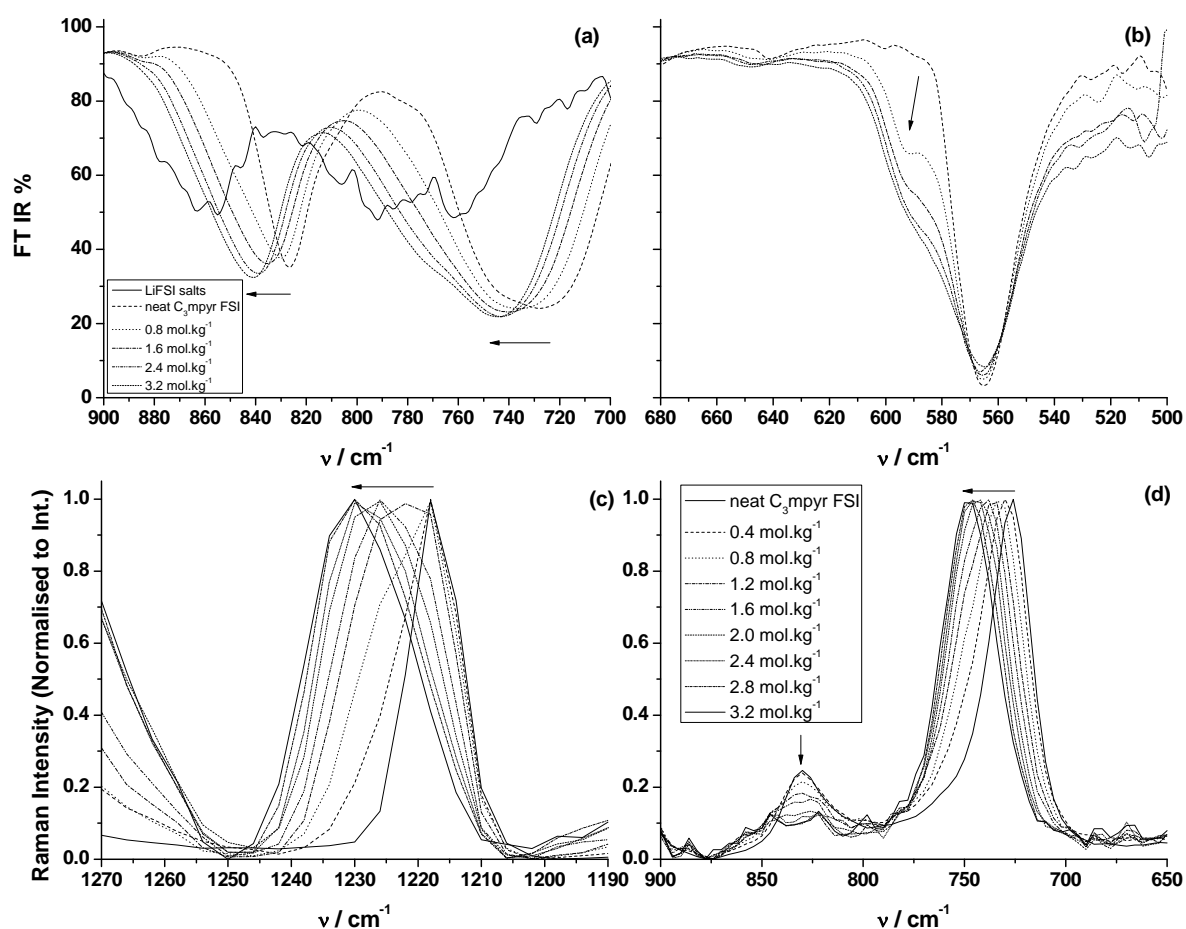
Figure 8 FT-IR transmittance and Raman spectra; (a) FT-IR from 900 to 700 cm^{-1}, (b) FT-IR from 680 to 500 cm^{-1}, (c) Raman from 1270 to 1190 cm^{-1}, (d) Raman from 900 to 650 cm^{-1}. Note that the intensities of the LiFSI salt spectra in FT-IR (a) (thin black) were magnified.
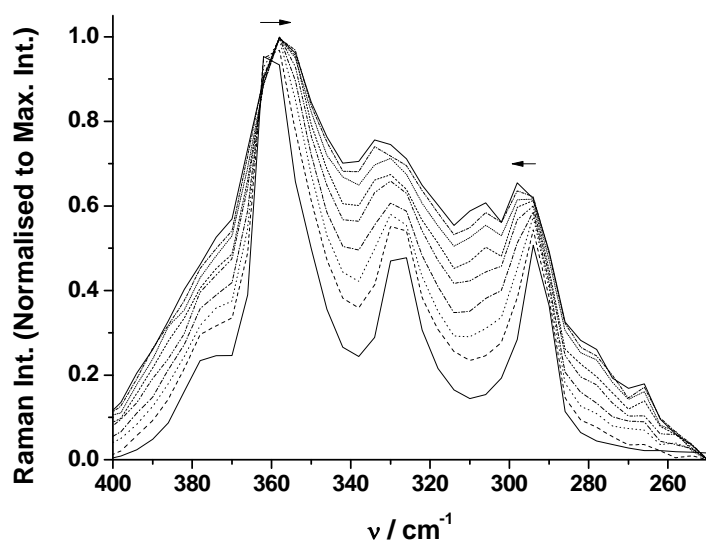
Figure 9 Selected regions of Raman spectra in 400 – 250 cm^{-1} range. Note that all peaks were baseline corrected and normalized to the maximum intensity or area. Arrow indicates direction of increasing LiFSI concentration.
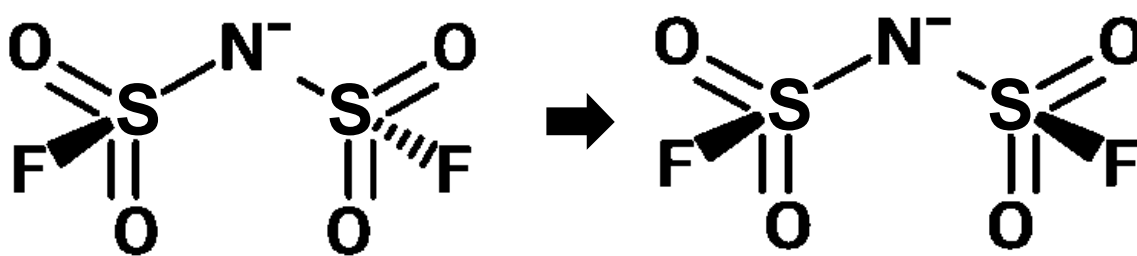
Figure 10 trans- and cis- conformations of FSI⁻

Physical properties of *N*-propyl-*N*-methylpyrrolidinium bis(fluorosulfonyl)imide in high LiFSI concentration: Supplement figures

Hyungook Yoon,[†,‡,§] Patrick C. Howlett,[§] Adam S. Best,[*,‡] Maria Forsyth,[§] and Douglas R. MacFarlane [†]

[†] School of Chemistry, Monash University, 3800 Victoria, Australia

[*,‡] Commonwealth Scientific and Industrial Research Organisation (CSIRO), Division of Energy Technology, Bayview Ave., Clayton, 3169 Victoria, Australia; Tel: ▓▓▓▓▓▓▓▓▓ E-mail: ▓▓▓▓▓▓▓▓▓

[§] ARC Centre of Excellence for Electromaterials Science (ACES), Institute for Frontier Materials (IFM), Deakin University, Burwood, Victoria 3125, Australia

KEYWORDS : Ionic liquids, FSI, concentration, conformation, diffusivity
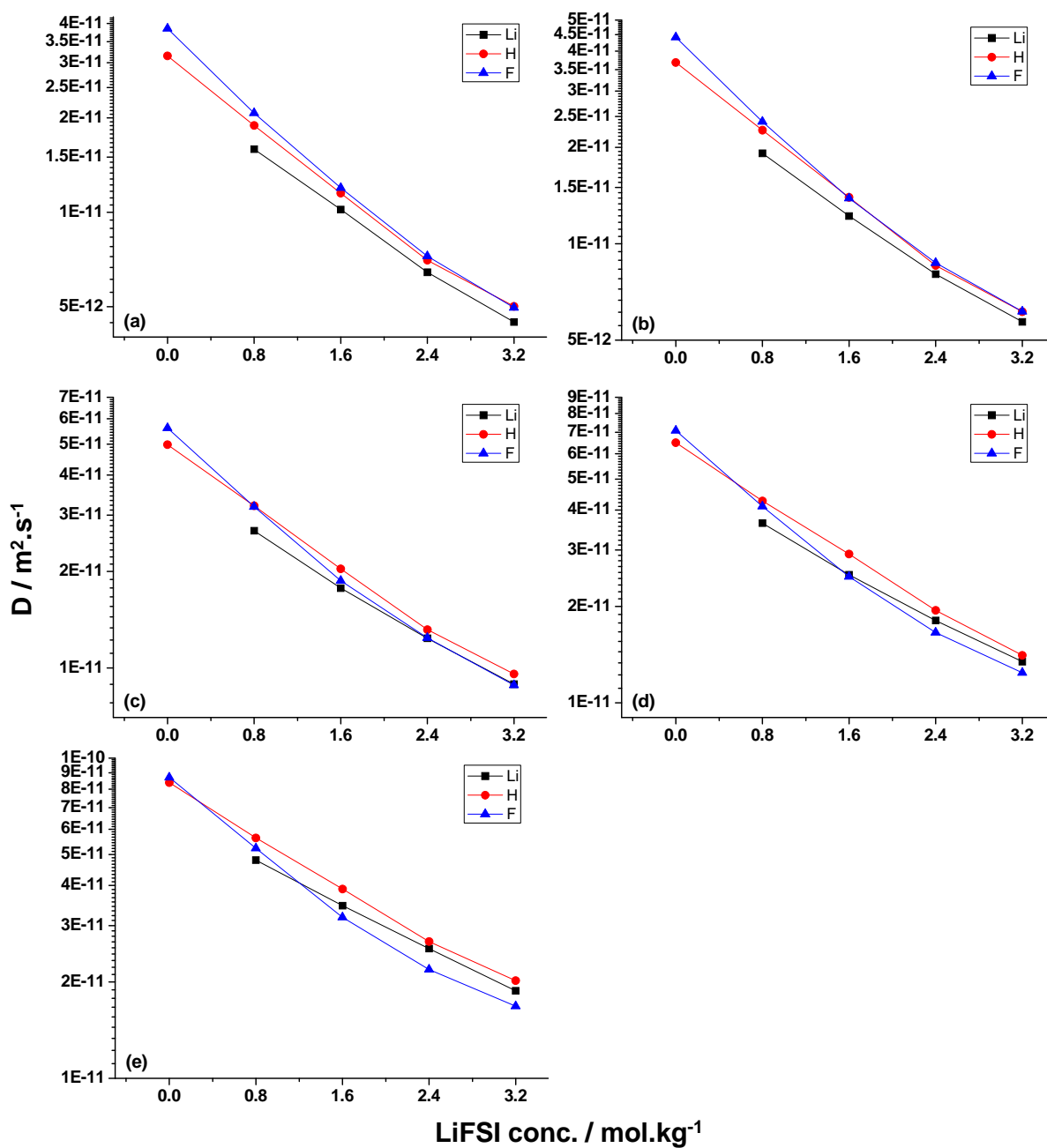
Supplement Figure 1: Diffusivities of Li$^+$, C$_3$mpyr$^+$ and FSI$^-$ ions measured using PFG-STE NMR by salt concentration (a) at 25 °C, (b) at 30 °C, (c) at 40 °C, (e) at 50 °C, (f) at 60 °C.

vibrational mode	neat C_3mpyrFSI	0.8 mol.kg^{-1} LiFSI in IL	1.6 mol.kg^{-1} LiFSI in IL	2.4 mol.kg^{-1} LiFSI in IL	3.2 mol.kg^{-1} LiFSI in IL
υCH_2 C_3mpyr	2980	2981	2982	2982	2983
υCH_2 C_3mpyr	2889	2889	2890	2890	2891
δCH_2, $CH_3 C_3$mpyr	1469	1469	1469	1469	1469
δCH_2 C_3mpyr	1433	1433	1433	1432	1432
$\upsilon_{as}SO_2$	1376	1376	1376	1375	1374
$\upsilon_{as}SO_2$	1359	1359	1358	1358	1357
$\upsilon_s SO_2$	1217	1217	1218	1219	1220
$\upsilon_s SO_2$	1171	1170	1170	1168	1168
FSI(?)	1100	1105	1109	1112	1114
Ring mode C_3mpyr	1003	1003	1003	1003	1003
	970	970	970	970	970
	939	939	939	939	939
	905	905	905	905	905
$\upsilon_{as}SNS$ and υSF	826	830	835	839	841
$\upsilon_s SNS$	730	736	741	744	746
δSNS	641	644	645	648	648
$\delta_a SO_2$	564	565	566	567	566

Supplement Table 1: FT-IR Peak positions (υ: stretching, δ: bending)
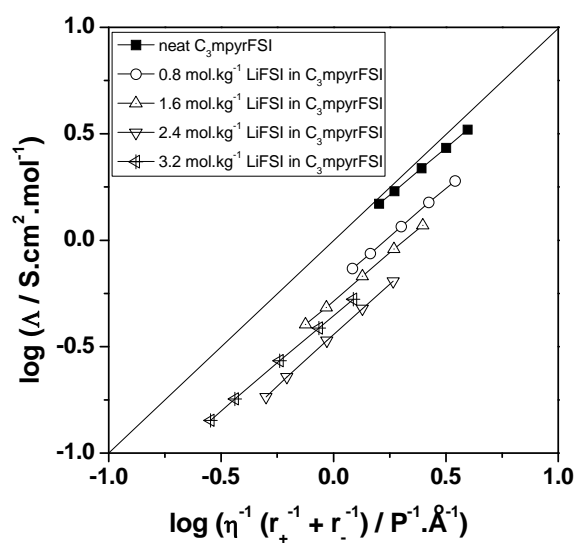
Supplement Figure 2: Modified Walden plot, Atomic radius from 'MacFarlane, D. R.; Forsyth, M.; Izgorodina, E. I.; Abbott, A. P.; Annat, G.; Fraser, K., Phys. Chem. Chem. Phys. 2009, 11 (25), 4962-4967.'
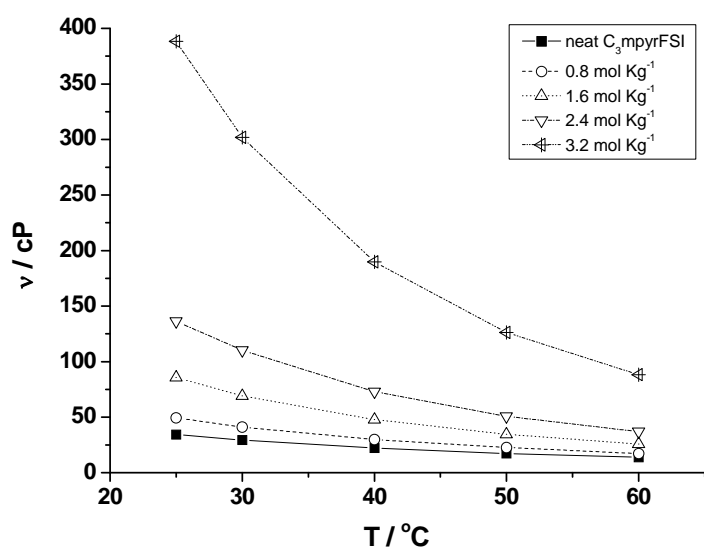
Supplement Figure 3: Viscosity plot of C₃mpyrFSI with different LiFSI salt concentrations.

Chapter 4. Studies of dicyanamide (DCA) ionic liquids

Introduction

In the previous chapter it was shown that lithium metal cells based on FSI IL electrolytes exhibit exceptionally good rate capability. However, the cost of perfluorinated lithium battery electrolytes remains high due to the presence of fluorine in the anion. Although the study of non-fluorinated electrolytes is essential to reduce the battery manufacturing cost, there are few publications in scientific literature which report lithium metal battery cycling with non-fluorinated ionic liquid due to the lack of suitable alternatives with sufficient electrochemical stability and ionic conductivity. This chapter describes the properties and lithium cell performance of low viscosity, high conductivity non-fluorinated ionic liquids based on the dicyanamide anion.

The first publication in this chapter compares the electrochemical stability and lithium salt solubility of some CN-functionalised ionic liquids based on dicyanamide ($N(CN)_2^-$ or DCA), tricyanomethide ($C(CN)_3^-$) and tetracyanoborate ($B(CN)_4^-$) anions. In particular, the role of moisture content of the DCA based electrolyte is investigated in Li metal | $LiFePO_4$ cells and is shown to be a critical factor determining cell performance. In addition, the performance of this IL in Li | $Li_4Ti_5O_{12}$ cells was studied. The cycling of Li | $LiFePO_4$ cells incorporating a plastic crystal analogue of the DCA IL was also demonstrated.

The second publication in this chapter describes the physical properties of a pyrrolidinium DCA IL with a range of lithium salts including LiTFSI, LiFSI, $LiBF_4$ and LiDCA. A range of properties including density, viscosity, conductivity and thermal phase behaviour were determined. In addition, the diffusivity of each ion was determined using pulse-field gradient stimulated echo (PFG-STE) diffusion measurements for the ^1H, ^7Li, ^{19}F, and ^{13}C nulcei. A 'Walden plot', which is an effective qualitative tool for understanding the degree of dissociation in an ionic liquid, was reviewed and compared with the concept of 'ionicity' in the presence of the various lithium salts.

Monash University

Declaration for Thesis Chapter 4

Declaration by candidate

In the case of Chapter 3, the nature and extent of my contribution to the work was the following:

Nature of contribution	Extent of contribution (%)
Cyclic Voltammetry, electrochemical impedance spectroscopy, coincell cycling, conductivity, viscosity, density, DSC, diffusion NMR (^{1}H, ^{7}Li, ^{19}F), solution preparation and electrode manufacture. Data analysis, manuscript writing.	85%

The following co-authors contributed to the work. Co-authors who are students at Monash University must also indicate the extent of their contribution in percentage terms:

Name	Nature of contribution	Extent of contribution (%) for student co-authors only
Douglas MacFarlane	Publication 4.1, 4.2: Project initiation, key ideas, editing, experiment planning.	
Maria Forsyth	Publication 4.1, 4.2: Project initiation, key ideas, editing, experiment planning.	
Patrick Howlett	Publication 4.1, 4.2: Project initiation, key ideas, editing, experiment planning.	
Adam Best	Publication 4.1, 4.2: Project initiation, key ideas, editing, experiment planning.	
Youssof Shekibi	Publication 4.1: Plastic crystal cell cycling results in figure 8 and 9. key ideas, editing.	
George Lane	Publication 4.1: Li | $Li_4Ti_5O_{12}$ coin cell cycling results in figure 7, key ideas, editing.	5%
Paul Bayley	Publication 4.2: ^{13}C diffusion NMR result in figure 4(c). key ideas, editing.	

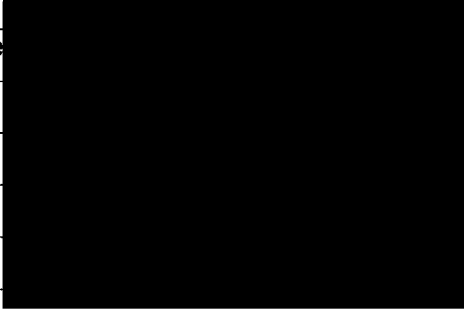| Candidate's Signature	Hyungook (Martin) Yoon	Date 21/06/2013

Declaration by co-authors

The undersigned hereby certify that:

(1) the above declaration correctly reflects the nature and extent of the candidate's contribution to this work, and the nature of the contribution of each of the co-authors.
(2) they meet the criteria for authorship in that they have participated in the conception, execution, or interpretation, of at least that part of the publication in their field of expertise;
(3) they take public responsibility for their part of the publication, except for the responsible author who accepts overall responsibility for the publication;
(4) there are no other authors of the publication according to these criteria;
(5) potential conflicts of interest have been disclosed to (a) granting bodies, (b) the editor or publisher of journals or other publications, and (c) the head of the responsible academic unit; and
(6) the original data are stored at the following location(s) and will be held for at least five years from the date indicated below:

Location(s) | **CSIRO Energy Technology, Clayton, Victoria, Australia**

[Please note that the location(s) must be institutional in nature, and should be indicated here as a department, centre or institute, with specific campus identification where relevant.]

			Date
Signature 1	D.R.MacFarlane		21/(/13
Signature 2	M.Forsyth		24/6/13
Signature 3	P.C.Howlett		21/6/13
Signature 4	A.S.Best		27/06/13
Signature 5	Y.Shekibi		24/06/2013
Signature 6	G.H.Lane		
Signature 7	P.M.Bayley		

PAPER

Lithium electrochemistry and cycling behaviour of ionic liquids using cyano based anions†

H. Yoon,[ab] G. H. Lane,[ab] Y. Shekibi,[b] P. C. Howlett,[c] M. Forsyth,[c] A. S. Best[*b] and D. R. MacFarlane[a]

Lithium based battery technologies are increasingly being considered for large-scale energy storage applications such as grid storage associated with wind and solar power installations. Safety and cost are very significant factors in these large scale devices. Ionic liquid (IL) electrolytes that are inherently non-volatile and non-flammable offer a safer alternative to mainstream lithium battery electrolytes, which are typically based on volatile and flammable organic carbonates. Hence, in recent years there have been many investigations of ionic liquid electrolytes in lithium batteries with some highly promising results to date, however in most cases cost of the anion remains a significant impediment to widespread application. Amongst the various possible combinations the dicyanamide (DCA) anion based ionic liquids offer exceptionally low viscosities and high conductivities – highly desirable characteristics for Li electrolyte solvents. DCA ILs can be manufactured relatively inexpensively because DCA is already a commodity anion, containing only carbon and nitrogen, which is produced in large amounts for the pharmaceutical industry. In this study we use the non-fluorinated ionic liquid N-methyl-N-butylpyrrolidinium dicyanamide to form non-volatile lithium battery electrolytes. We demonstrate good capacity retention for lithium metal and LiFePO$_4$ in such electrolytes and discharge capacities above 130 mAh.g^{-1} at 50 °C. We show that it is important to control moisture contents in this electrolyte system in order to reduce capacity fade and rationalise this observation using cyclic voltammetry and lithium symmetrical cell cycling. Having approximately 200 ppm of moisture content produces the optimum cycling ability. We also describe plastic crystal solid state electrolytes based on the DCA anion in the lithium metal–LiFePO$_4$ battery configuration and demonstrate over 150 mAh.g^{-1} discharge capacity without any significant capacity fading at 80 °C.

Broader context

Lithium battery technologies have applications in large-scale energy storage such as grid storage and electric vehicles. Safety, energy density, and cost are very crucial factors in the choice of large scale devices. Currently, mainstream lithium-ion battery electrolytes are based on volatile and flammable organic carbonates which introduce significant safety issues. Ionic liquid (IL) electrolytes, which are inherently non-volatile and non-flammable, offer a safer alternative. Additionally, ILs offer the promise of enabling a rechargeable lithium metal electrode to deliver significant increases in energy. Amongst the various possible cation and anion combinations, ILs using the dicyanamide (DCA) anion, which contain no fluorine reducing cost, offer exceptionally low viscosities and high conductivities – highly desirable characteristics for Li electrolyte solvents. We have investigated the ionic liquid N-methyl-N-butylpyrrolidinium dicyanamide to form lithium battery electrolytes which enable good capacity retention for a lithium metal–LiFePO$_4$ battery with discharge capacities above 130 mAh.g^{-1} at 50 °C. We also describe solid state electrolytes, based on plastic crystals with the DCA anion, in a lithium metal–LiFePO$_4$ battery and demonstrate over 150 mAh.g^{-1} discharge capacity without any significant capacity fading at 80 °C.

Introduction

Ionic liquid (IL) electrolytes, which are inherently non-volatile in nature,[1] offer a potentially safer alternative to mainstream lithium battery electrolytes which are based on volatile and flammable organic carbonates.[2,3] Hence, in recent years there have been many investigations of ionic liquid electrolytes in lithium batteries with some highly promising results to date.[4–8]

The suitability of any particular ionic liquid for use in a lithium battery is heavily dependent on the type of anode and

[a]School of Chemistry, Monash University, 3800 Victoria, Australia

[b]Commonwealth Scientific and Industrial Research Organisation (CSIRO) Division of Energy Technology, Bayview Ave, Clayton, 3169 Victoria, Australia. E-mail: ▮▮▮▮▮▮▮▮; Tel: ▮▮▮▮▮

[c]ARC Centre of Excellence for Electromaterials Science (ACES), Institute for Frontier Materials (IFM), Deakin University, Burwood, Victoria 3125, Australia

† Electronic supplementary information (ESI) available. See DOI: 10.1039/c3ee23753b

This journal is © The Royal Society of Chemistry 2013

Energy Environ. Sci., 2013, **6**, 979–986 | **979**

cathode materials used.[9] One anode material that is of particular interest to researchers is lithium metal. Lithium has an enormous specific capacity (3860 mAh.g^{-1})[10] compared to graphite (380 mAh.g^{-1}) which is commonly used in commercial lithium-ion devices. However lithium metal exhibits high reactivity in the presence of electrolytes based on aprotic organic solvents, leading to excessive electrode–electrolyte side reactions. Dendrite formation and excessive electrolyte degradation eventually stifles the proper functioning of the battery, and as yet a rechargeable lithium metal battery has not been successfully commercialised.[11,12]

An early study by Sakaebe and Matsumoto demonstrated successful cycling, albeit with some capacity fade, of lithium metal–LiCoO$_2$ batteries in ionic liquids based on the bis(trifluoromethanesulfonyl)imide (TFSI) anion.[13] Howlett et al. studied the lithium metal electrode in isolation using the IL N-methyl-N-propylpyrrolidinium TFSI (C$_3$mpyr TFSI) and reported excellent cycling behaviour,[14] thus concluding that the limited capacity fade observed by Sakaebe probably resulted from the cathode (LiCoO$_2$) side of the battery. Despite this, LiCoO$_2$, and its derivatives, continue to be used in many battery studies involving TFSI type ILs due to the need for high energy batteries.[15–17]

With the demonstrated excellent stability of lithium metal in some TFSI ILs, many researchers have since reported on the cycling of lithium metal batteries using TFSI based ILs for a range of cathode materials. More recently, another sulfonyl type anion, bis(fluoromethanesulfonyl)imide (FSI) has been the subject of investigation in lithium battery studies.[18–21] The FSI ILs, which are more fluid and conductive than their TFSI counterparts, have become favoured over TFSI ILs due to the excellent battery cycling behaviour at high rates that can be obtained using FSI IL electrolytes.[18,20,22] However, there are some concerns about the thermal stability of FSI.[23,24]

The relative expense (currently) of TFSI and FSI ILs compared to organic carbonate-based electrolytes detracts from their attractiveness as commercial electrolytes. Therefore, the investigation of alternative ILs based on less expensive anions, especially non-fluorinated anions, is of significance. To our knowledge there are no publications in the scientific literature which report lithium metal battery cycling using a non-fluorinated ionic liquid. In fact, in lithium metal systems using TFSI ILs, LiF has been identified as a major component of the solid electrolyte interphase (SEI) that acts to prevent ongoing degradation of the electrolyte.[4] Stable cycling behaviour of a fluorine free system would prove that LiF is not an indispensable SEI component in IL systems, and may promote the study of fluorine free ILs in the ongoing research effort.

Ionic liquids based on the dicyanamide (DCA) anion have exceptionally low viscosities,[25,26] a highly desirable characteristic for potential electrolyte solvents. DCA ILs can be manufactured relatively inexpensively as DCA is already a commodity anion produced in large amounts for the pharmaceutical industry. However, for lithium batteries, the DCA anodic stability is below that of TFSI, by at least 1 V,[25,26] therefore the lithium ion insertion potential of cathode, such as LiCoO$_2$, would be likely to exceed the anodic breakdown potential of a DCA type ionic liquid. This potential problem may explain the lack of investigation of these ILs in lithium batteries.

In this article we report on the use of IL electrolytes using DCA and two other related anions based on the cyano-moiety. In particular we will focus on ionic liquids and plastic crystals based on N-methyl-N-alkyl-pyrrolidinium dicyanamide (C$_x$mpyr DCA) in lithium batteries. We include investigations of lithium metal, Li$_4$Ti$_5$O$_{12}$, and LiFePO$_4$ electrode materials, with particular attention paid to batteries using a lithium metal anode and LiFePO$_4$ (LFP) cathode.

Experimental

Materials

N-Methyl-N-butylpyrrolidinium dicyanamide (C$_4$mpyr DCA with 90 ppm of H$_2$O) and N-methyl-N-butylpyrrolidinium tetracyanoborate (C$_4$mpyr TCB with 34 ppm of H$_2$O) were both sourced from Merck™, Germany. N-Methyl-N-butylpyrrolidinium tricyanomethanide (C$_4$mpyr TCM) was synthesized from N-methyl-N-butylpyrrolidinium bromide from Merck™, Germany and potassium tricyanomethanide from Alfa Aesar™, USA in dry acetonitrile. Lithium dicyanamide (LiDCA) was synthesized from sodium dicyanamide with LiCl in dry acetone in our laboratories.[27] N-N-Dimethylpyrrolidinium dicyanamide (C$_1$mpyr DCA) was synthesized following the previously reported method by MacFarlane et al.[26] Moisture contents were determined via a Karl Fisher titration 756KF coulometer.

Cyclic voltammetry

For cyclic voltammetric studies, a 500 μm dia. Pt working electrode and a Pt wire counter electrode were employed. The reference electrode consisted of a silver wire immersed in a solution of 10 mM silver triflate in N-methyl, N-butylpyrrolidinium bis(trifluoromethanesulfonyl)imide (C$_4$mpyr TFSI) and separated from the main solution by a glass frit as reported by Snook et al.[28] The scan rate was 20 mV s^{-1}. Measurements were obtained at ambient temperature. Potentiostatic control was provided by an Autolab pgstat302 (Eco Chemie, Netherlands) controlled with GPES (Version 4.9.005) software.

Coin cells

LiFePO$_4$ electrodes consisted of 75 wt% LiFePO$_4$ coated with carbon [1.6 wt%] (Phostech), 15 wt% carbon black (Shawinigan) and 10 wt% PVdF binder. Dry ingredients were milled together for 72 h, prior to the addition of the binder (dissolved in N-methylpyrrolidone) to form a slurry. The slurry was milled for a further 72 h prior to being spread on aluminium foil using a 100 μm graded roller giving its loading of 2.5 mg.cm^{-2}. Foils for the plastic crystal C$_1$mpyr DCA used a 60 μm graded roller giving its loading of 1.5 mg.cm^{-2}. All coated foils were allowed to dry overnight in a fume hood prior to being dried in a vacuum oven at 100 °C for 72 h.

Coin cells consisted of a CR2032 stainless steel coin cell case, a 10 mm diameter disc cathode, a 10 mm diameter disc of lithium foil (China Energy Lithium, 0.33 mm thick, cleaned with n-pentane) anode, and 30 μm thick Separion® (Evonik

980 | Energy Environ. Sci., 2013, **6**, 979–986

This journal is © The Royal Society of Chemistry 2013

Industries, Germany, dried under vacuum at 100 °C) separator. An internal spring and spacer provided uniform pressure inside the cells. Cells were assembled in an argon filled glove box (<5 ppm H_2O, 10 ppm O_2).

Cells were cycled on a Maccor series 4000 battery tester. The test temperature was 50 °C unless stated otherwise.

Results and discussion

Electrochemical windows

In order to determine the electrochemical stability of the cyano-based anions, we have chosen to use the pyrrolidinium cation for these experiments. Whilst ionic liquids using these cations do not have the highest conductivity or lowest viscosity, they have superior electrochemical stability when compared to imidazolium-based ionic liquids.[29,30]

We have checked the solubility of various lithium salts in C_4mpyr DCA, C_4mpyr TCM and C_4mpyr TCB (whose structures are shown in Fig. 1) to determine their possible application as lithium battery electrolytes. LiDCA salts could be dissolved into C_4mpyr DCA to approximately 0.75 mol.kg^{-1}, and up to 1.5 mol.kg^{-1} into C_4mpyr TCM. We have tried to solubilise a range of lithium salts (*e.g.*, LiDCA, LiTFSI, LiFSI, $LiPF_6$ and $LiBF_4$) into C_4mpyr TCB with no success above a concentration of 0.3 mol.kg^{-1}, which limits the viability of C_4mpyr TCB for use as a lithium battery electrolyte. Scheers *et al.*[31] have reported the same issue for TCB based ILs; in order to overcome this, they introduced glycol dimethyl ether to dissolve the Li salts in the mixture, which is similar to the approach of Watanabe and co-workers.[32–35] For C_4mpyr DCA, we have chosen to use a salt concentration of 0.5 mol.kg^{-1} LiDCA as this was found to exhibit the optimum Li|Li^+ behaviour in solution.

Fig. 2 shows the electrochemical windows of the ionic liquids chosen for this study. For the DCA, TCB and reference NTf_2 (or TFSI) ILs, the CV started at 0 V scanning reductively first. After completion of the scan, the working electrode was polished before starting at 0 V and scanning in the oxidative direction. Only in the TCM case did this change; the CV started at 0 V for reductive direction and −2 V in the oxidative direction. In this
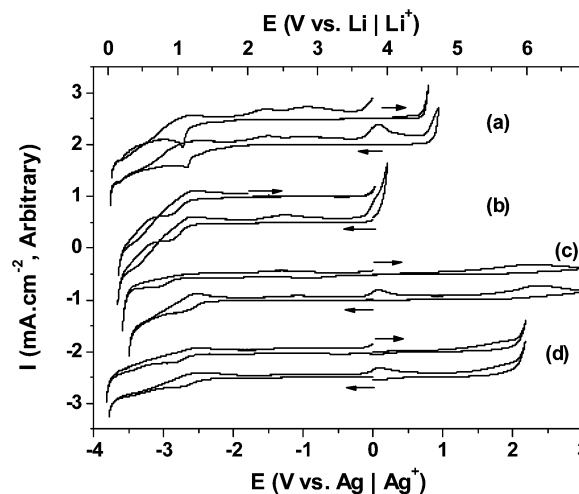

Fig. 2 Comparison of the electrochemical window of three cyano-based ionic liquids with a pyrrolidinium cation (scan rate: 20 mV s^{-1} at r.t.); where (a) C_4mpyr DCA, (b) C_4mpyr TCM, (c) C_4mpyr TCB, (d) C_4mpyr NTf_2 (added for comparative purposes).[28] Note values in the top *x*-axis are converted from Ag|Ag^+ to Li|Li^+ for comparative purpose. The moisture content of each IL was 90 ppm, 40 ppm, 28 ppm and 21 ppm for (a) to (d) respectively.

way, we sought to isolate the products generated as a result of the scan direction.

Fig. 2(a) shows that C_4mpyr DCA has wider electrochemical window than C_4mpyr TCM but narrower electrochemical window than C_4mpyr TCB. On the reverse (cathodic) scan, a noticeable peak is present at −2.7 V, which may be due to an unknown impurity or potential cation reduction. Using a threshold current density of 0.014 mA.cm^{-2} above background, the reductive breakdown of the IL is underway by −3.62 V, and the oxidative breakdown by +0.59 V, giving an electrochemical window of 4.2 V. C_4mpyr TCM in Fig. 2(b) exhibits the narrowest electrochemical window of the cyano-based ILs. The rapid oxidation behaviour at the electrochemical limit is not observed in the case of C_4mpyr TCB (Fig. 2(c)); it is unclear why this is the case.

The TCM and DCA ILs are at least 1 V (*vs.* Ag|Ag^+) less electrochemically stable than the NTf_2 ILs, limiting the scope for using these materials with common cathodes such as $LiCoO_2$ or $LiMn_2O_4$. For this reason in the battery cycling work described later, we have focused on $LiFePO_4$ (LFP) cathodes. Whilst the TCB based IL appears to have an equivalent electrochemical window to C_4mpyr NTf_2 (or TFSI) and FSI based ILs, the very limited Li salt solubility precludes its further study in this work. Consequently, we focused the further investigation described below on the DCA-based ionic liquids.

Cycling stability of C_4mpyr DCA with different moisture content

We have found that cyano based ionic liquids have a strong affinity for moisture and it is therefore very difficult to remove all moisture from the solution. Electrolytes composed of fluorine based anions or salts in the presence of moisture may have an unfavourable effect on the lithium plating process and SEI
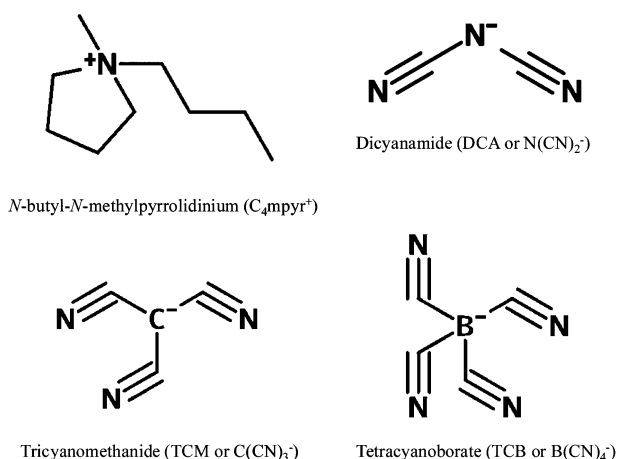

N-butyl-*N*-methylpyrrolidinium (C_4mpyr$^+$)

Dicyanamide (DCA or N(CN)$_2$$^-$)

Tricyanomethanide (TCM or C(CN)$_3$$^-$)

Tetracyanoborate (TCB or B(CN)$_4$$^-$)

Fig. 1 Structures of ions examined in this study.

formation.[36,37] There are few reports on the role of trace amounts of H_2O in non-fluorinated ionic liquid based electrolytes, however, Scheers *et al.* investigated the role of relatively large amount of H_2O in 4,5-dicyano-(2-trifluoromethyl)imidazolium based ionic liquids on lithium ion co-ordination behaviour.[38] Hence, we have conducted a number of experiments to understand the role of H_2O on the lithium electrochemistry in the electrolyte of C_4mpyr DCA + 0.5 mol.kg^{-1} LiDCA. We have systematically increased the moisture content of the electrolyte from 36 ppm up to 630 ppm. The electrolyte with 36 ppm of H_2O was prepared by eliminating moisture from the solution *via* contacting it with lithium metal for up to three months. The CV of this electrolyte, shown in Fig. 3(a), indicates

that no lithium dissolution was possible following a strong reduction peak at ∼ −3.7 V *vs.* Ag|Ag$^+$. We ascribe this peak to be related to ionic liquid decomposition, more specifically $C_x$mpyr reduction, due to insufficient moisture to form an SEI. We do note that the electrolyte was slightly discoloured after being exposed to the Li metal for the extended period of time.

Fig. 3(b) shows the cyclic voltammetry for the 0.5 mol.kg^{-1} LiDCA solution with 97 ppm H_2O. The Li$^+$ reduction peak, beginning at −3.9 V (*vs.* Ag|Ag$^+$), reaches a maximum current density of 4 mA.cm^{-2} on the first scan. On the reverse scan a clear bulk lithium metal stripping is present at −3.95 V (*vs.* Ag|Ag$^+$), along with some smaller peaks which are due to the stripping of Li from Li–Pt alloys.[14,39,40] The Li stripping peak of the 2nd scan is bigger than the first scan and then reduces in subsequent scans. We attribute this change to the formation of a passivation layer that grows with continued cycling. The tendency of decreasing peak currents for Li$^+$ deposition and Li stripping during cycles are commonly observed in all samples with different H_2O amount but, the highest peak current value was observed when the water content is 97 ppm. In all instances we have not found it possible to clearly resolve the deposition peak; it appears that bulk electrolyte decomposition is almost co-incident with lithium deposition. Of note is the increase in current density for the peak at −2.5 V *vs.* Ag|Ag$^+$ which can be attributed to the increasing presence of moisture in the electrolyte.

Fig. 3(c) shows a trend for the peak current density of the plating of lithium decreasing as increasing amounts of H_2O are added to the electrolyte. Comparing the sample which has 97 ppm H_2O and the sample which has 630 ppm of H_2O, a significant decrease in the current density for both Li$^+$ deposition and stripping can be seen, suggesting increasing amounts of moisture are detrimental to electrochemical kinetics. Cyclic voltammetry experiments clearly show the feasibility and stability of lithium cycling in the C_4mpyr DCA ionic liquid with non-fluorinated lithium salt and an optimum moisture content contributes to higher current densities and efficiencies.

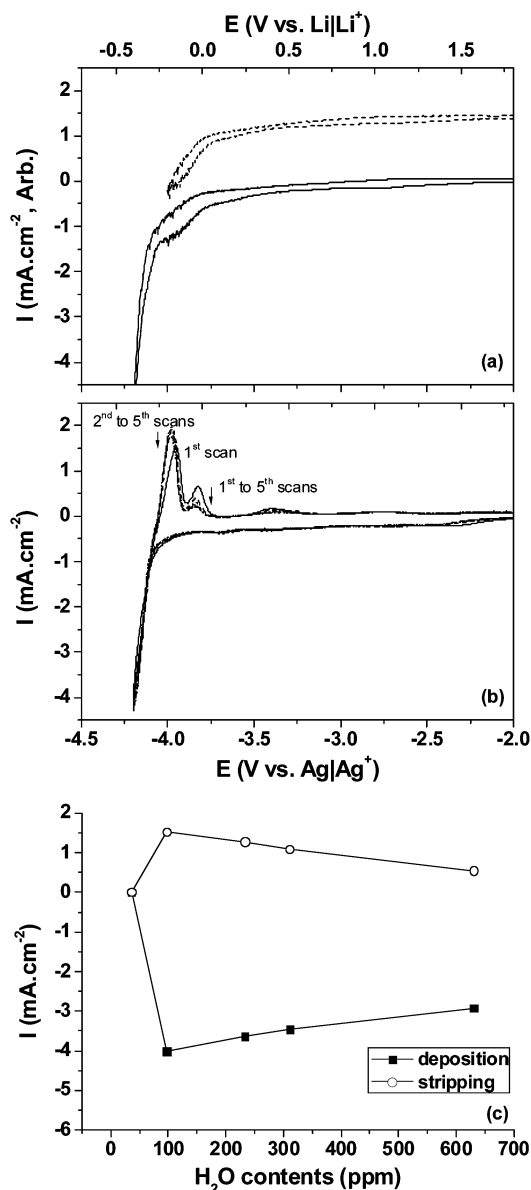## Cyclic performance of C_4mpyr DCA lithium symmetrical cells

Lithium symmetrical cells, with 0.5 mol.kg^{-1} LiDCA in C_4mpyr DCA and different moisture contents, were prepared and cycled 100 times at 50 °C and at a current density of 0.1 mA.cm^{-2} for 16 min (0.1 C cm^{-2}) for each polarisation. Fig. 4(b)–(d) show the cycling results using electrolytes and Fig. 4(f)–(h) show the EIS before and after the cycling with 226 ppm, 291 ppm and 443 ppm moisture respectively. In all cases, the over-potentials of the symmetrical cells start at approximately the same point; however, with continued cycling the cells exhibit increasing over-potentials, which vary dramatically with moisture content. We have ascribed this change to unrestrained growth of the SEI on the lithium metal electrode, leading to increased impedance and hence, the over-potential. The cell impedance of the electrolyte containing 36 ppm water increases most rapidly with cycling leading to the high over-potentials recorded here (Fig. 4a and e). From this experiment, it appears that a certain amount of moisture is required to form and stabilise an SEI layer in

Fig. 3 (a) CVs of 0.5 mol.kg^{-1} LiDCA in C_4mpyr DCA with 36 ppm H_2O showing 5 cycles at ambient temperature (scan rate is 20 mV s^{-1}). (b) CV with 97 ppm H_2O. (c) Li deposition and dissolution peak current at the first cycle with different amount of H_2O. Note: CVs for electrolytes with different H_2O content are presented in the ESI.†
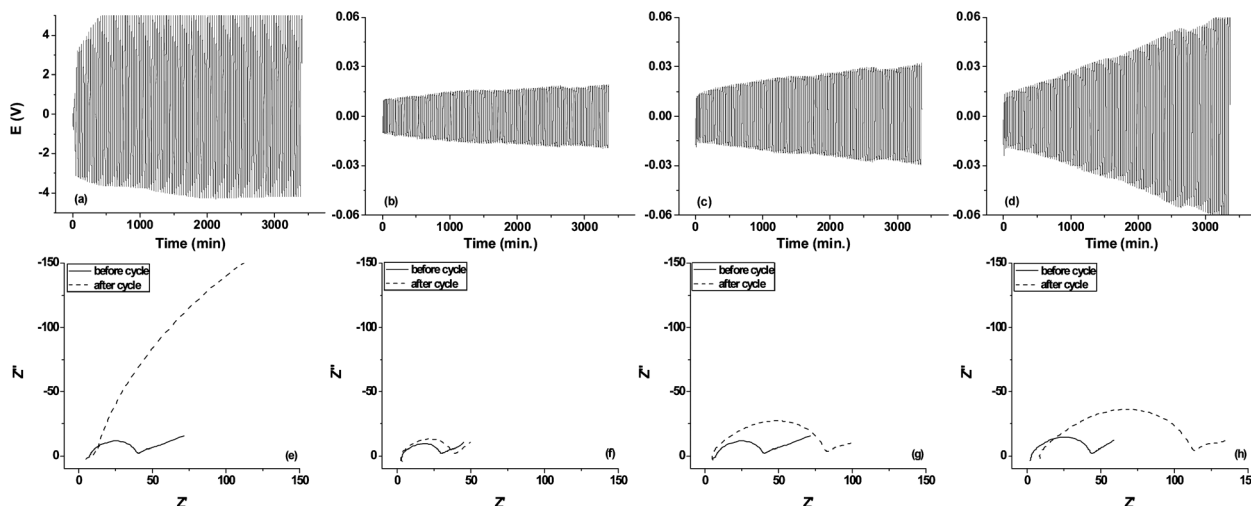
Fig. 4 Li symmetrical cell cycling and EIS results: 10 mm Li disc, 0.1 mA.cm^{-2} constant current for 16 minutes, 100 cycles at 50 °C using 0.5 mol.kg^{-1} LiDCA in C$_4$mpyr DCA with different H$_2$O contents; (a) and (e) 36 ppm, (b) and (f) 226 ppm, (c) and (g) 291 ppm, (d) and (h) 443 ppm.

presence of the DCA anion during lithium cycling. This indicates that the moisture content of the electrolyte has a significant effect on the SEI that forms on the lithium surface in DCA electrolyte systems; however, this can be managed to allow effective cycling of the cell.

In support of this assertion, we prepared a lithium symmetrical cell doped with 223 ppm of water and cycled the cell 100 times at 50 °C, with a 15 h, 1 h and 24 h interval after the 10th, 30th and 50th cycles, respectively. During the cycling interval, the cell was maintained at 50 °C and open circuit. Fig. 5 shows that even when no current is applied to the cell the impedance continues to increase during the storage period at 50 °C. This implies that the increasing cell impedance is not driven by a potential dependant thermodynamic reaction but rather by a temperature and time dependant kinetic reaction.

Li|LiFePO$_4$ cells

Li|LiFePO$_4$ cells were constructed using cathodes with a loading of 2.5 mg.cm^{-2} and LiDCA salt (0.5 mol.kg^{-1}) in C$_4$mpyr DCA
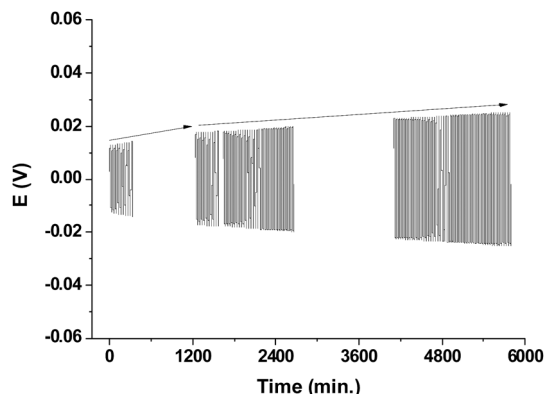

Fig. 5 Li symmetrical cell cycling results: 0.1 mA.cm^{-2} constant current for 16 minutes, 100 cycles at 50 °C using 0.5 mol.kg^{-1} LiDCA in C$_4$mpyr DCA at 223 ppm H$_2$O. Cycling procedure were 10 cycles, 15 hours at OCV or "rest", 10 cycles, 1 hour at OCV or "rest", 30 cycles, 24 hours at OCV or "rest", and 50 cycles.

with 226 ppm and 443 ppm of moisture. These cells were cycled between 3.0 V and 3.8 V with 0.35 mA.cm^{-2} constant current (about 1 C rate) at 50 °C. For each cell, we observed an initial capacity of more than 130 mAh.g^{-1} discharging capacity as shown in Fig. 6. The cell with 443 ppm of H$_2$O shows a larger initial irreversible capacity, lower efficiency (93–95% over 20 cycles) and more rapid capacity fade (93% of initial discharge capacity after 10th cycles) than the cell containing 226 ppm of H$_2$O, which has 137 mAh.g^{-1} maximum discharge capacity at the 2nd cycle, over 97% efficiency and over 97% discharge capacity remaining after 10 cycles. We ascribe the difference in the cycling efficiency and capacity fade to be due to the different amounts of moisture in the cell and the evolution of the SEI on the lithium metal electrode. Importantly, these results show that good performance in a real battery at a relatively high C rate can be achieved with this non-fluorinated electrolyte system.

Li|Li$_4$Ti$_5$O$_{12}$ cells

Li$_4$Ti$_5$O$_{12}$ is a cheap, high capacity and high cycleability material having zero strain with minimal SEI formation and has been researched vigorously for the application as an alternative anode material.[41,42] The compatibility of Li$_4$Ti$_5$O$_{12}$ with the C$_4$mpy DCA based electrolyte was also investigated. A Li|Li$_4$Ti$_5$O$_{12}$ cell was prepared with a loading of 1.23 mg.cm^{-2} and cycled at 50 °C. The cell was cycled at 1 C rate at 50 °C and displayed a capacity of around 130 mAh.g^{-1} (Fig. 7), the theoretical capacity for this material is 175 mAh.g^{-1}. Clearly Li$_4$Ti$_5$O$_{12}$ is a viable electrode material for C$_4$mpyr DCA based electrolytes.

Plastic crystal electrolytes based on C$_1$mpyr DCA

Plastic crystal electrolytes have also been researched widely since they have flexibility and durability during volumetric change.[43–45] Recently, Adebahr et al. have reported the possibility of using C$_1$mpyr DCA as a plastic crystal electrolyte having
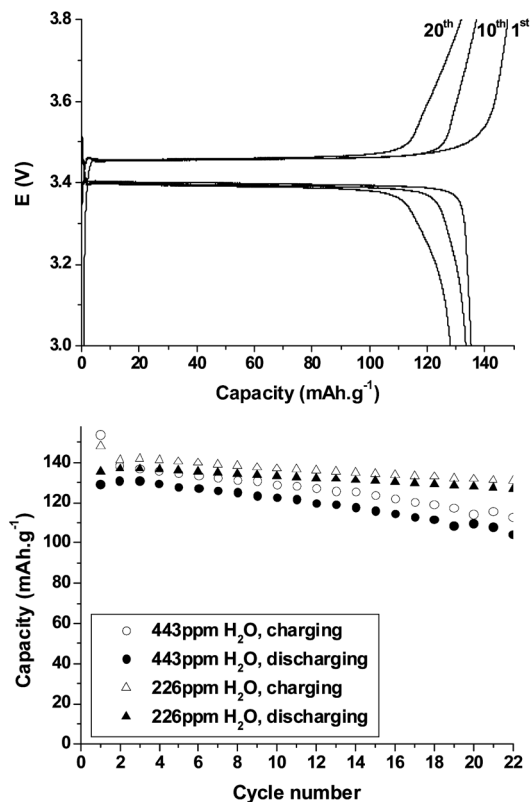
Fig. 6 Coin cell voltage profile of 226 ppm H_2O cell (upper) and the cycling result for a Li|LiFePO$_4$ using 0.5 mol.kg^{-1} LiDCA in C$_4$mpyr DCA with 226 ppm and 443 ppm H_2O (lower). Charging and discharging conditions are from 3.0 V to 3.8 V, with 0.35 mA.cm^{-2} constant current (about 1 C rate) at 50 °C.
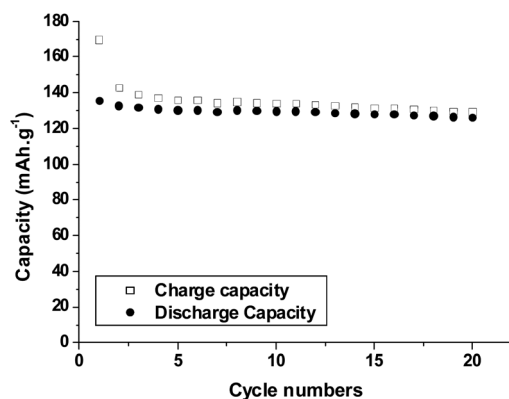
Fig. 8 Charge–discharge profiles at the 10th, 50th, and 100th cycle of a Li|LiFePO$_4$ cell at C/10 rate using C$_1$mpyr LiDCA in PVdF at 80 °C.

Fig. 9 Li|LiFePO$_4$ coin cell cycling at C/10 rate using C$_1$mpyr LiDCA in PVdF at 80 °C.

Fig. 7 Li|Li$_4$Ti$_5$O$_{12}$ coin cell cycling at 2/3 C rate at 50 °C using 0.5 mol.kg^{-1} LiDCA in C$_4$mpyr DCA with approx. 200 ppm of H_2O.

This combined assembly was then left at 130 °C for a further two hours. The assembly was cooled to room temperature before assembly with a Li metal anode in a battery cell. Cycling performance of the cell was tested at C/10 rate at 80 °C to examine the specific capacity and cycle-ability of this composite in its solid-state phase. Initially, the cell showed a capacity at about 162 mAh.g^{-1}, which was followed a by linear drop reaching 158 mAh.g^{-1} for the next 10 cycles (Fig. 8). Consequently, the cell showed a slow capacity loss from 158 mAh.g^{-1} to 140 mAh.g^{-1} after 200 cycles. Further studies need to be conducted on this composite electrolyte using a separator more suitable for application at higher temperatures.

Fig. 9 shows charge and discharge curves of the 10th, 50th and 100th cycles. The first 20 cycles, shows the cell to have poor efficiency and we ascribe this behaviour to the electrolyte decomposing slowly to form the SEI on Li metal, consistent with our earlier observations. At later cycles (>75), the cell reached and continuously maintained 98% efficiency.

Conclusions

The use of a non-fluorinated anion, as part of an ionic liquid and electrolyte thereof, goes to the heart of the challenge of adopting these exciting materials in lithium battery applications; affordability, availability and electrochemical stability. The

a high conductivity at elevated temperatures with the addition of lithium salts.[44]

Molten C$_1$mpyr DCA with 0.5 mol.kg^{-1} LiDCA binary composite electrolyte, was incorporated in a PVdF separator at 130 °C inside an argon filled glove box. This material was kept at this temperature for more than two hours until the electrolyte was fully absorbed into the separator. The laden separator was then placed on the surface of LiFePO$_4$, which was already wetted with a thin layer of molten electrolyte at the same temperature.
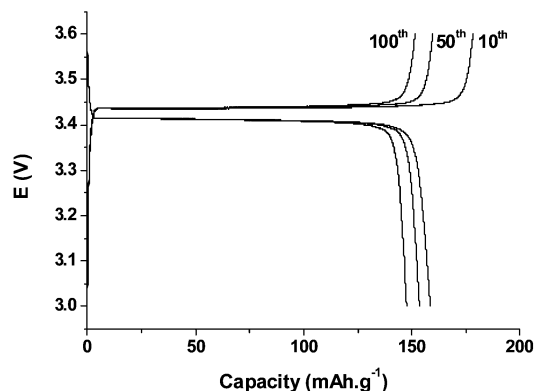
984 | *Energy Environ. Sci.*, 2013, **6**, 979–986

This journal is © The Royal Society of Chemistry 2013

Paper

Energy & Environmental Science

dicyanamide anion is well adopted in a number of different technology areas and is relatively cheap. We have now studied this important family of non-fluorinated ionic liquid electrolytes for potential application in lithium metal batteries. We show that there is promise in the use of these materials for energy storage.

Our studies have shown that the electrochemical stability of DCA is higher than TCM but lower than and TCB analogues. On the other hand, the Li salt solubility shows that the TCM is able to solubilise more salt than DCA and TCB (a very poor solvent for lithium salts). We do note, however, that the electrochemical window of this DCA is still inferior to NTf$_2$ based ionic liquids.

For the DCA based electrolytes, we have found a strong relationship with the amount of H$_2$O on the cycle-ability of the lithium anode. When there is less than 100 ppm of H$_2$O present in the electrolyte, this reduces the lithium cycle-ability significantly, whilst having between 100 and 200 ppm of H$_2$O provided the best cycling ability in Li|Li symmetrical cells.

Li|LiFePO$_4$ cells with C$_4$mpyr DCA ionic liquid showed over 130 mAh.g^{-1} of discharge capacity without a significant capacity reduction over to 20 cycles. We also demonstrated utility of Li| Li$_4$Ti$_5$O$_{12}$ cells at 50 °C. An organic ionic plastic crystal, C$_1$mpyr DCA, showed 150 mAh.g^{-1} discharge capacity in a Li|LiFePO$_4$ without a significant capacity fade for up to 200 cycles at 80 °C. In conclusion, these non-fluorinated ionic liquids based on cyano-based anions have proved to be a promising base for potentially safer and economical electrolytes for lithium metal batteries.

Acknowledgements

Notes and references

1 H. Ohno, in *Electrochemical Aspects of Ionic Liquids*, ed. O. Hiroyuki, 2005, pp. 1–3.

2 J. B. Goodenough and Y. Kim, *Chem. Mater.*, 2010, **22**, 587–603.

3 B. Scrosati and J. Garche, *J. Power Sources*, 2010, **195**, 2419–2430.

4 P. C. Howlett, N. Brack, A. F. Hollenkamp, M. Forsyth and D. R. MacFarlane, *J. Electrochem. Soc.*, 2006, **153**, A595–A606.

5 A. S. Best, A. I. Bhatt and A. F. Hollenkamp, *J. Electrochem. Soc.*, 2010, **157**, A903–A911.

6 G. T. Kim, S. S. Jeong, M. Z. Xue, A. Balducci, M. Winter, S. Passerini, F. Alessandrini and G. B. Appetecchi, *J. Power Sources*, 2012, **199**, 239–246.

7 G. B. Appetecchi, G. T. Kim, M. Montanino, F. Alessandrini and S. Passerini, *J. Power Sources*, 2011, **196**, 6703–6709.

8 K. Ui, K. Yamamoto, K. Ishikawa, T. Minami, K. Takeuchi, M. Itagaki, K. Watanabe and N. Koura, *J. Power Sources*, 2008, **183**, 347–350.

9 H. Sakaebe and H. Matsumoto, in *Electrochemical Aspects of Ionic Liquids*, ed. O. Hiroyuki, 2005, pp. 171–186.

10 J. I. Yamaki, S. I. Tobishima, Y. Sakurai, K. I. Saito and K. Hayashi, *J. Appl. Electrochem.*, 1997, **28**, 135–140.

11 D. Aurbach, E. Zinigrad, Y. Cohen and H. Teller, *Solid State Ionics*, 2002, **148**, 405–416.

12 D. Aurbach, E. Zinigrad, H. Teller, Y. Cohen, G. Salitra, H. Yamin, P. Dan and E. Elster, *J. Electrochem. Soc.*, 2002, **149**, A1267–A1277.

13 H. Sakaebe and H. Matsumoto, *Electrochem. Commun.*, 2003, **5**, 594–598.

14 P. C. Howlett, D. R. MacFarlane and A. F. Hollenkamp, *Electrochem. Solid-State Lett.*, 2004, **7**, A97–A101.

15 H. Sakaebe, H. Matsumoto and K. Tatsumi, *Electrochim. Acta*, 2007, **53**, 1048–1054.

16 N. Serizawa, S. Seki, S. Tsuzuki, K. Hayamizu, Y. Umebayashi, K. Takei and H. Miyashiro, *J. Electrochem. Soc.*, 2011, **158**, A1023–A1030.

17 J. Reiter, M. Nadherna and R. Dominko, *J. Power Sources*, 2012, **205**, 402–407.

18 H. Matsumoto, H. Sakaebe, K. Tatsumi, M. Kikuta, E. Ishiko and M. Kono, *J. Power Sources*, 2006, **160**, 1308–1313.

19 J. Saint, A. S. Best, A. F. Hollenkamp, J. Kerr, J. H. Shin and M. M. Doeff, *J. Electrochem. Soc.*, 2008, **155**, A172–A180.

20 Q. Zhou, W. A. Henderson, G. B. Appetecchi, M. Montanino and S. Passerini, *J. Phys. Chem. B*, 2008, **112**, 13577–13580.

21 E. Paillard, Q. Zhou, W. A. Henderson, G. B. Appetecchi, M. Montanino and S. Passerini, *J. Electrochem. Soc.*, 2009, **156**, A891–A895.

22 A. Guerfi, S. Duchesne, Y. Kobayashi, A. Vijh and K. Zaghib, *J. Power Sources*, 2008, **175**, 866–873.

23 R. Vijayaraghavan, M. Surianarayanan, V. Armel, D. R. MacFarlane and V. P. Sridhar, *Chem. Commun.*, 2009, 6297–6299.

24 Y. Wang, K. Zaghib, A. Guerfi, F. F. C. Bazito, R. M. Torresi and J. R. Dahn, *Electrochim. Acta*, 2007, **52**, 6346–6352.

25 D. R. MacFarlane, J. Golding, S. Forsyth, M. Forsyth and G. B. Deacon, *Chem. Commun.*, 2001, 1430–1431.

26 D. R. MacFarlane, S. A. Forsyth, J. Golding and G. B. Deacon, *Green Chem.*, 2002, **4**, 444–448.

27 A. P. Purdy, E. Houser and C. F. George, *Polyhedron*, 1997, **16**, 3671–3679.

28 G. A. Snook, A. S. Best, A. G. Pandolfo and A. F. Hollenkamp, *Electrochem. Commun.*, 2006, **8**, 1405–1411.

29 J. M. Pringle, J. Golding, C. M. Forsyth, G. B. Deacon, M. Forsyth and D. R. MacFarlane, *J. Mater. Chem.*, 2002, **12**, 3475–3480.

30 S. A. Forsyth, S. R. Batten, Q. Dai and D. R. MacFarlane, *Aust. J. Chem.*, 2004, **57**, 121–124.

31 J. Scheers, J. Pitawala, F. Thebault, J.-K. Kim, J.-H. Ahn, A. Matic, P. Johansson and P. Jacobsson, *Phys. Chem. Chem. Phys.*, 2011, **13**, 14953–14959.

32 T. Tamura, T. Hachida, K. Yoshida, N. Tachikawa, K. Dokko and M. Watanabe, *J. Power Sources*, 2010, **195**, 6095–6100.

33 S. Seki, K. Takei, H. Miyashiro and M. Watanabe, *J. Electrochem. Soc.*, 2011, **158**, A769–A774.

This journal is © The Royal Society of Chemistry 2013

Energy Environ. Sci., 2013, **6**, 979–986 | **985**

34 K. Yoshida, M. Tsuchiya, N. Tachikawa, K. Dokko and M. Watanabe, *J. Electrochem. Soc.*, 2012, **159**, A1005–A1012.

35 K. Ueno, K. Yoshida, M. Tsuchiya, N. Tachikawa, K. Dokko and M. Watanabe, *J. Phys. Chem. B*, 2012, **116**, 11323–11331.

36 D. Aurbach, I. Weissman, A. Zaban and P. Dan, *Electrochim. Acta*, 1999, **45**, 1135–1140.

37 D. Aurbach, M. D. Levi, E. Levi and A. Schechter, *J. Phys. Chem. B*, 1997, **101**, 2195–2206.

38 J. Scheers, L. Niedzicki, G. Z. Zukowska, P. Johansson, W. Wieczorek and P. Jacobsson, *Phys. Chem. Chem. Phys.*, 2011, **13**, 11136–11147.

39 R. Wibowo, S. E. W. Jones and R. G. Compton, *J. Phys. Chem. B*, 2009, **113**, 12293–12298.

40 R. Wibowo, L. Aldous, S. E. W. Jones and R. G. Compton, *Chem. Phys. Lett.*, 2010, **492**, 276–280.

41 K. Zaghib, M. Simoneau, M. Armand and M. Gauthier, *J. Power Sources*, 1999, **81**, 300–305.

42 A. S. Prakash, P. Manikandan, K. Ramesha, M. Sathiya, J. M. Tarascon and A. K. Shukla, *Chem. Mater.*, 2010, **22**, 2857–2863.

43 G. Annat, J. Adebahr, I. R. McKinnon, D. R. MacFarlane and M. Forsyth, *Solid State Ionics*, 2007, **178**, 1065–1071.

44 J. Adebahr, M. Forsyth and D. R. MacFarlane, *Electrochim. Acta*, 2005, **50**, 3853–3858.

45 Y. Shekibi, T. Ruether, J. Huang and A. F. Hollenkamp, *Phys. Chem. Chem. Phys.*, 2012, **14**, 4597–4604.

986 | *Energy Environ. Sci.*, 2013, **6**, 979–986

This journal is © The Royal Society of Chemistry 2013

Ionicity and lithium interfacial properties of *N*-butyl-*N*-methylpyrrolidinium dicyanamide ionic liquid - lithium salt electrolytes

Hyungook Yoon,[†,‡] Paul M. Bayley,[§] Patrick C. Howlett,[§] Adam S. Best,[*‡] Maria Forsyth,[§] and Douglas R. MacFarlane [†]

[†] School of Chemistry, Monash University, 3800 Victoria, Australia
[*‡] Commonwealth Scientific and Industrial Research Organisation (CSIRO), Division of Energy Technology, Bayview Ave., Clayton, 3169 Victoria, Australia; Tel: ███████████ E-mail: ███████████
[§] ARC Centre of Excellence for Electromaterials Science (ACES), Institute for Frontier Materials (IFM), Deakin University, Burwood, Victoria 3125, Australia

ABSTRACT: The physical properties of the ionic liquid *N*-butyl-*N*-methylpyrrolidinium dicyanamide (C$_4$mpyrDCA), with a range of salts including LiNTf$_2$, LiFSI, LiBF$_4$ and LiDCA have been investigated, including density, viscosity, conductivity, DSC and the diffusivity of each ion from Pulse-field gradient stimulated echo (PFG-STE) diffusion measurements for ^{1}H, ^{7}Li, ^{19}F, and ^{13}C. When the same amount of lithium salts are added to the IL, LiDCA showed the lowest viscosity and highest ion mobility for all ionic species in the solution while LiBF$_4$ showed the highest viscosity and lowest ion mobility. Comparing the results in the perspective of the Walden and Ionicity plots, suggests that there is greater ion aggregation in the lithium salt mixtures. Correlation of the physical properties with the SEI forming properties of the mixtures shows that more ion aggregation reduces the surface impedance of lithium surface.

INTRODUCTION

Due to their non-volatility, which potentially offers a safer alternative to the mainstream volatile and flammable organic carbonate-based lithium battery electrolytes,[1-2] ionic liquids (ILs) have been investigated for application in a range of different lithium battery types. A

major concentration of these studies has centered around ILs based on either the NTf_2 or FSI

anions, based on their relatively higher conductivity and lower viscosity with several

significant results reported on these materials.[3-6] However, the relative expense of these

materials when compared to organic carbonate-based electrolytes has been a significant

barrier to their commercial use in energy storage devices. Therefore, studies on alternative

ILs which could be potentially less expensive, especially those consist no fluorine in its

components, are necessary. Of note, there are few academic publications or patents on this

topic compared with ILs utilizing fluorinated anions.[7-10]

In the search for non-fluorinated ILs, we have examined the cyano-based family of anions

including tricyanomethanide, tetracyanoborate and dicyanamide. Of these three anions,

dicyanamide ($N(CN)_2^-$ or DCA) based ionic liquids, exhibit moderate electrochemical

windows and have exceptionally low viscosities and relatively low cost.[8, 11-12] MacFarlane, et

al. first introduced and investigated the pyrrollidinium based DCA anion ionic liquids,

investigating their physical and electrochemical properties, showing that they were promising

candidate as electrolytes for many electrochemical devices.[13] These DCA ionic liquids with

various other cations have been investigated for the use in gel polymer electrolyte, plastic

crystal electrolytes,[14-16] and dye-sensitized solar cell applications.[17-18] Compared to the other

similar anions having nitrile group, such as $C(CN)_3^-$ or $B(CN)_4^-$, DCA ionic liquids have

relatively high solubility for various lithium salts.[12] We have also demonstrated that the

capacity and cycleability of lithium metal cells with this non-fluorinated anion in our recent

report.[12] There was also an attempt to utilize a partly fluorinated $B(CN)_4^-$ derivative by

Scheers, et al. in their non-fluorinated IL research.[7, 19]

On the other hand, LiF, a bi-product during charging and discharging of lithium cells based

on fluorine containing ILs, was thought to be an important component in the formation of a

stable, solid electrolyte interphase (SEI)[20-21] . Our recent work showed that stable SEI layers

could be formed from in the DCA case in the presence of small but significant amounts of water, suggesting that it had a critical role in the chemistry of the SEI. In this paper, to explore whether the excellent SEI forming properties of the fluorinated anions could be introduced via the lithium salt, we have further investigated the properties of *N*-butyl-*N*-methylpyrrolidinium dicyanamide (C$_4$mpyrDCA) IL when it is mixed with a range of fluorinated lithium salts, LiNTf$_2$, LiFSI, LiBF$_4$, using the IL-LiDCA as the basis for comparison at constant composition. Correlations between SEI formation and physical properties of the mixtures are discussed.

EXPERIMENTAL

Materials:

N-butyl-*N*-methylpyrrolidinium dicyanamide (C$_4$mpyrDCA), 90 ppm H$_2$O, synthesis grade, Merck™) was used as received after checking moisture contents (< 200 ppm) via Karl Fisher titrations (Metrohm). Lithium dicyanamide (LiDCA) was synthesized from sodium dicyanamide with LiCl in dry acetone in our laboratories as described in our previous paper.[12,22] Lithium bis(trifluoromethanesulfonyl)imide (LiNTf$_2$) and lithium tetrafluoroborate (LiBF$_4$) were sourced from Stella Corporation and lithium bis(fluorosulfonyl)imide (LiFSI) was sourced from Suzhou Fluolyte Co., Ltd. All lithium salts were dried at 140 °C under vacuum for 48 hours before use. Electrolytes in this experiment were prepared by adding 0.5 mol.kg^{-1} of each salt into C$_4$mpyrDCA IL and stirring for 24 hours at 50 °C in an Ar-filled glove box. Moisture contents were determined (less than 130 ppm for all solutions) via Karl Fisher titration 756 coulometer.

An Anton Paar™ DMA 4500M was used to measure density from 20 °C to 60 °C and an Anton Paar™ Automated Micro Viscometer with VisioLab ver. 1.0.1 was used to measure viscosity over the same temperature range.

Differential scanning calorimetry (DSC) was carried out on a TA instruments™ DSC 2910. Samples (~10 mg) were sealed in Al hermetic pans and lids and then were cooled by liquid nitrogen at 10-20 °C.min⁻¹ to 150 °C. The DSC traces were recorded during heating at 10 °C.min⁻¹ to 100 °C.

Ionic conductivity was measured with a sealed glass conductivity dip-cell equipped with two porous platinum electrodes; all preparations took place inside an Ar-filled glove box and the moisture contents were determined again after conductivity measurement; even though we used a sealed dip-cell, the moisture contents after conductivity measurement were increased to ~ 400 ppm for all samples. A 0.01 M KCl solution was used to determine the cell constant, before and after each sample measurement. The ionic conductivity was measured from -30 to 100 °C and then back to 30 °C to check for any hysteresis.

Pulse-field gradient stimulated echo (PFG-STE) diffusion measurements for ^1H for C_4mpyr^+, ^7Li and ^{19}F were performed on a Bruker 300 MHz Ultrashield with Avance I console utilizing a Diff30 diffusion probe and GREAT60 amplifier for ^1H for C_4mpyr^+, ^7Li and ^{19}F, following the method described by Bayley et al.[23] and another Bruker 500 MHz Ultrashield with Avance I console was used for ^{13}C diffusion for DCA anion. Each sample was packed to a height of 50mm in a 5mm Schott E NMR tube in an Ar filled glove box and sealed with Teflon tape and a cap. Each sample was measured from 278 – 333 K.

CR2032 size lithium symmetric cells were prepared for EIS measurement with 2 10 mm2 diameter lithium discs and a 30 mm thick Separion® (Evonik Industries, Germany, dried under vacuum at 100 °C) separator in an Ar-filled glove box. The EIS was measured using 1 mV perturbation after cell preparation preparation and the cells were polarized with a constant voltage of 1.0 V for 5 minutes at 25 °C and the EIS was measured. These experiments were conducted using a Solartron™ 1470 Battery test unit connected to a 1255B Frequency response analyzer with Corrwave ver. 3.1c and Z-plot ver. 3.1c.

RESULTS AND DISCUSSION

Density, Viscosity, DSC and Conductivity:

Density and viscosity of C_4mpyrDCA with the various lithium salts is shown in figure 1. The density and dynamic viscosity of neat C_4mpyrDCA is 1.01 g.cm^{-3} and 35 cP at 25 °C, consistent with other recently published data for this compound.[19] However, the measured density is higher and the viscosity is lower than older reported values of 0.95 g.cm^{-3} and 50 cP respectively,[13, 24] which may be due the different impurity and moisture content between these reports. The density increases when 0.5 mol.kg^{-1} of the lithium salt is added and the increase follows the molecular weight of each salt. The viscosity which is shown in figure 1(b) shows a different behavior. LiDCA, the lowest molecular weight lithium salt in this report, showed the lowest density and lowest viscosity. However, LiBF$_4$, shows higher viscosity than the larger and heavier lithium salts such as LiNTf$_2$or LiFSI.
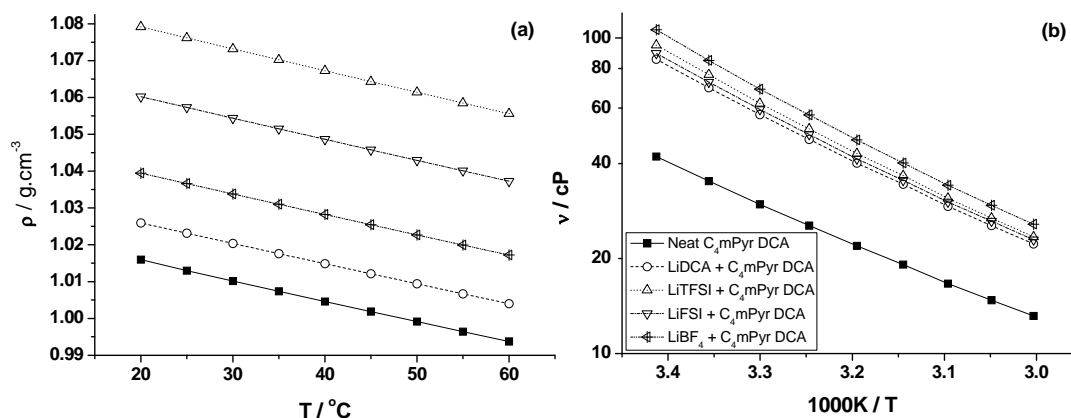
Figure 1 (a) Density and (b) Dynamic viscosity of C_4mpyrDCA with 0.5 mol.kg^{-1} of various lithium salts

DSC traces for both the neat IL and electrolytes thereof are presented in figure 2. The onset temperature of melting in the neat IL is -16 °C. A transition is observed at -89 °C which we ascribe to the glass transition in the quenched material and this is followed by a large, broad exothermic peak during heating at -44 °C, due to crystallization of the neat IL.[25] When 0.5

mol.kg^{-1} LiDCA was added, the crystallization peak at -44 °C and melting peak disappear, showing only the glass transition at between -99 °C and -89 °C. This is also observed in a similar temperature range when the IL is mixed with the other lithium salts. Another broad peak was also observed in the lithium salt mixtures between 0 °C and 40 °C. This peak which is shown clearly with LiNTf$_2$, but not so clearly with LiDCA may be related to the solubility of the lithium salts. We hypothesize that the lithium salts crystallize during cooling due to low solubility at lower temperature and dissolve again during heating in this temperature range.
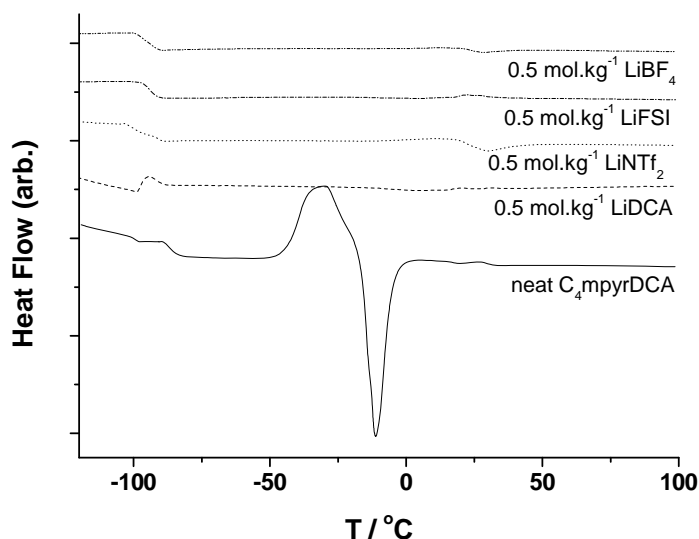
Figure 2 DSC of C$_4$mpyrDCA with various lithium salts (Exo up, heating rate : 10 ^{o}C.min^{-1})

Table S1 provides the summary of the physical properties of some reported ionic liquids having the DCA anion with various cation species. The conductivity of the C$_4$mpyrDCA – lithium salt mixtures is presented in figure 3. The conductivity of neat C$_4$mpyrDCA is 6 mS.cm^{-1} at 25 °C which is lower than the previously reported value of C$_3$mpyrFSI but higher than the on of C$_4$mpyrNTf$_2$.(Table S2) This conductivity decreases with temperature and

rapidly drops from -15 °C as it passes the melting point as we saw in the DSC data. When 0.5 mol.kg^{-1} of salt is added to the IL, the drop due to the freezing of the IL is eliminated. The mixture containing LiDCA shows the highest conductivity followed by LiFSI, LiBF$_4$ and LiNTf$_2$ order at 25 °C. However, the temperature dependency of LiBF$_4$ containing solution is higher than the others, such that it showed the lowest conductivity at -30 °C.

Figure 3 Conductivity of C$_4$mpyrDCA with 0.5 mol.kg^{-1} of various lithium salts

Table S1 Physical properties of DCA ionic liquids with various cations

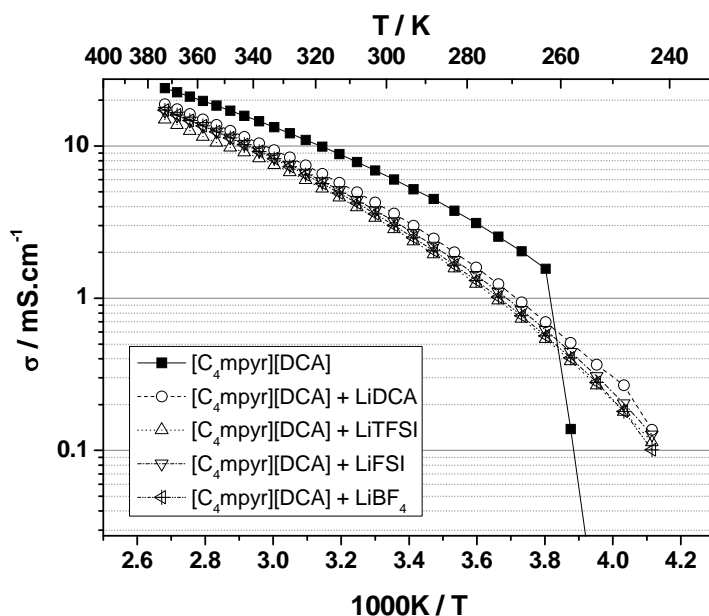| Cation	Tg (°C)	M.P (°C)	Density (g.cm^{-3}, at 25°C)	Vis.(cP, at 25°C)	Cond.(mS.cm^{-1}, at 25°C)	Ref.
1,3-dimethylimidazolium		34	1.14 (at 20°C)	15.5	36	[26]
1-ethyl-3-methylimidazolium	-104	-21	1.06	21		[11, 13, 27]
	-101	-15				[15]
1-butyl-3-methylimidazolium	-90	-6	1.06 (at 24°C)			[28]
	-94	-10	1.06	29.3	11	[29]
1-hexyl-3-methylimidazolium	-90		1.04 (at 20°C)	47.4	5.1	[26]
1-oxyl-3-methylimidazolium	-89	-49	1.00			[30]
	-93			34		[31]
1-decyl-3-methylimidazolium	-23			76		[31]
1-benzyl-3-methylimidazolium	-78			40		[31]
1,3-dibenzylimidazolium	-45			202		[31]
1-(n-butyl)-2,3-dimethylimidazolium	-81	26	1.09	67.2	4.9	[29]
1-(n-butyl)-1,3'-dimethyl-2,2'-biimidazolium	-42		1.17	977	0.41	[29]
1-(i-butyl)-3-methylimidazolium	-80		1.08	61.1	5.5	[29]
1-(t-butyl)-3-methylimidazolium		59	1.12		0.046	[29]
N-Pentyl-N,N,N-triethylammonium	-85					[11]
N-Hexyl-N,N,N-triethylammonium	-82					[11, 13]
N-Hexyl-N,N,N-tributylammonium		-43				[11, 13]
tricapryl-methylammonium	-90			300		[31]
benzyltriethylammonium	-83					[31]
phynyltrimethylammonium	-117					[31]

dimethyldihexylguanidinium	-77			267		[31]
1-ethyl-2-methylpyrazolium		13	1.16 (at 20°C)	24.6	17	[26]
N-ethylthiazolium		57				[26]
N,N-dimethylpyrrolidinium		115				[11,13]
N-Ethyl-N-methylpyrrolidinium		-10				[11,13]
		-14	1.06 (at 20°C)	27.5	20	[26]
N-Propyl-N-methylpyrrolidinium		-35	0.92	45		[11,13]
N-Butyl-N-methylpyrrolidinium	-106			50		[11,13]
N-Hexyl-N-methylpyrrolidinium	-100	-11	0.92	45		[11,13]

Table 2 Physical properties of ionic liquids with lithium salts

Electroylte	Tg (°C)	m.p. (°C)	Cond. (S.cm^{-1})	Viscosity (mm^2.s^{-1})	^{19}F (m^2.s^{-1}) (FSI)	^{19}F (m^2.s^{-1}) (NTf$_2$)	^{7}Li (m^2.s^{-1})	^{1}H (m^2.s^{-1}) (Pyr.)
C$_3$mpyrNTf$_2$	-73[32]	12[32]	1.4e-3(60 °C) [33]	138 (20 °C) [33] 89 (25 °C)[34]		1.47e-11 (20 °C) [33] 7.54e-11 (60 °C) [33]		3.42e-11 (60 °C) [33]
C$_3$mpyrNTf$_2$+ 0.5 mol.kg^{-1} Li NTf$_2$		-14[33]	8.8e-4 (20 °C) [33] 3.5e-3(60 °C) [33]	157 (20 °C) [33]		4.68e-12(20 °C) [33] 3.48e-11(60 °C) [33]	3.1e-11(60 °C) [33]	
C$_4$mpyrNTf$_2$		10[32]						
C$_3$mpyrFSI		5[33]	9.14e-3(20 °C) [33]	37(20 °C) [33] 12(60 °C) [33]	3.44e-11(20 °C) [33] 1.24e-10(60 °C) [33]			2.87e-11(20 °C) [33] 1.05e-10(60 °C) [33]
C$_3$mpyrFSI+ 0.5 mol.kg^{-1} Li NTf$_2$		-28[33]	1.12e-3(20 °C) [33] 6.90e-3(50 °C) 2) [33]	60(20 °C) [33] 17(60 °C) [33]	2.01e-11(20 °C) [33] 6.38e-11(60 °C) [33]	1.06e-11(20 °C) [33] 4.95e-11(60 °C) [33]	4.67e-11(60 °C) [33]	1.74e-11(20 °C) [33] 4.86e-11(60 °C) [33]
C$_3$mpyrDCA		-35[11,13]	1.93e-4(25 °C) [35]	25.6(25 °C) [35] 45 (25 °C) [11,13]				
C$_4$mpyrDCA	-106[11,13]			50[11,13]				

PFG-STE NMR:

Figure 4 shows the diffusivity of each ion in the neat IL and each lithium salt containing electrolyte measured by PFG-STE NMR. The ^{1}H NMR results in figure 4(a) for the C$_3$mpyr cation shows that it has the highest mobility in the neat IL and that the addition of the lithium salts causes a significant drop in diffusivity. The mixture containing LiBF$_4$ has the lowest diffusivity followed by LiNTf$_2$, LiFSI and LiDCA. This order is the same as the order that we have seen at the dynamic viscosity data in figure 1(b). The ^{7}Li NMR results in figure 4(b)

also show the same trends. In the case of ^{13}C NMR signal from the DCA anion in figure 4(c), due to its experimental complexity and resulting experimental error, the diffusivity difference between each salt containing solution is not as clear, but it is still obvious that the LiDCA containing solution shows the highest diffusivity except the neat IL, while the LiBF$_4$ containing solution shows the lowest diffusivity.
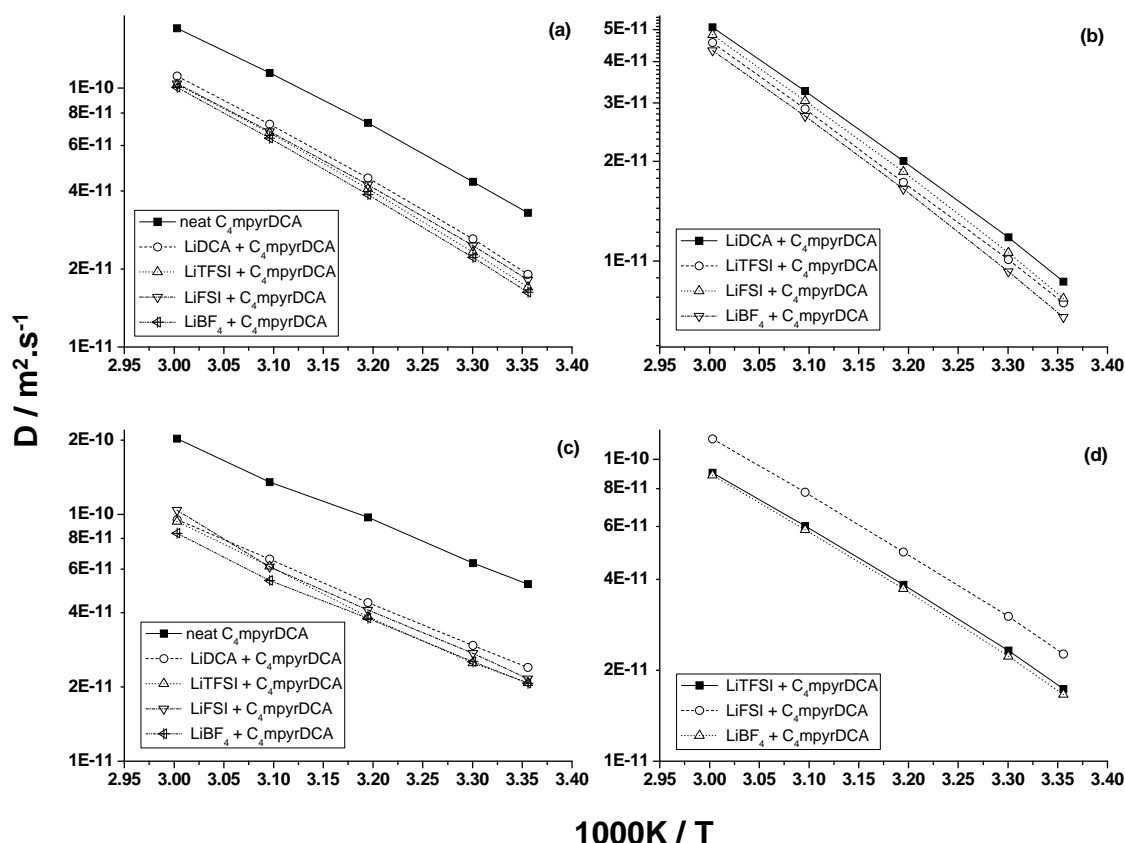

Figure 4 The diffusivity of each ions measured by PFG-STE NMR, a) ^{1}H diffusion for C$_4$mpyr$^+$, b) ^{7}Li diffusion for Li$^+$, c) ^{13}C diffusion for DCA anion, d) ^{19}F diffusion for the added anion from lithium salts. Measured from 25 ^{o}C to 60 ^{o}C

An interesting behavior was found in the ^{19}F diffusion data, figure 4(d); the diffusivity of the fluorinate containing anions is slowest for BF$_4^-$ followed by NTf$_2^-$ and FSI$^-$. However, the diffusivity of ^{19}F FSI$^-$ is unusually high comparing to the other ^{1}H, ^{7}Li and ^{13}C diffusivity. It

also should be noted that while the ^{19}F diffusivities are similar to the ^{1}H diffusivities in

LiNTf$_2$ or LiBF$_4$ added solution, ^{19}F diffusivity in LiFSI added solution are noticeably higher

than the diffusivity of other ions. This indicates that the surrounding environment of FSI$^-$ in

this IL is different from the surrounding environment of NTf$_2^-$ or BF$_4^-$, and makes FSI$^-$ more

mobile. This may indicates that the ion pares or clusters formed in LiFSI containing solution

does not contain FSI$^-$, while NTf$_2^-$ or BF$_4^-$ are more bound to the ion pares or clusters..

Walden plot and Ionicity:

A log-log plot of molar conductivity versus inverse viscosity, as described by Angell and co-

workers, is a useful depiction of the Walden rule.[2, 36]

$$\Lambda \eta^{\alpha} = C \qquad\qquad (1)$$

where Λ is the molar conductivity and η is the viscosity, α is an adjustable parameter and C is

temperature dependent constant. A reference line is added to the plot based on data from

infinitely dilute aqueous KCl data in the temperature range $15 - 50°C$,[37] as these solutions are

thought to represent good example of well dissociated ions that are able to move

independently of one another.[37] The temperature dependence of the infinitely diluted KCl

data is such that α in equation 1 is 0.87 and thus the reference line has a slope that is different

to the traditionally used line on these plots which is based on a single temperature only. It is

important to note that the Walden rule applies equally well to molten salts and the same

reference line equally describes a number of well characterised molten salt systems.[38] Where

substantial negative deviations from this rule are observed, this has been interpreted as an

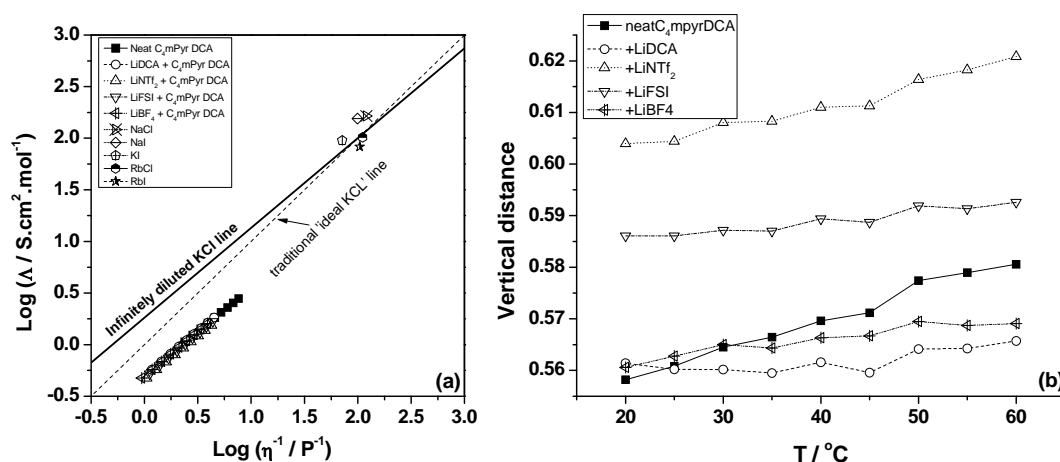indication of ion aggregation or pairing.[9]

Figure 5 (a) Relationships between log inversed viscosity and log molar conductivity (Walden plot) for C$_4$mpyrDCA with 0.5 mol.kg^{-1} of various lithium salts (some high temperature molten salt data also included for comparision) and (b) the vertical distance from the infinitely dilute KCl line.

The Walden plot of C$_4$mpyrDCA with each of the lithium salt mixtures is presented in figure 5(a). The non-unity value of α, which is evident from the non-unity slope of the line is very evident in these data sets. It has been known that a 'good IL' in Walden plot shows proximity to the ideal line (α = 1, C = 0).[2, 36] Linear fitting in figure 5(a) reveals values of 0.82 for the neat IL and 0.84 to 0.86 for the salt containing solutions, similar to those generally observed in other ILs.[2, 39-42] The vertical distance from the traditional ideal KCl line, C values, are similar for all solutions having strong temperature dependency (affected by α). However, the vertical distances from the infinitely diluted KCl line which representing the 'fractional Walden rule'[37] (presented in figure 5(b)) more clearly shows that the temperature dependency is reduced when LiDCA or LiFSI is added in C$_4$mpyrDCA. It was also shown that LiNTf$_2$ and LiFSI added solution show the most non-ideal behavior comparing to the other solution. Therefore, more ions are associated in LiNTf$_2$ and LiFSI containing solutions than the others.[43] We also tried to adapt the 'modified Walden plot' which included the effect of ion

sizes introduced by MacFarlane, et al.[8] to see the difference between neat IL and LiDCA, LiBF$_4$ containing solution, but that also showed the same trend.

Having a similar purpose to a Walden plot, the 'ionicity', the ratio of differently obtained conductivity by impedance spectroscopy and diffusion NMR, $\Lambda_{imp} / \Lambda_{NMR}$ also describes the degree of ion dissociation in the ionic liquid since the value obtained by impedance spectroscopy, Λ_{imp}, is contributed by all species in the solution while the calculated conductivity from the diffusion NMR by the Nernst-Einstein equation (equation 2) includes contributions from associated species.[44]

$$\Lambda = \frac{N_A e^2}{kT} \left(2 \sum D_i x_i \right) \qquad (2)$$

where N_A is the Avogadro's number, k is Boltzmann's constant, and D_i is the diffusivity of each ion and x_i is the mol fraction of each ion.
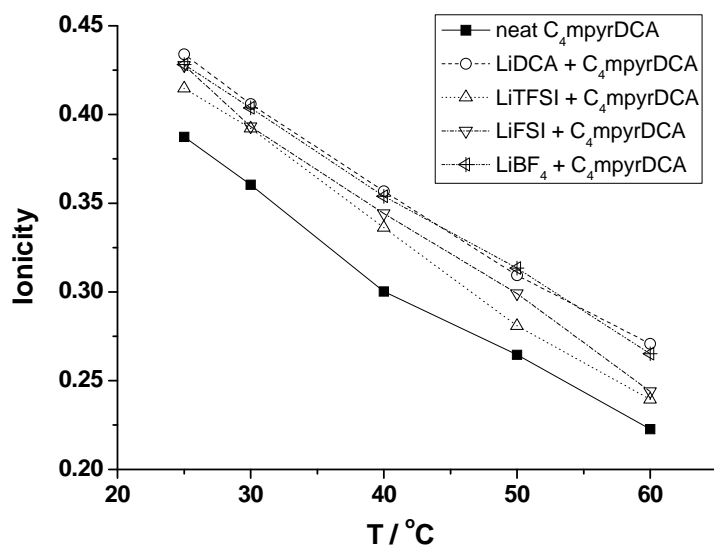

Figure 6 The ratio of molar conductivity from EIS and NMR conductivity ($\Lambda_{imp} / \Lambda_{NMR}$, 'Ionicity') of C$_4$mpyrDCA with various lithium salts.

Figure 6 shows the ionicity of each salt containing solution at different temperatures. It is shown that the ionicity decreases with increased temperature, which indicates ions more tend to form pairs or neural clusters at higher temperature in these tested solutions. An interesting observation is the ionicity of neat IL is the lowest and all lithium salt added solution showed higher ionicity. The solution containing LiDCA or LiBF₄ showed the highest ionicity, which is the opposite of the result from the Walden plot presented in figure 5. This result was compared with a different plotting method which was described by MacFarlane, et al, [36] the 'ionicity plot' in figure 7 and the vertical distance from the ideal line in table 3, which also shows the same trend shown in figure 6. This observation also correlates with the viscosity result presented at figure 1(b) of the solution having LiBF₄, which has lower density but shows higher viscosity.
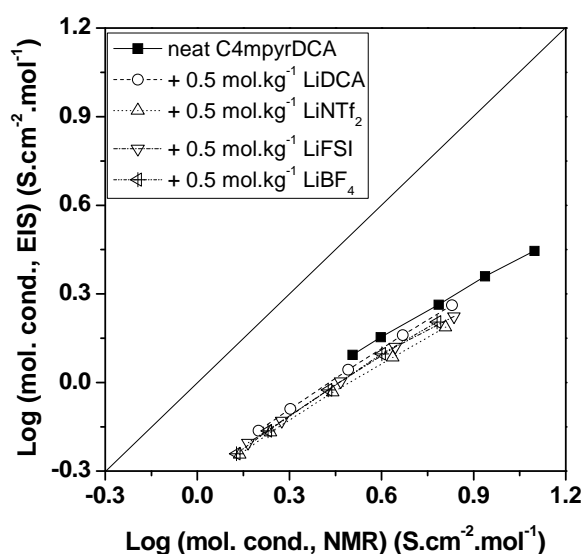

Figure 7 The 'Ionicity plot'; molar conductivity from EIS vs. molar NMR conductivity of C₄mpyrDCA with various lithium salts.

There are 2 possibilities for this inconsistency between the 'Walden plot' and 'Ionicity'. At first, the Walden rule may not be directly used for a solution containing salts, having more

than 2 ionic species in the solution for comparative purposes with a neat IL. Secondly, there is a possibility that $LiBF_4$ and LiDCA containing solutions tend to form "salt rich" clusters with high numbers of ions that lowering the diffusivity of each ion in the solution than the expected values when ions were dissociated or only forms ion pairs.

Table 3 Vertical distance of each solution from the ideal line in figure 7

Temperature (°C)	Neat C$_4$mpyrDCA	0.5 mol.kg^{-1} LiDCA in C$_4$mpyrDCA	0.5 mol.kg^{-1} Li NTf$_2$ in C$_4$mpyrDCA	0.5 mol.kg^{-1} LiFSI in C$_4$mpyrDCA	0.5 mol.kg^{-1} LiBF$_4$ in C$_4$mpyrDCA
25	0.41	0.36	0.38	0.37	0.37
30	0.44	0.39	0.41	0.41	0.39
40	0.52	0.45	0.47	0.46	0.45
50	0.58	0.51	0.55	0.52	0.50
60	0.65	0.57	0.62	0.61	0.58

Symmetrical cell EIS:

Li symmetrical cells were prepared to determine the dependence of the electrochemical behaviour to lithium metal surface on the different dissolved Li salts. EIS spectra were measured 2 hours after cell preparation. The cells were then subjected to a 1 V polarisation for 5 min and subsequent EIS spectra were acquired. The EIS spectra are presented in figure 8.
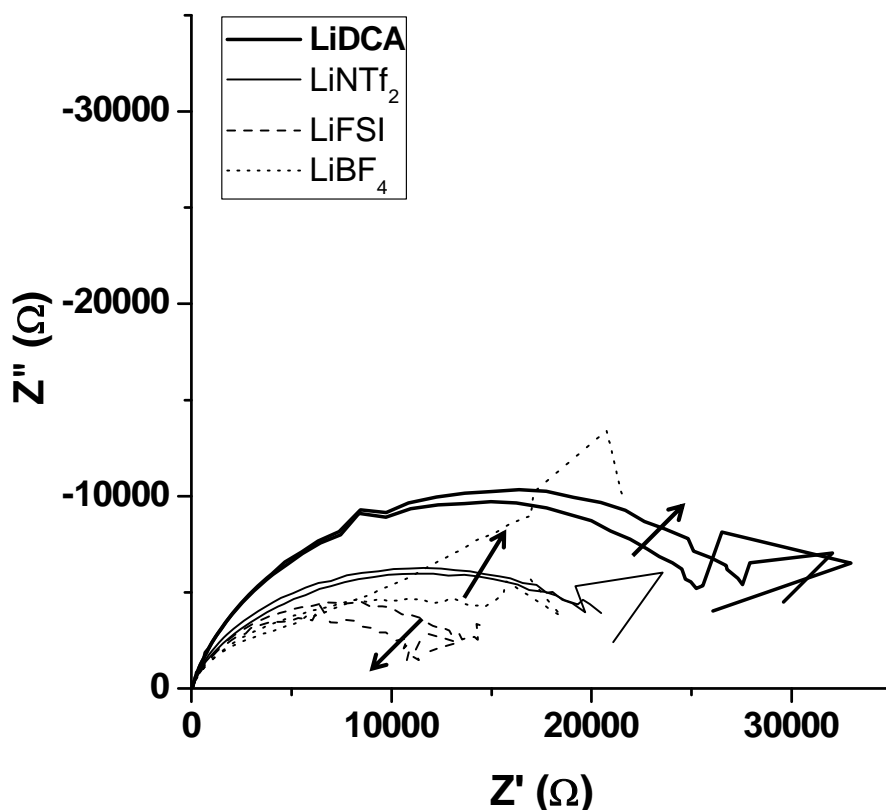
Figure 8 EIS of Li symmetrical coin cells containing of each solution; 2 EIS curves with arrows for each solution indicate 1st, after the cell prepared (before polarized) and 2nd after polarized.

It is immediately obvious that the addition of perfluorinated salts produces lower interfacial impedance at the Li surface compared to the DCA system in these cells. The initial impedance of the EIS spectra acquired from the 0.5 mol.kg^{-1} LiDCA in C$_4$mpyrDCA cell ranged from 10 to 20 thousand ohms the impedance did not change significantly after cell polarization. Similar stability after polarization was also observed with the cell with LiNTf$_2$ salt. However, when the cell contained LiBF$_4$ salt, the impedance increased rapidly after polarization. The solution with LiFSI salt showed the lowest impedance in the prepared solutions and the second measured impedance was lower than the first measurement. This

may be caused by increasing lithium surface area by a corrosion process during the initial polarization, which was reported previously.[45-47]
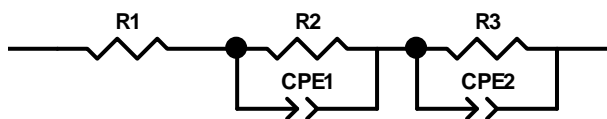

Figure 9 Fitting model for the EIS with 2 constant phase elements.

The surface impedance was modelled by fitting the equivalent circuit shown in figure 9 and the results are presented in table 4. The surface impedance of the cells after polarisation (R2 + R3) was high when LiDCA or LiBF$_4$ salts were used, while LiNTf$_2$ or LiFSI salts shows relatively lower surface impedance. This may correlate with the relatively high ionicity of the solutions with LiDCA or LiBF$_4$ compared to LiNTf$_2$ or LiFSI as shown here. It has previously been shown[47] that chemical processes derived from decomposition of the IL anion often dominate the surface impedance. However, it is not clear what role the degree of ionic association in the IL or the ability of the IL to structure at the interface play in this process. We will investigate the relationship between ionicity and Li surface impedance in further work. The initial measurements shown here indicate that the use of alternative Li salts in DCA based ILs offer a promising method to control the development of surface impedance in Li based cells, with potential for improved performance.

Table 4 EIS fitting results (numbers in the bracket indicates the fitting errors)

EIS	R1 (Ω)	R2 (Ω)	R3 (Ω)
0.5 mol.kg^{-1} LiDCA, before polarization	20 (2.5%)	22,417 (16.4%)	8,055 (42.8%)
0.5 mol.kg^{-1} LiDCA, after polarization	20 (2.9%)	22183 (13.3%)	5,976 (47.5%)
0.5 mol.kg^{-1} Li NTf$_2$, before polarization	62 (1.7%)	16,447 (6.7%)	4,400 (19.0%)
0.5 mol.kg^{-1} Li NTf$_2$,	48 (1.7%)	15,396 (9.2%)	5,961 (19.1%)

after polarization			
0.5 mol.kg^{-1} LiFSI, before polarization	20 (4.4%)	9,524 (9.7%)	6,393 (15.8%)
0.5 mol.kg^{-1} LiFSI, after polarization	21 (5.0%)	5,089 (18.7%)	7,746 (13.4%)
0.5 mol.kg^{-1} LiBF$_4$, before polarization	14 (14.4%)	27,360 (8.2%)	4,491 (11.9%)
0.5 mol.kg^{-1} LiBF$_4$, after polarization	15 (11.0%)	27,426 (7.1%)	5,102 (8.0%)

CONCLUSIONS

We have investigated the physical properties of C$_4$mpyrDCA with a class of lithium salts

dissolved in it by density, viscosity, DSC, conductivity and diffusion NMR experiments. It

was shown that when LiDCA was added, the solution has the lowest viscosity and highest

ionic mobility with highest degree of ionization while when LiBF$_4$ was added the solution has

the opposite properties. Unlike the other added salt anion species, BF$_4^-$ was shown to make a

larger cluster than simple ion pairs. FSI- anion also showed different behaviours from the

other anions, which has unusually high mobility which can be interpreted to be isolated from

a cluster formed by other ionic species in this DCA solution. We also note that the fractional

Walden plots with infinitely diluted KCl line distinguish more effectively than the traditional

Walden plot the difference between the solutions having different salts. The 'ionicity', the

ratio of the molar electroscopic conductivity versus the conductivity obtained by the diffusion

NMR by Nernst-Einstein equation represent better than the Walden plot when comparing a

neat IL to a salt mixed system. The EIS experiments show the positive correlation between

ionicity and lithium surface impedance.

REFERENCES

1.   Angell, C. A.; Xu, W.; Yoshizawa, M.; Hayashi, A.; Belieres, J.-P.; Lucas, P.; Videa, M., Physical Chemistry of Ionic Liquids, Inorganic and Organic, Protic and Aprotic. In *Electrochemical Aspects of Ionic Liquids*, Hiroyuki, O., Ed. 2005; pp 5-23.

2.   Angell, C. A.; Byrne, N.; Belieres, J.-P., Parallel developments in aprotic and protic ionic liquids: Physical chemistry and applications. *Accounts of Chemical Research* **2007,** *40* (11), 1228-1236.

3.   Armand, M.; Choquette, Y.; Gauthier, M.; Michot, C.; Chobuette, Y.; Kapfer, B. Salts of perfluorinated amides - useful materials with ionic and electronic conduction, as colourants and catalysts. EP850920-A; WO9829358-A; etc., Dec 30 1997.

4.   Sakaebe, H.; Matsumoto, H., N-Methyl-N-propylpiperidinium bis(trifluoromethanesulfonyl)imide (PP 13-TFSI) - novel electrolyte base for Li battery. *Electrochemistry Communications* **2003,** *5* (7), 594-598.

5.   Garcia, B.; Lavallee, S.; Perron, G.; Michot, C.; Armand, M., Room temperature molten salts as lithium battery electrolyte. *Electrochimica Acta* **2004,** *49* (26), 4583-4588.

6.   Matsumoto, H.; Sakaebe, H.; Tatsumi, K.; Kikuta, M.; Ishiko, E.; Kono, M., Fast cycling of Li/LiCoO2 cell with low-viscosity ionic liquids based on bis(fluorosulfonyl)imide FSI (-). *Journal of Power Sources* **2006,** *160* (2), 1308-1313.

7.   Scheers, J.; Johansson, P.; Jacobsson, P., Anions for lithium battery electrolytes: A spectroscopic and theoretical study of the B(CN)(4)(-) anion of the ionic liquid C-2mim B(CN)(4). *Journal of the Electrochemical Society* **2008,** *155* (9), A628-A634.

8.   Lane, G.; Best, A.; MacFarlane, D.; Forsyth, M.; Hollenkamp, T.; Begic, S., Lithium battery electrolytes based on the ionic liquid N-methyl-N-butylpyrrolidinium dicyanamide:compatibility with different electrode materials including lithium metal, Li4Ti5O12, LiFePO4 and LiCoO2. CSIRO, Monash University: Clayton, VIC, 2010.

9.   Scheers, J.; Pitawala, J.; Thebault, F.; Kim, J.-K.; Ahn, J.-H.; Matic, A.; Johansson, P.; Jacobsson, P., Ionic liquids and oligomer electrolytes based on the B(CN)(4)(-) anion; ion association, physical and electrochemical propertiesw. *Physical Chemistry Chemical Physics* **2011,** *13* (33), 14953-14959.

10.   Younesi, R.; Hahlin, M.; Treskow, M.; Scheers, J.; Johansson, P.; Edstrom, K., Ether Based Electrolyte, LiB(CN)(4) Salt and Binder Degradation in the Li-O-2 Battery Studied by Hard X-ray Photoelectron Spectroscopy (HAXPES). *Journal of Physical Chemistry C* **2012,** *116* (35), 18597-18604.

11.   MacFarlane, D. R.; Forsyth, S. A.; Golding, J.; Deacon, G. B., Ionic liquids based on imidazolium, ammonium and pyrrolidinium salts of the dicyanamide anion. *Green Chemistry* **2002,** *4* (5), 444-448.

12.   Yoon, H.; Lane, G. H.; Shekibi, Y.; Howlett, P. C.; Forsyth, M.; Best, A. S.; MacFarlane, D. R., Lithium electrochemistry and cycling behaviour of ionic liquids using cyano based anions. *Energy & Environmental Science* **2013,** *6* (3), 979-986.

13.   MacFarlane, D. R.; Golding, J.; Forsyth, S.; Forsyth, M.; Deacon, G. B., Low viscosity ionic liquids based on organic salts of the dicyanamide anion. *Chemical Communications* **2001,** (16), 1430-1431.

14.   Seeber, A. J.; Forsyth, M.; Forsyth, C. M.; Forsyth, S. A.; Annat, G.; MacFarlane, D. R., Conductivity, NMR and crystallographic study of N,N,N,N-tetramethylammonium dicyanamide plastic crystal phases: an archetypal ambient temperature plastic electrolyte material. *Physical Chemistry Chemical Physics* **2003,** *5* (12), 2692-2698.

15.   Tiyapiboonchaiya, C.; Pringle, J. M.; MacFarlane, D. R.; Forsyth, M.; Sun, J. Z., Polyelectrolyte-in-ionic-liquid electrolytes. *Macromolecular Chemistry and Physics* **2003,** *204* (17), 2147-2154.

16.   Adebahr, J.; Grozema, F. C.; deLeeuw, S. W.; MacFarlane, D. R.; Forsyth, M., Structure and dynamics of the plastic crystal tetramethylammonium dicyanamide - a molecular dynamics study. *Solid State Ionics* **2006,** *177* (33-34), 2845-2850.

17.   Wang, P.; Zakeeruddin, S. M.; Moser, J. E.; Gratzel, M., A new ionic liquid electrolyte enhances the conversion efficiency of dye-sensitized solar cells. *Journal of Physical Chemistry B* **2003,** *107* (48), 13280-13285.

18.   Chen, J.; Officer, D. L.; Pringle, J. M.; MacFarlane, D. R.; Too, C. O.; Wallace, G. G., Photoelectrochemical solar cells based on polyterthiophenes containing Porphyrins using ionic liquid electrolyte. *Electrochemical and Solid State Letters* **2005,** *8* (10), A528-A530.

19.   González, E. J.; González, B. a.; Macado, E. n. A., Thermophysical Properties of the Pure Ionic Liquid 1-Butyl-1-methylpyrrolidinium Dicyanamide and Its Binary Mixtures with Alcohols. *Journal of Chemical & Engineering Data* **2013,** *58*, 1440-1448.

20.   Peled, E.; Golodnitsky, D.; Ardel, G., Advanced model for solid electrolyte interphase electrodes in liquid and polymer electrolytes. *Journal of the Electrochemical Society* **1997,** *144* (8), L208-L210.

21.   Howlett, P. C.; Brack, N.; Hollenkamp, A. F.; Forsyth, M.; MacFarlane, D. R., Characterization of the lithium surface in N-methyl-N-alkylpyrrolidinium bis(trifluoromethanesulfonyl) amide room-temperature ionic liquid electrolytes. *Journal of the Electrochemical Society* **2006,** *153* (3), A595-A606.

22.   Purdy, A. P.; Houser, E.; George, C. F., Lithium dicyanamide, its reactions with cyanuric chloride, and the crystal structures of LiN(CN)(2)(MeCN)(2) and LiCN(C5H5N)(2). *Polyhedron* **1997,** *16* (20), 3671-3679.

23.   Bayley, P. M.; Lane, G. H.; Rocher, N. M.; Clare, B. R.; Best, A. S.; MacFarlane, D. R.; Forsyth, M., Transport properties of ionic liquid electrolytes with organic diluents. *Physical Chemistry Chemical Physics* **2009,** *11* (33), 7202-7208.

24.   Emel'yanenko, V. N.; Verevkin, S. P.; Heintz, A.; Corfield, J. A.; Deyko, A.; Lovelock, K. R. J.; Licence, P.; Jones, R. G., Pyrrolidinium-based ionic liquids. 1-butyl-1-methyl pyrrolidinium dicyanoamide: Thermochemical measurement, mass spectrometry, and ab initio calculations. *Journal of Physical Chemistry B* **2008,** *112* (37), 11734-11742.

25.   Zhou, Q.; Henderson, W. A.; Appetecchi, G. B.; Montanino, M.; Passerini, S., Physical and Electrochemical Properties of N-Alkyl-N-methylpyrrolidinium Bis(fluorosulfonyl)imide Ionic Liquids: PY13FSI and PY14FSI. *Journal of Physical Chemistry B* **2008,** *112* (43), 13577-13580.

26.   Yoshida, Y.; Baba, O.; Saito, G., Ionic liquids based on dicyanamide anion: Influence of structural variations in cationic structures on ionic conductivity. *Journal of Physical Chemistry B* **2007,** *111* (18), 4742-4749.

27.   Forsyth, S. A.; Pringle, J. M.; MacFarlane, D. R., Ionic liquids - An overview. *Australian Journal of Chemistry* **2004,** *57* (2), 113-119.

28.   Fredlake, C. P.; Crosthwaite, J. M.; Hert, D. G.; Aki, S.; Brennecke, J. F., Thermophysical properties of imidazolium-based ionic liquids. *Journal of Chemical and Engineering Data* **2004,** *49* (4), 954-964.

29.   Yoshida, Y.; Baba, O.; Larriba, C.; Saito, G., Imidazolium-based ionic liquids formed with dicyanamide anion: Influence of cationic structure on ionic conductivity. *Journal of Physical Chemistry B* **2007,** *111* (42), 12204-12210.

30.   Papaiconomou, N.; Yakelis, N.; Salminen, J.; Bergman, R.; Prausnitz, J. M., Synthesis and properties of seven ionic liquids containing 1-methyl-3-octylimidazolium or 1-butyl-4-methylpyridinium cations. *Journal of Chemical and Engineering Data* **2006,** *51* (4), 1389-1393.

31.   Kulkarni, P. S.; Branco, L. C.; Crespo, J. G.; Nunes, M. C.; Raymundo, A.; Afonso, C. A. M., Comparison of physicochemical properties of new ionic liquids based on imidazolium, quaternary ammonium, and guanidinium cations. *Chemistry-a European Journal* **2007,** *13* (30), 8478-8488.

32.   Johansson, K. M.; Adebahr, J.; Howlett, P. C.; Forsyth, M.; MacFarlane, D. R., N-methyl-N-alkylpyrrolidinium bis(perfluoroethylsulfonyl) amide (NPf(2) (-)) and tris(trifluoromethanesulfonyl) methide (CTf3 (-)) salts: Synthesis and characterization. *Australian Journal of Chemistry* **2007,** *60* (1), 57-63.

33.   Saint, J.; Best, A. S.; Hollenkamp, A. F.; Kerr, J.; Shin, J. H.; Doeff, M. M., Compatibility of LixTiyMn1-yO2 (y=0, 0.11) electrode materials with pyrrolidinium-based ionic liquid electrolyte systems. *Journal of the Electrochemical Society* **2008,** *155* (2), A172-A180.

34.   Ugo, P.; Moretto, L. M.; De Leo, M.; Doherty, A. P.; Vallese, C.; Pentlavalli, S., Diffusion regimes at nanoelectrode ensembles in different ionic liquids. *Electrochimica Acta* **2010,** *55* (8), 2865-2872.

35.   Cai, N.; Zhang, J.; Zhou, D. F.; Yi, Z. H.; Guo, J.; Wang, P., N-Methyl-N-Allylpyrrolidinium Based Ionic Liquids for Solvent-Free Dye-Sensitized Solar Cells. *Journal of Physical Chemistry C* **2009,** *113* (10), 4215-4221.

36.   MacFarlane, D. R.; Forsyth, M.; Izgorodina, E. I.; Abbott, A. P.; Annat, G.; Fraser, K., On the concept of ionicity in ionic liquids. *Physical Chemistry Chemical Physics* **2009,** *11* (25), 4962-4967.

37.   Schreiner, C.; Zugmann, S.; Hartl, R.; Gores, H. J., Fractional Walden Rule for Ionic Liquids: Examples from Recent Measurements and a Critique of the So-Called Ideal KCl Line for the Walden Plot. *Journal of Chemical & Engineering Data* **2010,** *55* (5), 1784–1788.

38.   Smedley , S. I., *The interpretation of ionic conductivity in liquids*. New York : Plenum Press: 1980.

39.   Makino, T.; Kanakubo, M.; Umecky, T.; Suzuki, A.; Nishida, T.; Takano, J., Electrical Conductivities, Viscosities, and Densities of N-Methoxymethyl- and N-Butyl-N-methylpyrrolidinium Ionic Liquids with the Bis(fluorosulfonyl)amide Anion. *Journal of Chemical and Engineering Data* **2012,** *57* (3), 751-755.

40.   Ferrari, S.; Quartarone, E.; Mustarelli, P.; Magistris, A.; Protti, S.; Lazzaroni, S.; Fagnoni, M.; Albini, A., A binary ionic liquid system composed of N-methoxyethyl-N-methylpyrrolidinium bis(trifluoromethanesulfonyl)-imide and lithium bis(trifluoromethanesulfonyl)imide: A new promising electrolyte for lithium batteries. *Journal of Power Sources* **2009,** *194* (1), 45-50.

41.   Xu, W.; Cooper, E. I.; Angell, C. A., Ionic liquids: Ion mobilities, glass temperatures, and fragilities. *Journal of Physical Chemistry B* **2003,** *107* (25), 6170-6178.

42.   Ueno, K.; Tokuda, H.; Watanabe, M., Ionicity in ionic liquids: correlation with ionic structure and physicochemical properties. *Physical Chemistry Chemical Physics* **2010,** *12* (8), 1649-1658.

43.   Fraser, K. J.; Izgorodina, E. I.; Forsyth, M.; Scott, J. L.; MacFarlane, D. R., Liquids intermediate between "molecular" and "ionic" liquids: Liquid Ion Pairs? *Chemical Communications* **2007,** (37), 3817-3819.

44.   Noda, A.; Hayamizu, K.; Watanabe, M., Pulsed-gradient spin-echo H-1 and F-19 NMR ionic diffusion coefficient, viscosity, and ionic conductivity of non-chloroaluminate room-temperature ionic liquids. *Journal of Physical Chemistry B* **2001,** *105* (20), 4603-4610.

45.   Best, A. S.; Bhatt, A. I.; Hollenkamp, A. F., Ionic Liquids with the Bis(fluorosulfonyl) imide Anion: Electrochemical Properties and Applications in Battery Technology. *Journal of the Electrochemical Society* **2010,** *157* (8), A903-A911.

46.   Bhatt, A. I.; Best, A. S.; Huang, J.; Hollenkamp, A. F., Application of the N-propyl-N-methyl-pyrrolidinium Bis(fluorosulfonyl)imide RTIL Containing Lithium Bis(fluorosulfonyl)imide in Ionic Liquid Based Lithium Batteries. *Journal of the Electrochemical Society* **2010,** *157* (1), A66-A74.

47.   Bhatt, A. I.; Kao, P.; Best, A. S.; Hollenkamp, A. F., Understanding the Morphological Changes of Lithium Surfaces during Cycling in Electrolyte Solutions of Lithium Salts in an Ionic Liquid. *Journal of the Electrochemical Society* **2013,** *160* (8), A1171-A1180.

Chapter 5. Summary and future work

This chapter summarizes the conclusion of this thesis and comments more broadly on the issues facing ionic liquid based electrolytes for battery applications as well as possible directions for future research.

<u>Summary</u>

This thesis examined two different ionic liquids; a fluorinated anion based ionic liquid, FSI and a non-fluorinated ionic liquid, based on the DCA anion. FSI was chosen for its higher conductivities and diffusivities than the corresponding NTf_2 compounds, and DCA for its relatively wide electrochemical window and high lithium salt solubility among other non-fluorinated nitrile compounds.

FSI anion based ILs showed excellent rate capability (even higher than that of standard EC : DMC with 1M $LiPF_6$ standard battery electrolyte) at high lithium concentrations (3.2 mol.kg^{-1} LiFSI in C_3mpyr FSI, or 1:1 molar ratio of the salt : IL), with both the lithium metal electrode and $LiCoO_2$ cathode, in spite of their significantly higher viscosities and lower conductivities. This unusual behaviour was investigated using electrochemical and spectroscopic techniques and it was rationalised that the FSI electrolyte containing the highest salt concentration (1:1 salt to IL molar ratio) showed more ideal behaviour in the Walden plot, with greater ionic dissociation and higher mobility of lithium ions compared to the other ions, which means that the partial conductivity of Li$^+$ is higher at higher concentration. Spectroscopic measurements including FT-IR, Raman and NMR showed that the trans-FSI conformation changed to cis with increasing Li salt concentration. These observations suggest that the Li$^+$ transport mechanism at high salt concentrations is strongly influenced by the trans- to cis- conformational change of the FSI anion.

Amongst the nitrile anion based ILs, it was shown that the electrochemical stability of DCA was higher than TCM but lower than its TCB analogues. However, TCM is able to solubilise more salt than DCA and TCB. The electrochemical window of the DCA IL is inferior to the NTf_2 based ILs. The cycle-ability of the lithium anode in DCA based electrolytes has a strong relationship with the amount of H_2O in the IL, indicating some role for water in the formation of the SEI layer. A Li | $LiFePO_4$ cell with C_4mpyrDCA electrolyte showed over 130 mAh.g^{-1} of discharge capacity without significant capacity reduction beyond 20 cycles. The physical properties of this DCA IL were characterised with a range of salts including $LiNTf_2$, LiFSI, $LiBF_4$ and LiDCA. LiDCA showed the lowest viscosity and highest ion mobility for all ionic species in the solution while $LiBF_4$ showed the highest viscosity and lowest ion mobility forming large clusters. FSI anion in DCA based electrolyte also showed different behaviours from the other salt anions, which has unusually high mobility which can be interpreted to be isolated from a cluster formed by other ionic species in this DCA solution. It was also shown

that the 'ionicity' concept is better to describe the properties than the 'Walden plot' when a salt is added in the IL so the solution has several different ionic species.

Challenges remaining for IL electrolyte applications in Li batteries.

In spite of the superior rate capability of FSI based electrolytes with high concentration of LiFSI salts found in this research, several drawbacks have been reported previously. Wang, *et al*. who tested several ionic liquids including C_3mpyrFSI and showed that in their Accelarating Rate Calorimetry tests, C_3mpyrFSI is not safer than organic electrolytes.[1] Vijayaraghavan, *et al*. also investigated various ionic liquids and showed that, some ionic liquids containing FSI exhibited exothermic and self-heating behaviours over 200 ^{o}C, accompanied by pressure increases.[2] Another problem in the FSI system reported by Abouimrane, *et al*. showed that an electrolyte containing LiFSI corrodes the aluminium current collector at 3.3 V vs. Li | Li$^+$.[3]

It also should be noted that unlike previous reports showing that additional lithium salts increased the cathodic electrochemical stability in imidazolium-based NTf$_2$ ILs,[4-5] increasing the amount of LiFSI salts in C_4mpyrFSI decreased the cathodic stability in the study of Paillard et al which was attributed to the high level of impurities in the commercial grade LiFSI salt used.[6] There was no evidence found in this thesis that the increased amount of LiFSI in C_3mpyrFSI increases the cathodic electrochemical stability. Many of the Li | LiCoO$_2$ cells prepared failed cycling after a few cycles and the best cycled cell (one of 3.2 mol.kg^{-1} LiFSI in C_3mpyrFSI) also failed after 20 cycles without reaching 4.2V during the charging process. This may be caused by its relatively low cathodic stability above 4.0V vs. Li | Li$^+$ compared to the NTf$_2$ anion. There are some reports that the FSI anion could establish a solid electrolyte interphase (SEI) on graphite anodes without the need for additives,[6] however, the trial to duplicate that experiment on graphite anodes during this research period failed, showing less than 10% of initial discharge capacity of the theoretical capacity of graphite. Hence further investigation of the modes of cathode instability and the optimum materials for use with FSI electrolytes are needed.

It was shown that the DCA based electrolyte is extremely sensitive to the amount of moisture, having around 200 ppm as an optimum moisture concentration in the solution for improved Li metal battery cycling. The mechanism of the moisture sensitivity is not yet fully understood and needs further investigation. This extreme moisture sensitivity is an important issue in commercialising this electrolyte for lithium battery applications. The relatively low cathodic electrochemical stability[7-8] also prevents its use with LiCoO$_2$ cathode materials or other high voltage cathode materials. It is also interesting that this low viscosity IL does not show any cycling ability at room temperature, but only at higher temperatures such as 50 ^{o}C.

Tetracyanoborate (TCB) is an attractive candidate for non-fluorinated ionic liquid for lithium battery electrolyte since it has relatively high cathodic electrochemical stability as shown in this thesis. However, there is a problem that it has poor lithium salt solubility. To avoid this problem, Scheers, *et al.*[9] have successfully demonstrated glycol dimethyl ether as an additive in this TCB to maximise the salt solubility. This approach is worthy of further investigation. Using equimolar glycol to lithium salt mixtures to make ionic liquid like structures as suggested by Watanabe and co-workers[10-13] may also be a possible approach.

Future work

The research trends in lithium secondary batteries are currently mainly focused on electric vehicle applications to increase range and reduce costs.[14] To accomplish this goal, several research directions are progressing widely, including improving cathode, anode and electrolyte performance as well as including new types of batteries. One of the important research trends is high voltage cathode materials. Several significant steps have been reported in this field[15-18] but, there is still a lack of electrolyte candidates for these high voltage applications. Ionic liquid based electrolytes have been regarded as promising candidates, but due to its stability NTf$_2$ ILs are still the only viable candidates. The electrochemical origins of this feature of IL properties is an important area for future study

Another important research field is fast charging battery technology, which is mainly regarded as a matter more related to electrode performance than the electrolyte.[19-20] However, research into the lithium transport mechanisms in the high rate materials discovered in this thesis could produce greater understanding of its origins and potentially indicate further improvements.

References

1.   Wang, Y.; Zaghib, K.; Guerfi, A.; Bazito, F. F. C.; Torresi, R. M.; Dahn, J. R., Accelerating rate calorimetry studies of the reactions between ionic liquids and charged lithium ion battery electrode materials. *Electrochimica Acta* **2007,** *52* (22), 6346-6352.
2.   Vijayaraghavan, R.; Surianarayanan, M.; Armel, V.; MacFarlane, D. R.; Sridhar, V. P., Exothermic and thermal runaway behaviour of some ionic liquids at elevated temperatures. *Chemical Communications* **2009,** (41), 6297-6299.
3.   Abouimrane, A.; Ding, J.; Davidson, I. J., Liquid electrolyte based on lithium bis-fluorosulfonyl imide salt: Aluminum corrosion studies and lithium ion battery investigations. *Journal of Power Sources* **2009,** *189* (1), 693-696.
4.   Shin, J. H.; Henderson, W. A.; Appetecchi, G. B.; Alessandrini, F.; Passerini, S., Recent developments in the ENEA lithium metal battery project. *Electrochimica Acta* **2005,** *50* (19), 3859-3865.

5.   Randstroem, S.; Appetecchi, G. B.; Lagergren, C.; Moreno, A.; Passerini, S., The influence of air and its components on the cathodic stability of N-butyl-N-methylpyffolidinium bis(trifluoromethanesulfonyl)imide. *Electrochimica Acta* **2007,** *53* (4), 1837-1842.

6.   Paillard, E.; Zhou, Q.; Henderson, W. A.; Appetecchi, G. B.; Montanino, M.; Passerini, S., Electrochemical and Physicochemical Properties of PY(14)FSI-Based Electrolytes with LiFSI. *Journal of the Electrochemical Society* **2009,** *156* (11), A891-A895.

7.   MacFarlane, D. R.; Forsyth, S. A.; Golding, J.; Deacon, G. B., Ionic liquids based on imidazolium, ammonium and pyrrolidinium salts of the dicyanamide anion. *Green Chemistry* **2002,** *4* (5), 444-448.

8.   MacFarlane, D. R.; Meakin, P.; Sun, J.; Amini, N.; Forsyth, M., Pyrrolidinium imides: A new family of molten salts and conductive plastic crystal phases. *Journal of Physical Chemistry B* **1999,** *103* (20), 4164-4170.

9.   Scheers, J.; Pitawala, J.; Thebault, F.; Kim, J.-K.; Ahn, J.-H.; Matic, A.; Johansson, P.; Jacobsson, P., Ionic liquids and oligomer electrolytes based on the B(CN)(4)(-) anion; ion association, physical and electrochemical propertiesw. *Physical Chemistry Chemical Physics* **2011,** *13* (33), 14953-14959.

10.   Tamura, T.; Hachida, T.; Yoshida, K.; Tachikawa, N.; Dokko, K.; Watanabe, M., New glyme-cyclic imide lithium salt complexes as thermally stable electrolytes for lithium batteries. *Journal of Power Sources* **2010,** *195* (18), 6095-6100.

11.   Seki, S.; Takei, K.; Miyashiro, H.; Watanabe, M., Physicochemical and Electrochemical Properties of Glyme-LiN(SO2F)(2) Complex for Safe Lithium-ion Secondary Battery Electrolyte. *Journal of the Electrochemical Society* **2011,** *158* (6), A769-A774.

12.   Yoshida, K.; Tsuchiya, M.; Tachikawa, N.; Dokko, K.; Watanabe, M., Correlation between Battery Performance and Lithium Ion Diffusion in Glyme-Lithium Bis(trifluoromethanesulfonyl)amide Equimolar Complexes. *Journal of the Electrochemical Society* **2012,** *159* (7), A1005-A1012.

13.   Ueno, K.; Yoshida, K.; Tsuchiya, M.; Tachikawa, N.; Dokko, K.; Watanabe, M., Glyme-Lithium Salt Equimolar Molten Mixtures: Concentrated Solutions or Solvate Ionic Liquids? *Journal of Physical Chemistry B* **2012,** *116* (36), 11323-11331.

14.   Aurbach, D., A review on new solutions, new measurements procedures and new materials for rechargeable Li batteries. *Journal of Power Sources* **2005,** *146* (1-2), 71-78.

15.   Goodenough, J. B., Cathode materials: A personal perspective. *Journal of Power Sources* **2007,** *174* (2), 996-1000.

16.   Goodenough, J. B.; Kim, Y., Challenges for Rechargeable Li Batteries. *Chemistry of Materials* **2010,** *22* (3), 587-603.

17.   Yamamoto, T.; Hara, T.; Segawa, K.; Honda, K.; Akashi, H., 4.4 V lithium-ion polymer batteries with a chemical stable gel electrolyte. *Journal of Power Sources* **2007,** *174* (2), 1036-1040.

18.   Borgel, V.; Markevich, E.; Aurbach, D.; Semrau, G.; Schmidt, M., On the application of ionic liquids for rechargeable Li batteries: High voltage systems. *Journal of Power Sources* **2009,** *189* (1), 331-336.

19.   Matsumoto, H.; Sakaebe, H.; Tatsumi, K.; Kikuta, M.; Ishiko, E.; Kono, M., Fast cycling of Li/LiCoO2 cell with low-viscosity ionic liquids based on bis(fluorosulfonyl)imide [FSI]. *Journal of Power Sources* **2006,** *160* (2), 1308-1313.

20.   Kang, K. S.; Meng, Y. S.; Breger, J.; Grey, C. P.; Ceder, G., Electrodes with high power and high capacity for rechargeable lithium batteries. *Science* **2006,** *311* (5763), 977-980.